University of Cyprus
Faculty of Engineering
Department of Architecture

ADAPTABLE DUAL CONTROL SYSTEMS

by

Tonia Sophocleous-Lemonari

Diploma of Civil Engineering, National Technical University of Athens, Greece
M.Sc. in General Management, Mediterranean Institute of Management, Cyprus

Submitted to the Department of Architecture of the University of Cyprus in partial fulfillment of the requirements for the degree of

Doctor of Philosophy

Nicosia, September 2012

ADAPTABLE DUAL CONTROL SYSTEMS

by

Tonia Sophocleous-Lemonari

Thesis supervisor:

Dr. Marios C. Phocas, Associate Professor
Department of Architecture, University of Cyprus

Examination committee:

Dr. Nadia Charalambous, Lecturer (*Chairman)*
Department of Architecture, University of Cyprus

Dr. Marios C. Phocas, Associate Professor
Department of Architecture, University of Cyprus

Dr. Odysseas Kontovourkis, Lecturer
Department of Architecture, University of Cyprus

Dr. Ioannis Balafas,
Department of Civil and Environmental Engineering, University of Cyprus

Dr. Adrian Pocanschi, Privatdozent
Institute of Building Structures and Structural Design, University of Stuttgart

University of Cyprus
Faculty of Engineering
Department of Architecture

APPROVAL PAGE

Doctor of Philosophy Dissertation

Adaptable Dual Control Systems

by

Tonia Sophocleous-Lemonari

Research Supervisor: _____

Dr. Marios C. Phocas

Committee Member (Chairman) _____

Dr. Nadia Charalambous (Chairman)

Committee Member _____

Dr. Odysseas Kontovourkis

Committee Member _____

Dr. Ioannis Balafas

Committee Member _____

Dr. Adrian Pocanschi

ABSTRACT

"Adaptable Dual Control Systems"

The addition of secondary members within the primary frame to compose dual systems has proven to be beneficial under static loading in terms of reduction of self-weight of members, ease of construction and structural design optimization through attractive design configurations. The nature of dual response in frame systems leads to an overall improved behavior under static loading, but has not been investigated for dynamic excitations. Concerned with the logic of adaptable response through a dual action of frame systems the proposals made refer to the use of inventive seismic resisting technology methods suitable for basic forms of general architectural design applications.

The technology of passive seismic control systems is realized though the addition of damping devices with bracings to compose a secondary system within the primary frame. The structural aim of the added members is to succeed in resisting seismic ground motions through dissipation of the input energy leaving the primary frame to resist in its elastic region. The method provides configuration designs of energy dissipation systems, which incorporate conventional sections of braces. Such mechanisms sometimes fail to effectively develop a continuous activation of energy dissipation during a complete cycle of vibration, due to compression buckling of the bracings members. Alternatively, a few most recently developed research proposals involve the use of flexible members as bracings, which are able to develop kinetic mechanisms during the energy dissipation process while working only in tension.

Contributing to the field of research and development of kinetic mechanisms, the current research work investigates, through numerical simulations and parametric studies, the effects of potential application of Adaptable Dual Control Systems in frame structures for seismic passive control. Common denominator for every aspect of the present research comprises the integration of a bracing-damper mechanism in frame structures that consists of tension-only members and hysteretic steel plates, for the development of an adaptable dual response behavior against moderately strong, extremely irregular motions. The effects

of Adaptable Dual Control Systems on the performance of frame structures are demonstrated using four different configuration design alternatives.

The investigation is concentrated in simulation and modeling research techniques to test the conceptual design idea and its implementation potential. The basic mechanical behavior principles of ADCS are illustrated using a single degree of freedom structural model utilized in a Finite-Element analysis software, SAP2000. The analytical investigations revealed the dominating design parameters for ADCS. The non-linear link parameter, defined as the ratio of the stiffness to the yield force of the hysteretic damper, DR, characterizes the behavior of the controlled systems in each configuration. Optimum DR values are proposed for each system configuration in achieving high energy dissipation capacity, while preventing possible increase of the maximum base shear and relative displacements.

ADCS dynamic behavior is analytically provided under three international seismic records and it is verified under ten records of the Mediterranean region. Some interesting conclusions are indicated as regards the potential use of ADCS alternative configuration designs in passive seismic control applications, aiming at maximization of the energy dissipation capacity and practically a negligible coupling effect of the added secondary slender bracings and hysteretic damper plates to the primary frame.

ΠΕΡΙΛΗΨΗ

«Προσαρμόσιμα Συστήματα Δυαδικού Ελέγχου»

Η προσθήκη δευτερευόντων μελών εντός της πρωτεύουσας πλαισιακής κατασκευής για τη σύνθεση δυαδικών συστημάτων έναντι στατικών φορτίων έχει αποδειχθεί ότι υπερτερεί ως προς τη μείωση του ίδιου βάρους της κατασκευής, την ευκολία της ανέγερσης της και τη βελτιστοποίηση του δομικού σχεδιασμού μέσω ελκυστικών μορφοποιήσεων. Η φύση της δυαδικής μορφής της απόκρισης πλαισιακών συστημάτων επιφέρει βελτίωση στη συμπεριφορά κατά την απόκριση καθολικά έναντι στατικής φόρτισης, ενώ δεν έχει διερευνηθεί για δυναμικές φορτίσεις. Οι εισηγήσεις εντός του πλαισίου της λογικής μιας προσαρμόσιμης συμπεριφοράς κατά την απόκριση, ικανές να αναπτύξουν δυαδική λειτουργία, επιστρατεύουν καινοτόμες μεθόδους αντισεισμικής τεχνολογίας κατάλληλες για εφαρμογή σε βασικές μορφές γενικών αρχιτεκτονικών μορφοποιήσεων δομικών συστημάτων.

Η τεχνολογία συστημάτων παθητικού σεισμικού ελέγχου γίνεται εφικτή μέσω της προσθήκης στοιχείων απόσβεσης με συνδέσμους ακαμψίας που συνιστούν ένα δευτερεύον σύστημα εντός του πρωτεύοντος πλαισίου. Ο δομικός στόχος των πρόσθετων μελών είναι η επιτυχής απόκριση έναντι σεισμικών εδαφικών δονήσεων μέσω της απόσβεσης της εισαγόμενης ενέργειας επιτρέποντας στο πρωτεύον πλαίσιο να συμπεριφερθεί ελαστικά. Η μέθοδος παρέχει λύσεις για μορφοποίηση συστημάτων απόσβεσης ενέργειας, οι οποίες εμπεριέχουν συμβατικές διατομές συνδέσμων. Συναφείς μηχανισμοί κάποτε αποτυγχάνουν να αναπτύσσουν αποτελεσματικά συνεχή ενεργοποίηση απόσβεσης ενέργειας καθ' όλη τη διάρκεια ενός πλήρους κύκλου της επαναληπτικής φόρτισης της διέγερσης εξαιτίας του φαινομένου λυγισμού των θλιβόμενων μελών ακαμψίας. Εναλλακτικά έχουν εντοπιστεί σποραδικές πρόσφατες ερευνητικές προτάσεις που αφορούν τη χρήση εύκαμπτων μελών σαν συνδέσμους, οι οποίοι είναι ικανοί να αναπτύξουν κινητικούς μηχανισμούς κατά τη διαδικασία απόσβεσης ενέργειας ενώ ενεργοποιούνται μόνον σε εφελκυσμό.

Συνεισφέροντας στο πεδίο έρευνας και ανάπτυξης των κινητικών μηχανισμών, η

παρούσα ερευνητική εργασία διερευνά, μέσω αριθμητικής προσομοίωσης και παραμετρικών αναλύσεων, τις επιδράσεις της πιθανής εφαρμογής των προσαρμόσιμων συστημάτων δυαδικού ελέγχου σε πλαισιακές κατασκευές για σκοπούς παθητικού σεισμικού ελέγχου. Κοινός παρονομαστής για κάθε μέρος της παρούσας έρευνας αποτελεί η ένταξη εφελκυόμενων μελών ακαμψίας και υστερετικού μηχανισμού απόσβεσης ενέργειας από μεταλλικά ελάσματα, σε πλαισιακές κατασκευές, ώστε να είναι δυνατή η ανάπτυξη μιας προσαρμόσιμης και δυαδικής συμπεριφοράς κατά την απόκριση έναντι σχετικά ισχυρών, ιδιαιτέρως ακανόνιστων μετακινήσεων. Παρουσιάζονται οι επιδράσεις των προσαρμόσιμων συστημάτων δυαδικού ελέγχου χρησιμοποιώντας τέσσερις διαφορετικούς δυνατούς τρόπους μορφοποίησης.

Η διερεύνηση επικεντρώνεται σε τεχνικές προσομοίωσης και μοντελοποίησης για την επιτελεστικότητα της ιδέας σχεδιασμού και της δυνατότητας εφαρμογής της. Οι βασικές αρχές της μηχανικής συμπεριφοράς των προσαρμόσιμων συστημάτων δυαδικού ελέγχου παρουσιάζονται χρησιμοποιώντας μονοβάθμιο στατικό μοντέλο στο απλοποιητικό λογισμικό ανάλυσης πεπερασμένων στοιχείων, SAP2000. Η αναλυτική διερεύνηση έχει αποκαλύψει τις δεσπόζουσες παραμέτρους σχεδιασμού των προσαρμόσιμων συστημάτων δυαδικού ελέγχου. Η μη γραμμική παράμετρος συνδέσμου που ορίζεται σαν ο λόγος της ακαμψίας ως προς τη δύναμη διαρροής του υστερητικού αποσβεστήρα, DR , καθορίζει τη συμπεριφορά των συστημάτων ελέγχου για κάθε δυνατή μορφοποίηση. Προτείνονται βέλτιστες τιμές DR για κάθε μία από τις δυνατές μορφοποιήσεις ώστε να προσδίδεται υψηλή ικανότητα απόσβεσης ενέργειας και να αποτρέπει πιθανή αύξηση της τέμνουσας και των σχετικών μετακινήσεων.

Παρουσιάζονται τα αποτελέσματα από διεξοδικές αναλύσεις ως προς τη δυναμική απόκριση υπό τρεις διαφορετικές σεισμικές διεγέρσεις από το διεθνή χώρο και η συμπεριφορά των συστημάτων επικυρώνεται υπό δέκα καταγραφές από την περιοχή της Μεσογείου. Επισημάνονται ενδιαφέροντα συμπεράσματα που σχετίζονται με την προοπτική χρήσης των εναλλακτικών μορφοποιήσεων προσαρμόσιμων συστημάτων δυαδικού ελέγχου σε εφαρμογές σεισμικού παθητικού ελέγχου που έχουν στόχο τη μεγιστοποίηση της δυνατότητας απόσβεσης ενέργειας και πρακτικά αμελητέας

αλληλεπίδρασης των επιπρόσθετων δευτερευόντων εύκαμπτων συνδέσμων και ελασμάτων υστερητικής απόσβεσης με το πρωτεύον πλαίσιο.

ACKNOWLEDGMENTS

I would like to take this opportunity to express my deep and intense gratitude to my thesis supervisor, Dr. Marios C. Phocas. It is difficult to overstate my gratitude to Dr. Phocas who was the most important person in both the creation of my Ph.D. research and also my academic and personal development. With his enthusiasm, his inspiration and his great effort he provided encouragement, sound advice, excellent teaching and company. I would have been lost without him.

I am indebted to Dr. Nadia Charalambous, Dr. Odysseas Kontovourkis and Dr. Ioannis Balafas who worked with me supporting both my academic and personal achievements.

I would also like to thank my colleagues, researchers and students from Archimedes Research Center at the Department of Architecture and Department of Civil and Environmental Engineering of the University of Cyprus and the University of Nicosia for providing a stimulating environment in which to learn and grow.

Lastly and most importantly I wish to thank my family for providing a loving environment for me.

Dedicated to Dr. Adrian Pocanschi, who conceived the idea of Steel Frames with Bracing Mechanism and Hysteretic Damper.

TABLE OF CONTENTS

CHAPTER 1 INTRODUCTION 27

1.1 Structures Configurations 27

1.2 Energy Dissipation for Frames 27

1.3 Motivation 28

1.4 Literature Review 29

1.5 Adaptable Dual Control Systems 29

1.6 Research Outline 31

CHAPTER 2 DUAL STATIC SYSTEMS 33

2.1 Dual Static Systems Characteristics 33

2.2 Primary Frames 34

2.3 Dual Static Frames with Stayed Cables 35

2.4 Dual Static Frame with Suspended Cables 38

2.5 Sub-Tensioned Dual Static Frames with Struts 39

2.6 General Remarks 43

CHAPTER 3 PASSIVE STRUCTURAL CONTROL 45

3.1 Passive Structural Control 45

3.2 Damping Devices for Passive Seismic Control 46

3.3 Kinetic Systems in Frame Structures 51

3.3.1 Eccentrically braced frames 51

3.3.2 Buckling restraint bracing dampers 52

3.3.3 Toggle and scissors-jack bracing configurations 52

3.4 Kinetic Systems with Tension-Only Members 54

3.4.1 Tension-only bracings with friction dampers 54

3.4.2 Tension-only bracings with metallic dampers *56*

3.5 General Remarks 59

CHAPTER 4 ADAPTABLE DUAL CONTROL SYSTEMS 61

4.1 Systems Characteristics 61

4.2 ADCS Design Requirements 62

4.3 ADCS0 Design 63

4.3.1 General for ADCS0 design *63*

4.3.2 Configuration design for ADCS0 ..... *64*

4.3.3 Kinetic model of ADCS0 ..... *64*

4.3.4 Construction design of ADCS0 ..... *65*

4.4 ADCS1 Design 65

4.4.1 General for ADCS1 design *65*

4.4.2 Configuration design of ADCS1 ..... *66*

4.4.3 Kinetic model of ADCS1 ..... *66*

4.4.4 Construction design of ADCS1 ..... *67*

4.5 ADCS2 Design 68

4.5.1 General for ADCS2 design *68*

4.5.2 Configuration design of ADCS2 ..... *68*

4.5.3 Kinetic model of ADCS2 ..... *69*

4.5.4 Construction design of ADCS2 ..... *70*

4.6 ADCS3 Design 71

4.6.1 General for ADCS3 design *71*

4.6.2 Configuration design of ADCS3 ..... *71*

4.6.3 Kinetic model of ADCS3 ..... *72*

4.6.4 Construction design of ADCS3 ..... *73*

CHAPTER 5 ADCS MODELS AND MECHANICAL PROPERTIES 75

5.1 Primary System 75

5.2 ADCS Model 75

5.3 Seismic Input Records 76

5.4 ADCS Mechanical Properties 78

5.4.1 General 78

5.4.2 Mechanical properties of hysteretic damper 78

5.4.3 ADCS mechanical properties investigation 81

CHAPTER 6 DYNAMIC RESPONSE 83

6.1 ADCS0 Dynamic Response 83

6.1.1 General for ADCS0 design 83

6.1.2 Energy dissipation results for ADCS0 84

6.1.3 Base shear results for ADCS0 86

6.1.4 Relative displacement results for ADCS0 87

6.1.5 Damper deformations in ADCS0 89

6.2 ADCS1 Dynamic Response 90

6.2.1 Natural period identification for ADCS1 90

6.2.2 Energy dissipation results for ADCS1 91

6.2.3 Base shear results for ADCS1 95

6.2.4 Relative displacement results for ADCS1 98

6.2.5 Damper deformations in ADCS1 102

6.2.6 Bracings axial forces identification for ADCS1 103

6.3 ADCS2 Dynamic Response 104

6.3.1 Natural period identification for ADCS2 104

6.3.2 Energy dissipation results for ADCS2 105

6.3.3 Base shear results for ADCS2 108

6.3.4 Relative displacement results for ADCS2 ..... *110*
6.3.5 Damper deformations in ADCS2 ..... *114*
6.3.6 Bracings axial forces identification for ADCS2 ..... *115*
6.4 ADCS3 Dynamic Response 116
6.4.1 Natural period identification for ADCS3 ..... *116*
6.4.2 Energy Dissipation results for ADCS3 ..... *116*
6.4.3 Base shear results for ADCS3 ..... *120*
6.4.4 Relative displacement results for ADCS3 ..... *123*
6.4.5 Damper deformations in ADCS3 ..... *127*
6.4.6 Bracings axial forces identification for ACDS3 ..... *128*
6.5 ADCS selected effective stiffness ratios 129
CHAPTER 7 DYNAMIC RESPONSE VERIFICATION 131
7.1 Dynamic Response Verification 131
7.1.1 Seismic records of the Greek-Mediterranean area *131*
7.2 ADCS1 Dynamic Response Verification 133
7.2.1 Energy dissipation verification for ADCS1 ..... *133*
7.2.2 Base shear verification for ADCS1 ..... *137*
7.2.3 Relative displacements verification for ADCS1 ..... *138*
7.3 ADCS2 Dynamic Response Verification 139
7.3.1 Energy dissipation verification for ADCS2 ..... *139*
7.3.2 Base shear verification for ADCS2 ..... *143*
7.3.3 Relative displacements verification for ADCS2 ..... *144*
7.4 ADCS3 Dynamic Response Verification 145
7.4.1 Energy dissipation verification for ADCS3 ..... *145*
7.4.2 Base shear verification for ADCS3 ..... *149*
7.4.3 Relative displacements verification for ADCS3 ..... *150*

CHAPTER 8 CONCLUSIONS 153

8.1 Research Contributions 153

8.2 Research Results 154

8.3 Future Work 158

REFERENCES 159

LIST OF FIGURES

Figure 2.1 Primary frames under uniform vertical load: (a) models and deformed shapes; (b) shear forces; (c) bending moments. 35

Figure 2.2 System with stayed cables: (a) model; (b) deformed shape; (c) axial forces; (d) bending moments. 36

Figure 2.3 System with stayed cables and single under strut: (a) model; (b) deformed shape; (c) axial forces; (d) bending moments. 37

Figure 2.4 System with suspended cables: (a) model; b) deformed shape; (c) axial forces; (d) bending moments. 38

Figure 2.5 Sub-tensioned, two-strut system: (a) model; (b) deformed shape; (c) axial forces; (d) bending moments. 40

Figure 2.6 Sub-tensioned, triple-strut system: (a) model; (b) deformed shape; (c) axial forces; (d) bending moments. 41

Figure 2.7 Sub-tensioned two-strut cross system: (a) load; (b) deformed shape; (c) axial forces; (d) bending moments. 42

Figure 3.1 Passive structural control in frame structures. 45

Figure 3.2 Viscoelastic dampers on chevron bracings. 46

Figure 3.3 Hysteretic behavior of VE-damper. 47

Figure 3.4 Viscous damper on chevron and diagonal bracing. 48

Figure 3.5 Hysteretic behavior of VF-damper ([3.6]). 48

Figure 3.6 Friction dampers on cross and diagonal bracings. 49

Figure 3.7 Hysteretic behavior of friction damper. 49

Figure 3.8 Metallic dampers on chevron bracings. 50

Figure 3.9 Hysteretic behavior of metallic dampers ([3.35]). 51

Figure 3.10 Eccentrically braced frames. 51

Figure 3.11 Buckling restraint bracing dampers. 52

Figure 3.12 Scissor-jack system with viscous damper. 53

Figure 3.13 Toggle bracing with filled accordion metallic dampers. 53

Figure 3.14 Kinematics of friction mechanism ([3.9]). 55

Figure 3.15 Hysteretic behavior of friction mechanism ([3.9]). 55

Figure 3.16 System and kinematics of rotational friction damper ([3.22]). 56

Figure 3.17 Hysteretic behavior of rotational friction damper ([3.23]). 56

Figure 3.18 System and kinematics of light-weight dissipative bracing system ([3.28]) 57

Figure 3.19 Hysteretic behavior of light-weight dissipative bracing system ([3.28]) 57

Figure 3.20 Kinematics of central energy dissipater ([3.17]) 58

Figure 3.21 Hysteretic behavior of central energy dissipater ([3.17]). 58

Figure 4.1 ADCS0 with cross bracing-damper mechanism. 64

Figure 4.2 ADCS0 kinetic model. 65

Figure 4.3 ADCS1 with portal bracing-damper mechanism. 66

Figure 4.4 ADCS1 kinetic model. 67

Figure 4.5 Connection principle of ADCS1 with rotating disc and hysteretic damper. 68

Figure 4.6 ADCS2 with portal and chevron bracing-damper mechanism. 69

Figure 4.7 ADCS2 kinetic model. 70

Figure 4.8 Connection principle of ADCS2 with rotating discs and hysteretic damper. 71

Figure 4.9 ADCS3 with diagonal bracing-damper mechanism. 72

Figure 4.10 ADCS3 kinetic model. 73

Figure 4.11 Connection principle of ADCS3 with rotating discs and hysteretic damper. 74

Figure 5.1 International seismic input records. 77

Figure 6.1 ADCS0 hysteretic damper's energy dissipation and force-deformation behavior (damper: 1012205): (a) seismic case A; (b) seismic case B; (c) seismic case C. 85

Figure 6.2 Primary frame's and ADCS0 base shear BS time history (damper: 1012205): (a) seismic case A; (b) seismic case B; (c) seismic case C. 87

Figure 6.3 Primary frame's and ADCS0 relative displacement U_x time history (damper: 1012205): (a) seismic case A; (b) seismic case B; (c) seismic case C. 89

Figure 6.4 Damper's shear deformation D_d and ADCS0 relative displacement U_x time history (damper: 1012205): (a) seismic case A; (b) seismic case B; (c) seismic case C. 90

Figure 6.5 ADCS1 fundamental period T to damper's stiffness k_d, yield force P_y and damper ratio DR values. 91

Figure 6.6 ADCS1 effective energy deformation index EEDI to damper ratio DR 92

Figure 6.7 ADCS1 hysteretic damper's energy dissipation and force-deformation behavior (damper: 2282510): (a) seismic case A; (b) seismic case B; (c) seismic case C. 94

Figure 6.8 ADCS1 maximum base shear BS to damper ratio DR and fundamental period T for seismic case A. 95

Figure 6.9 ADCS1 maximum base shear BS to damper ratio *DR* and fundamental period T for seismic case B. 96

Figure 6.10 ADCS1 maximum base shear BS to damper ratio *DR* and fundamental period T for seismic case C. 96

Figure 6.11 Primary frame's and ADCS1 base shear BS time history (damper: 2282510): (a) seismic case A; (b) seismic case B; (c) seismic case C. 98

Figure 6.12 ADCS1 maximum relative displacement U_x to damper ratio *DR* and fundamental period T for seismic case A. 99

Figure 6.13 ADCS1 maximum relative displacement U_x to damper ratio *DR* and fundamental period T for seismic case B. 100

Figure 6.14 ADSC1 maximum relative displacement U_x to damper ratio *DR* and fundamental period T for seismic case C. 100

Figure 6.15 Primary frame's and ADCS1 relative displacement U_x time history (damper: 2282510): (a) seismic case A; (b) seismic case B; (c) seismic case C. 102

Figure 6.16 Damper's shear deformation D_d and ADCS1 relative displacement U_x time history (damper: 2282510): (a) seismic case A; (b) seismic case B; (c) seismic case C. 103

Figure 6.17 ADCS2 fundamental period T to damper's stiffness k_d, yield force P_y and damper ratio DR values. 105

Figure 6.18 ADCS2 effective energy deformation index EEDI to damper ratio DR 106

Figure 6.19 ADCS2 hysteretic damper's energy dissipation and force-deformation behavior (damper: 616355): (a) seismic case A; (b) seismic case B; (c) seismic case C. 107

Figure 6.20 ADCS2 maximum base shear BS to damper ratio *DR* and fundamental period T for seismic case A. 108

Figure 6.21 ADCS2 maximum base shear BS to damper ratio *DR* and fundamental period *T* for seismic case B. 109

Figure 6.22 ADCS2 maximum base shear BS to damper ratio *DR* and fundamental period *T* for seismic case C. 109

Figure 6.23 Primary frame's and ADCS2 base shear BS time history (damper: 616355): (a) seismic case A; (b) seismic case B; (c) seismic case C. 110

Figure 6.24 ADCS2 maximum relative displacement U_x to damper ratio *DR* and fundamental period *T* for seismic case A. 111

Figure 6.25 ADCS2 maximum relative displacement U_x to damper ratio *DR* and fundamental period *T* for seismic case B. 111

Figure 6.26 ADCS2 maximum relative displacement U_x to damper ratio *DR* and fundamental period *T* for seismic case C. 112

Figure 6.27 Primary frame's and ADCS2 relative displacement U_x time history (damper: 616355): (a) seismic case A; (b) seismic case B; (c) seismic case C. 113

Figure 6.28 Damper's shear deformation D_d and ADCS2 relative displacement U_x time history (damper: 616355): (a) seismic case A; (b) seismic case B; (c) seismic case C. 115

Figure 6.29 ADCS3 fundamental period *T* to damper's stiffness k_d, yield force P_y and damper ratio *DR* values. 116

Figure 6.30 ADCS3 effective energy deformation index EEDI to damper ratio *DR* 117

Figure 6.31 ADCS3 hysteretic damper's energy dissipation and force-deformation behavior (damper: 612155): (a) seismic case A; (b) seismic case B; (c) seismic case C. 119

Figure 6.32 ADCS3 maximum base shear BS to damper ratio *DR* and fundamental period *T* for seismic case A. 120

Figure 6.33 ADCS3 maximum base shear BS to damper ratio *DR* and fundamental period *T* for seismic case B. 121

Figure 6.34 ADCS3 maximum base shear BS to damper ratio *DR* and fundamental period *T* for seismic case C. 121

Figure 6.35 Primary frame's and ADCS3 base shear BS time history (damper: 612155) (a) seismic case A; (b) seismic case B; (c) seismic case C. 123

Figure 6.36 ADCS3 maximum relative displacement U_x to damper ratio *DR* and fundamental period *T* for seismic case A. 124

Figure 6.37 ADCS3 maximum relative displacement U_x to damper ratio *DR* and fundamental period *T* for seismic case B. 124

Figure 6.38 ADCS3 maximum relative displacement U_x to damper ratio *DR* and fundamental period *T* for seismic case C. 125

Figure 6.39 Primary frame's and ADCS3 relative displacement U_x time history (damper: 612155): (a) seismic case A; (b) seismic case B; (c) seismic case C. 127

Figure 6.40 Damper's shear deformation D_d and ADCS3 displacement U_x time history (damper: 612155): (a) seismic case A; (b) seismic case B; (c) seismic case C. 128

Figure 7.1 Greek Mediterranean seismic input records. 132

Figure 7.2 ADCS1 hysteretic damper's energy dissipation and force-deformation behavior (damper: 2282510): (a) seismic case 1; (b) seismic case 2; (c) seismic case 3; (d) seismic case 4; (e) seismic case 5; (f) seismic case 6; (g) seismic case 7; (h) seismic case 8; (i) seismic case 9; (j) seismic case 10. 137

Figure 7.3 ADCS2 hysteretic damper's energy dissipation and force-deformation behavior (damper: 616355): (a) seismic case 1; (b) seismic case 2; (c) seismic case 3; (d) seismic case 4; (e) seismic case 5; (f) seismic case 6; (g) seismic case 7; (h) seismic case 8; (i) seismic case 9; (j) seismic

case 10. 143

Figure 7.4 ADCS3 hysteretic damper's energy dissipation and force-deformation behavior (damper: 612155): (a) seismic case 1; (b) seismic case 2; (c) seismic case 3; (d) seismic case 4; (e) seismic case 5; (f) seismic case 6; (g) seismic case 7; (h) seismic case 8; (i) seismic case 9; (j) seismic case 10. 149

LIST OF TABLES

Table 2.1 Sections of primary frame and dual frame composed members. 43

Table 5.1 International seismic input records. 77

Table 5.2 ADCS's mechanical properties investigation values. 81

Table 6.1 Primary frame's and ADCS0 (damper: 1012205) maximum base shear BS and effective energy dissipation index EEDI. 86

Table 6.2 Primary frame's and ADCS0 (damper: 1012205) maximum relative displacements U_x. 88

Table 6.3 Primary frame's and ADCS1 (damper: 2282510) maximum base shear BS and effective energy dissipation index EEDI. 97

Table 6.4 Primary frame's and ADCS1 (damper: 2282510) maximum relative displacements U_x. 101

Table 6.5 ADCS1 bracing members' axial forces (damper: 2282510). 104

Table 6.6 Primary frame's and ADCS2 (damper: 616355) maximum base shear BS and effective energy dissipation index EEDI. 109

Table 6.7 Primary frame's and ADCS2 (damper: 616355) maximum relative displacements U_x. 113

Table 6.8 ADCS2 bracing members' axial forces (damper: 616355). 115

Table 6.9 Primary frame's and ADCS3 (damper: 612155) maximum base shear BS and effective energy dissipation index EEDI. 122

Table 6.10 Primary frame's and ADCS3 (damper: 612155) maximum relative displacements U_x. 126

Table 6.11 ADCS3 bracing members' axial forces (damper: 612155). 129

Table 6.12 Controlled systems optimum effective stiffness ratios. 129

Table 7.1 Seismic records of the Greek Mediterranean area. 131

Table 7.2 Primary frame's and ADCS1 (damper: 2282510) maximum base shear BS. 138

Table 7.3 Primary frame's and ADCS1 (damper: 2282510) maximum relative displacements U_x. 139

Table 7.4 Primary frame's and ADCS2 (damper: 616355) maximum base shear BS. 144

Table 7.5 Primary frame's and ADCS2 (damper: 616355) maximum relative displacements U_x. 145

Table 7.6 Primary frame's and ADCS3 (damper: 612155) maximum base shear BS. 150

Table 7.7 Primary frame's and ADCS3 (damper: 612155) maximum relative displacements U_x. 151

CHAPTER 1 **INTRODUCTION**

1.1 Structures Configurations

The design of any structural system to provide interesting solutions and achieve a clear, stable and controllable load-bearing behavior comprises a challenge for engineers and architects. This challenge is made more complex for earthquake resistant systems.

In the present study several significant proposals are made for structures to better resist both static and dynamic loads. The moment resisting frames' static behavior is improved with the addition of a secondary strengthening system of cables and struts. Such composed systems, defined as dual systems, are beneficial due to the effective distribution of internal stresses and they may provide interesting solutions in terms of the configuration designs. The dual-system concept is investigated under seismic loads, aiming at a stable behavior. In moment resisting steel frames with an eccentric bracing for example, the more rigid eccentric braces provide primarily a stable seismic behavior, while the moment frame provides good flexural behavior. Steel-moment resisting frames and passive seismic control devices provide high damping that significantly reduces the seismic loads imparted to the primary frames.

1.2 Energy Dissipation for Frames

Structural control through energy dissipation systems has been increasingly implemented internationally in the last years and has proven to be a most promising strategy for earthquake safety of the structures. The control concept is based on the integration of passive damping devices within the structure for the necessary energy dissipation and the elastic response of the primary system. Passive metallic yielding, friction, viscoelastic and viscous damping devices may be added to frame structures to dissipate the input energy during an earthquake and to substantially reduce or eliminate damage to the primary frames ([1.4], [1.7]).

1.3 Motivation

The design of frame structures with added control members for earthquake resistance refers primarily to the need for the primary systems to exhibit a linear elastic behavior under seismic actions. In principle the damping devices are added in moment resisting frames, attached on steel bracings of large hollow sections. Such bracing components increase the overall stiffness of the system, as they consist of steel members stressed in compression, tension and bending. Before any hysteretic action is undertaken by the damper, the stiff bracings may reduce inter-story displacements, while producing high accelerations ([1.5]). In addition, the application of the members under compression leads under cyclic loading, to a relatively inefficient behavior of the system: in every half-loading cycle the compression diagonal buckles and it therefore cannot participate in the energy dissipation process.

Slender bracing members for the integration of dampers in frame structures have found up to date limited applications ([1.2]). A reason for this is their tendency of becoming slack under tension yielding and compression buckling. In addition sudden increases of the tensile forces in the slender braces create detrimental impact loadings on the connections and the other structural members ([1.13]). On the other hand, the application of light-weight secondary systems for earthquake resistance seems to be a promising alternative as regards the avoidance of stiffness interaction with the primary system, as well as the achievement of both, simplicity and aesthetic qualities of the structures in the broader architectural context. The implementation of tension-only bracings with damping devices in frame structures may only be realized through the development of suitable bracing-damper configurations, whereas all bracing members would effectively contribute during the entire load duration to the operation of the integrated damper. In this way, optimization of the control system's operation principles, for earthquake structural resistance, may be achieved.

1.4 Literature Review

A control mechanism that enables the contribution of all structural members in the energy dissipation process is the Pall-Marsh friction mechanism with slender cross braces, as described in ([1.3]). Under lateral loads, one pair of braces is subjected to tension and the other to compression. The rectangular damper deforms into a parallelogram, dissipating energy at the bolted joints through sliding friction. With the completion of a loading cycle, the resulting areas of the hysteretic loops are identical for both braces. An alternative of this friction mechanism with cross braces has been proposed in ([1.15]). An implementation of chevron cable members with a friction damper that consists of three rotating plates and circular friction pad discs placed in between is described in ([1.8]).

In few other recently proposed light-weight control systems, hysteretic dampers are connected with slender bracing members that activate the former for the necessary energy dissipation through their joints' relative displacements. Effective energy deformation is achieved through the optimization of the integrated hysteretic damper plates' section. Along this line, the cross braces with the articulated quadrilateral with steel dissipaters work only in tension, whereas energy dissipation develops through elasto-plastic flexure of the steel plates with varying depth ([1.11]). A similar cross cable bracing configuration has been proposed in ([1.6]), with a central energy dissipater consisting of two steel plates that are interconnected through a rotational spring and eight elastic cables. All cables are in tension under lateral loads. Under seismic excitation four cables in tension rotate the steel plates in opposite directions. The remaining cables connected across the shortened diagonal are stressed elastically in compression and do not become slack, when the loading direction changes, due to the permanent rotation of the steel plates.

1.5 Adaptable Dual Control Systems

Adaptable Dual Control Systems, ADCS that are developed and investigated in their dynamic behavior in the present study, consist of tension-only bracing members with closed circuit and a hysteretic damper of steel plates. The implementation of ADCS in frame structures enables a dual function of the composed system, leading to two practically

uncoupled systems, i.e. the primary frame, responsible for the static vertical and static horizontal forces and the bracing-damper mechanism, for the earthquake forces and the necessary energy dissipation. In all cases the aim is for the hysteretic damper to utilize effectively the relative displacements between its connection joints, i.e. a bracing- and a primary frame's member, through its own yielding deformations for the necessary energy dissipation. Parametric dynamic analyses of the SDOF system's responses are performed based on three representative international earthquake motions of differing frequency content. The dynamic response behavior is verified based on ten selected seismic input records of the Mediterranean earthquake prone area. A non-linear link parameter, equal to the ratio of the stiffness to the yield force of the hysteretic damper, DR, is defined to characterize the behavior of each controlled system for the range of the relative stiffness ratios of the composed members. Optimum DR values are proposed for each configuration for achieving high energy dissipation capacity of the systems preventing possible related increase of the maximum base shear and relative displacements.

The initial ADCS proposal describing a cross bracing mechanism of closed circuit with a hysteretic damper of steel plates was studied in ([1.9]). During strong ground motions relative displacements between the bracing and the frame member interconnected through the hysteretic damper, yield to the damper's own deformations and energy dissipation. This kinetic system's principle is applied in the development and improvement of further possible configurations for ADCS ([1.10]). In principle, ADCS introduce a prototype connections' design for the bracing members, based on rotating discs. The connection principle may be applied in different bracing configurations that share common features in respect to the kinetic model and the control behaviour of the system ([1.12]). Furthermore, the hysteretic damper applied in ADCS, may follow the section principles of hysteretic dampers subjected to shear forces at their connections. The dampers consist of X- or triangular-shaped steel plates for achieving uniform deformation curvatures over the sections' height, as applied in the examples of ADAS- and TADAS-devices ([1.1], [1.14]). The present analysis refers to four particular ADCS-configurations, the cross bracing as a reference, ADCS0, a portal bracing, ADCS1, a portal- and a chevron bracing, ADCS2 and

a bracing that forms with three cables a triangular shape, ADCS3. Each bracing's configuration obviously provides a differentiated seismic performance, but also an alternative structural form that can be applied within the broader architectural context of the building.

1.6 Research Outline

Chapter 1 provides an introduction to some of the key issues involved in the configuration of dual frame systems that have to resist external loads through the development of an adaptable behavior, i.e. dual behavior for the purpose of structural control. It includes a summary of the up-to-date methods of energy dissipation for passive control.

Chapter 2 outlines the beneficial characteristics of dual systems behavior under uniform vertical static loading. It acknowledges the need for possible improvements as regards configurations of frame systems towards minimal architectural impact, while it poses the research interest in developing attractive dual systems for earthquake resistance.

Chapter 3 explains the method of passive structural seismic control through the use of energy dissipation devices. It presents the state of the art as regards available configurations of moment resisting frames with added bracing for the integration of damping mechanisms within. It distinguishes the energy dissipation systems from the concept of kinetic mechanisms and emphasizes the benefits of contributions to this new field of research and development: the energy dissipation mechanisms through the activation of movement in response.

Chapter 4 introduces the adaptable dual control systems concept. It describes the principle characteristics based on four different configurations and exemplifies the kinetic mechanisms, which activate the integrated hysteretic device to dissipate most part of the input seismic energy. The systems' configuration designs are developed and the construction design of the connections is presented.

Chapter 5 presents the SDOF-model used in the analytical simulations. The selection of international seismic input records is shown. The chapter concludes with the predominant

mechanical properties of the hysteretic damper as they result from respective sensitivity analyses, while the range of population to capture the important features of the controlled systems is presented.

Chapter 6 outlines the results of the dynamic responses of all four ADCS configurations under the international seismic input records. It emphasizes ADCS potential for maximum energy dissipation for each configuration, as well as different mechanical characteristics of the integrated damper. The resulting systems' performance in terms of base shear and relative displacements is emphasized. Provided in this chapter are also the optimization studies' results for the selection of the optimum design parameters for each configuration.

Chapter 7 concentrates on the results for the optimum design parameters, as far as the dynamic responses of three configurations of ADCS, subjected to ten records of seismic events of the Mediterranean region, are concerned. The potentials for promising dynamic responses by ADCS are verified in terms of energy dissipation, base shear and relative displacements of the controlled systems.

Chapter 8 addresses the conclusions of the current study.

CHAPTER 2 DUAL STATIC SYSTEMS

2.1 Dual Static Systems Characteristics

Dual static systems are defined through the linkage of two different component systems that are combined to resist forces by developing a specific mechanical behavior due to their different resisting nature ([2.1]). In principle, the dual systems' behavior depends on the parallel superposition of a primary frame and a secondary system, suspension or strengthening system, to the frame's linear members ([2.5]). Dual static frames employ cables to support the primary members as external supports and to create a unified reaction under both mechanical- (flow of forces and form of deflections) and visual considerations ([2.3]).

The principles of dual static systems behavior may be clarified through analytical investigations of differing configurations ([2.2]). The case examples presented in this chapter, contribute to the general field of architectural vision towards structural innovation through the design of structures ([2.4]). The following dual static systems' behavior is approached based on uniform vertical loading, whereas the weight of the primary frame is assumed to be adequate to counteract the uplift due to wind pressure. The cables' configuration follows in principle the moment diagram shape and aims at achieving an improved distribution of the internal stresses of the primary members. The design approach follows some basic assumptions: the tensile stays are inextensible, the primary beam is hinge-connected to the columns, the columns' bases are hinge-supported and the columns are enhanced to carry axial forces instead of bending moments. Optimization involves the reduction of the beam moments to a minimum, while a significant amount of load is carried by the beam in axial action. The dual system is internally indeterminate due to the elastic cables or the rods supports.

Different configurations of dual systems with hinge-connected primary members have been investigated in their static behavior under uniform vertical loading and compared to

the respective portal frame of the same geometrical characteristics of column height and beam length.

2.2 Primary Frames

The primary frames that are used for comparison purposes differ in their configuration as regards their supports and connection design. Three primary frames are defined: the fixed-supported, moment-resisting or rigidly-connected frame, the fixed-supported, hinge-connected frame and the hinge-supported, rigidly-connected frame (Figure 2.1).

The internal stresses developed in each of the three primary frames are discussed. In the fixed-supported, hinge-connected frame, the beam develops shear and bending moment, i.e. flexural resistance, while the columns contribute to the axial resistance only and they do not deflect due to their idealized hinge connection with the beam, since they do not have to carry shear forces or bending moments. The fixed-supported, rigidly-connected frame resists the external vertical loading by developing bending moments and shear forces in the beam and the columns, as a result of the rigid connections and therefore the transfer of the respective internal forces. The bending moments at the beam's midpoint decrease by approximately 45 %, since the frame's rigid joints are able to attract bending at the beam's ends. Therefore the moment-resisting primary frame, i.e. with rigidly-connected joints, develops reduced moments in the beam that has to resist 55 % at the field and 45 % at the joints of the respective maximum moment of the simply supported beam, whereas the hinge-supported beam, 64 % at the field and 40 % at the joints.

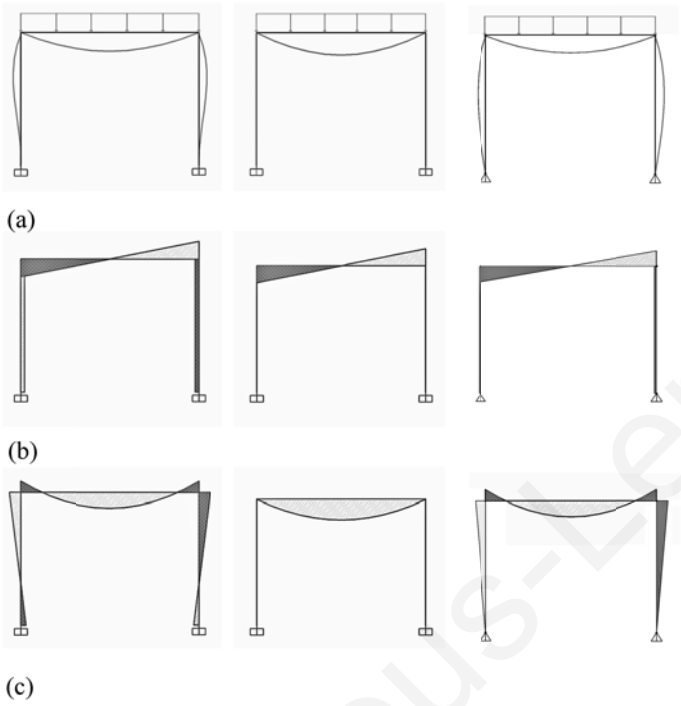

Figure 2.1 Primary frames under uniform vertical load: (a) models and deformed shapes; (b) shear forces; (c) bending moments.

2.3 Dual Static Frames with Stayed Cables

Dual static systems with stayed cables use intermediate supports through connection of the beam with tensile members from above (Figure 2.2), (Figure 2.3), (Figure 2.4). For the purpose of a preliminary structural analysis it is assumed that the stays give a quasi rigid support to the beam. The axial compression forces in the columns are obtained by balancing the forces at the top joint of the columns and stays. The tensile ties are anchored directly to the ground.

In the first example, the beam is supported by stayed cables that are arranged at 45^{o}, i.e. the back stay slope is the same as the main stay slope following a symmetrical configuration, to support the beam at a distance of 0.21L, where L is the length of the beam from column to column (Figure 2.2). The continuous beam is hinged to the columns that extend by 0.21L on top of the beam. Under uniform gravity load action, pure axial

compression is developed in the beam at a level of 2/3 of the equivalent force for the applied external load, although there is no force in the central span of the beam between the inner stays. The inner stays are subjected to maximum tension at the level of 70.37 % of the equivalent force for the applied external load. The flexure resistance is compared with that of the fixed-supported hinge-connected primary frame. The bending moment in the field at midpoint is reduced significantly, i.e. by 84.30 %, whereas at the points of the beam where the supporting stays are connected, the bending moment is reduced by 82.98 %. The maximum deflection at midpoint is 0.086L. Compared to the compression in the columns of the primary frame, the dual frame's columns have to resist 49.46 % more compression.

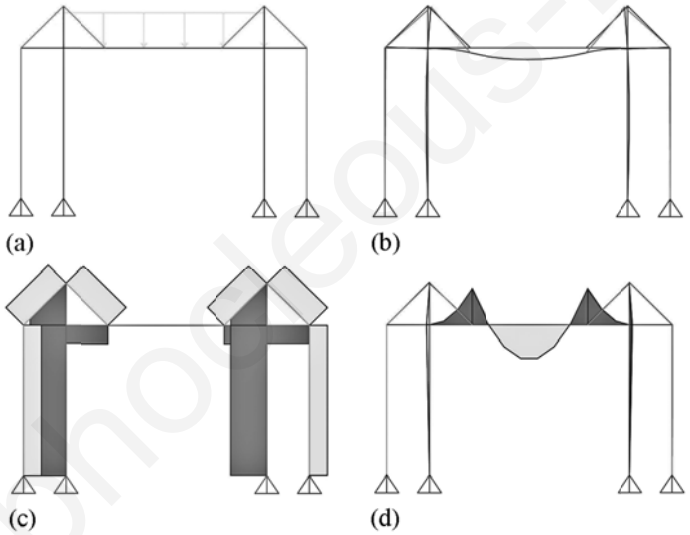

Figure 2.2 System with stayed cables: (a) model; (b) deformed shape; (c) axial forces; (d) bending moments.

In the dual static system with stayed cables and a single under-strut resting on cables, the tensile ties are guided back diagonally to the supports, so that they can resist also lateral forces, while in the center portion the cables continue below the beam and give support from below through a single strut at midpoint resting on diagonal cables underneath (Figure 2.3). Horizontal reaction forces are generated by the uniform vertical

load (e.g. an axial compression force in the beam between the columns across the entire length). In this case the added members support the beam at quarter spans following a symmetrical configuration. The columns extend by 0.25L above the beam. The beam carries a maximum compression force of 43.81 % compared to the assigned uniform load and the cables, a maximum tension of 37.16 % of the applied load. The static behavior is compared with that of the hinge-supported, rigidly-connected frame for the whole free length of the beam, i.e. column to column. The maximum compression for the columns is increased compared to the portal frame by 36.46 %. The deflection of the system accounts to 0.016L. Compared to the bending moment of the primary frame at midpoint in the field of the hinged beam, the maximum moment is spread at the four fields resulting to a maximum decrease of 95.49 %, which develops at the edge-field, and of 96.00 % at the edge supports.

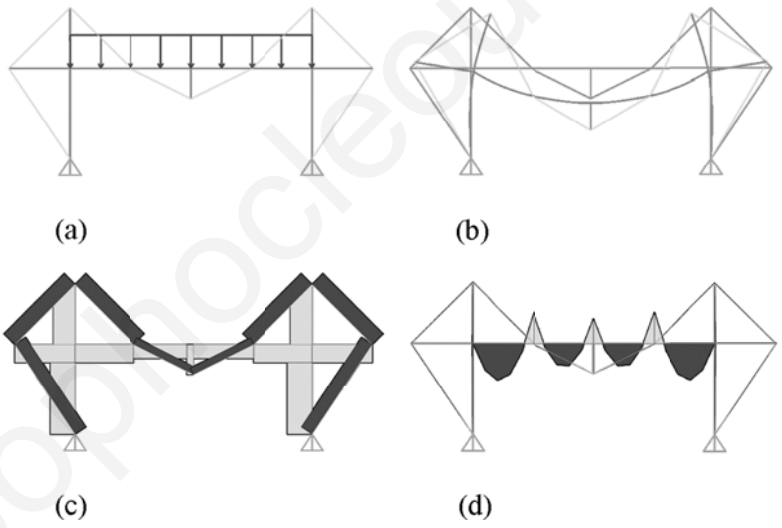

Figure 2.3 System with stayed cables and single under strut: (a) model; (b) deformed shape; (c) axial forces; (d) bending moments.

2.4 Dual Static Frame with Suspended Cables

In dual static frames with suspended cables the more rigid beam stabilizes the flexible tension members, i.e. suspended cables. The cables support the beam from above (Figure 2.4).

Vertical ties are connected with the suspended system at quarter spans of the beam's length. The columns extend by 0.6L above the beam, while the suspension cables are laterally tied at the ground at 0.625L, where L is the beam's span distance. The configuration results to zero requirements for the beam to carry any compression. The resolving axial force due to the applied load distributed along the beam is resisted by the suspended cables that develop maximum tension at the edged inner stays at the level of 45.42 % of the applied load's equivalent force. The static resistance to bending is compared with that of the fixed-supported, hinge-connected primary frame. Compared to the bending moment at midpoint of the respective primary frame, the beam is subjected to a significantly reduced moment of 6.00 % at the edge supports and 4.00 % at the edge fields of the respective frame's moment's magnitude. Conversely the compression of the columns increases to 181.00 %.

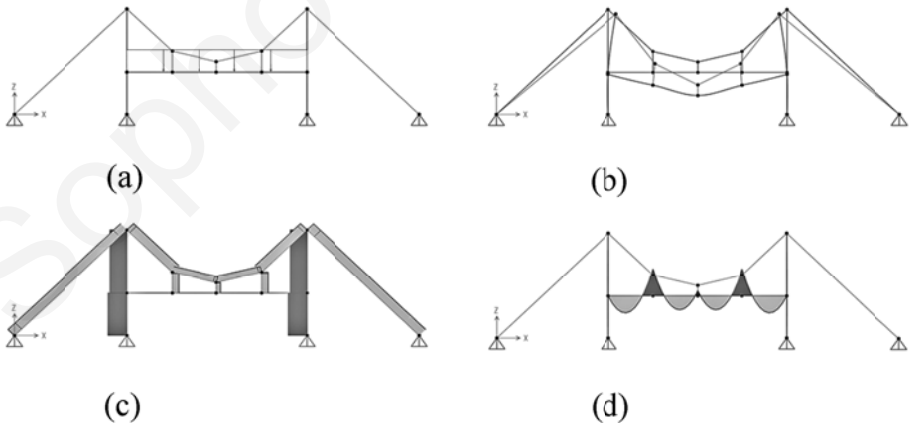

Figure 2.4 System with suspended cables: (a) model; b) deformed shape; (c) axial forces; (d) bending moments.

2.5 Sub-Tensioned Dual Static Frames with Struts

Sub-tensioned, dual static frames with struts give support to the frame from below, in contrary to conventional cable stayed structures giving support from above. They consist of a continuous beam, which functions in bending and a suspension system, i.e. the cables with compression struts, supporting the beam from below. They form truss-like systems with compression members as top chords, tension cables as bottom chords and compression struts as web members. The beam is compressed, the cables are under tension and the struts resist in less compression than the beam. There is a considerable effect of the secondary system's stiffness on the moment distribution of the beam. The configuration design may involve a single strut and a multi-strut cable supported beam (Figure 2.5), (Figure 2.6), (Figure 2.7). The behavior of the systems is compared with that of a fixed-supported, hinge-connected primary frame.

The sub-tensioned, two-strut system's behavior follows the principles of this type of systems (Figure 2.5). The two-strut cable-supported frame may succeed in minimizing the bending moment at midpoint of the beam of the respective frame, to 22.67 % at the field and 13.00 % at each point, where each strut supports the beam. The compression carried by the struts accounts to 48.15 % of the equivalent force to the applied load, and by the beam, to 95.64 %. All cables are stretched to the maximum carrying a tension of 96.12 % of the reference load equivalent force.

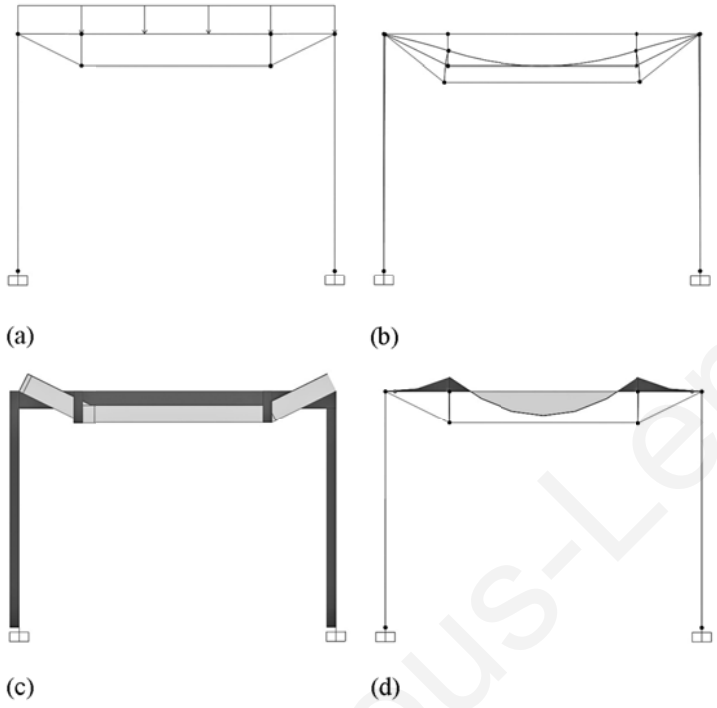

Figure 2.5 Sub-tensioned, two-strut system: (a) model; (b) deformed shape; (c) axial forces; (d) bending moments.

The sub-tensioned triple strut system is examined in (Figure 2.6). The effect of the support settlement is indicated when it is compared with the behavior of the primary frame: the tension in the two diagonal cables is equal to 157.00 % of the equivalent force for the load assigned; the compression in the beam is equal to 154.00 % while the center strut compresses up to 60.80 % of the same force. The bending moments are spread at the fields and supports that are formed through the configuration. The system enables up to 85.55 % moment decrease at the fields and 77.84 % at the middle support indicating the beneficial use of the added members.

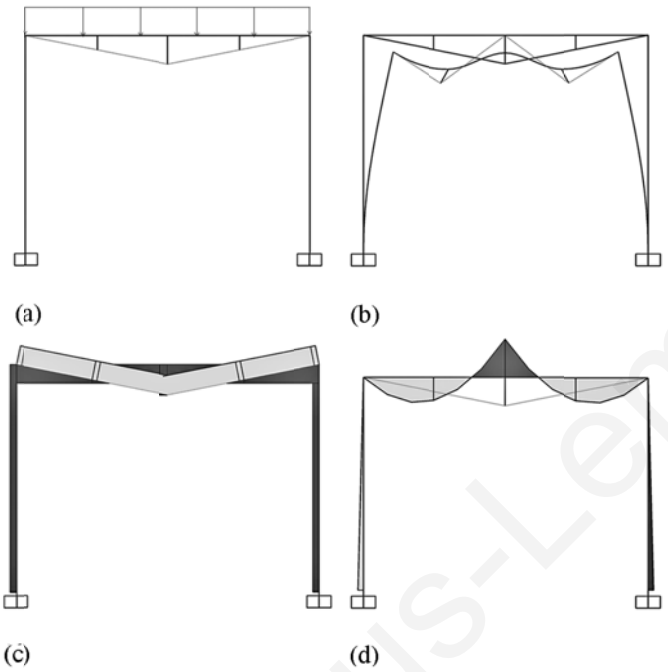

Figure 2.6 Sub-tensioned, triple-strut system: (a) model; (b) deformed shape; (c) axial forces; (d) bending moments.

The cables of the suspension system may follow a cross configuration. The beam is then supported by two struts underneath, which are connected with crossing cables at the center part (Figure 2.7). The columns height equals to 73.33% of the beam's length. Compared to the single beam of the respective primary frame, the bending moment in the dual system spreads in the three fields created by the supporting struts and reduces significantly up to 89.69 % in the edge fields. The beam has to resist in compression an equivalent force of 94.34 % of the applied load, whereas the cables are tensioned at a maximum force of 1.72 times of the assigned load's equivalent. The columns resist approximately the same level of compression, whereas a bending moment is generated at their fixed base, which accounts to 42.13 % of the respective maximum bending moment of the primary frame.

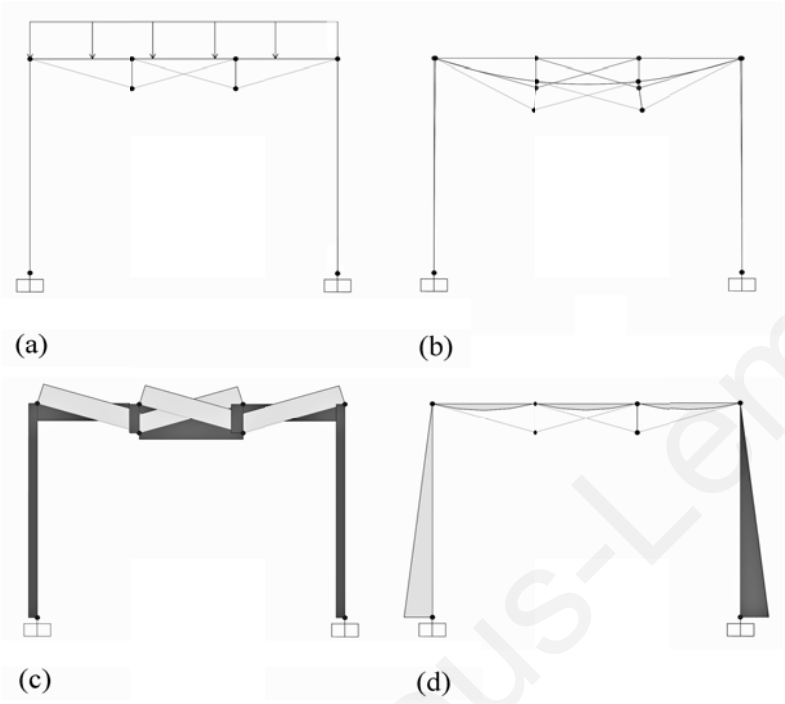

Figure 2.7 Sub-tensioned two-strut cross system: (a) load; (b) deformed shape; (c) axial forces; (d) bending moments.

We may conclude that it is possible to assign different functions to the composed systems of a dual frame. The continuous beam may be assigned to resist in reduced bending and the suspension system, i.e. cables and struts, to resist in axial manner and succeed in an effective distribution of moments, since the beam acts also as the top chord of the suspension system. The systems examined may be dimensioned to indicate the examples of application as described in (Table 2.1).

Table 2.1 Sections of primary frame and dual frame composed members.

System	Primary frame's beam	Dual frame's beam	Cables	Strut	Load: vertical, distributed	Length
	*	*	[D],(cm)	[D],(cm); [t],(mm)	(kN/m)	(m)
System with stayed cables	IPE600	IPE270	2.87	D=21.30, t=3.20	200	6
System with stayed cables and single under strut	IPB450	IPE220	5.00	D=7.30, t=14.00	100	12
System with suspended cables	IPB900	IPE360	5.08	D=5.08	50	24.38
Sub-tensioned two-strut system	IPE450	IPE240	2.00	D=3.34, t=3.37	100	6
Sub-tensioned triple-strut system	IPE600	IPE330	2.87	D=48.30, t=5.00	200	6
Sub-tensioned two-strut cross system	IPE600	IPE270	2.00	D=3.34, t=3.37	200	6

*DIN 1025 St 37-2, IPB: EURONORM 53-62 (HE-B); IPE: EURONORM 19

2.6 General Remarks

Improvements of the moment resisting frames involve alternative configurations with the addition of secondary members to compose dual systems. By adding cables and struts within the primary frame the following benefits in the static behavior of the systems may be achieved:

- The resistance primarily in tension and/or compression rather than bending reduces the requirement of self-weight, thus taking into account the construction process. The supporting frames are hinged rather than rigid or trussed and are laterally stabilized by diagonal bracing, while the site connections may generally be hinged.

- Members are hinge-connected to ease the construction standardization, while the attempt for the structural design optimization is for all members to be stressed at

their maximum to succeed in economy of the material as well.

- The design configurations are attractive in their simplicity and minimal proportions for the level of their free spans, whereas alterations of the basic forms of the systems may easily adjust to a broader range of requirements (e.g. by adding more struts or more stays to cover longer spans).

- The level of internal redundancy that upgrades due to the added members is effectively used as a second line of defense in the cases of local loss of strength or stability, of having to resist loads other than the design loads and of bracing the structure against lateral action.

- The assembly parts are clearly identified, i.e. rigid members, connections and tension hangers and diagonals, whereas particularly important are the details of the members' connections.

In general, the dual systems' design enables the creative synergy of the two component systems to result in an overall improved behavior considering stability, (since lack of bending stiffness makes them vulnerable to fluttering), resolution of bending to axial forces and best possible distribution of forces by activating all members to maximize their potential use in the static response.

On the other hand, dynamic loads may initiate vibrations and loads larger than the comparative static ones. The inquiry of the effectiveness of the dual nature of frame systems in resisting dynamic loads needs to be further investigated and developed. There are both a great concern and an interesting challenge in investigating new proposals, which may integrate inventive engineering technology and the process of construction into architectural design concerned with the logic of the structure.

CHAPTER 3 PASSIVE STRUCTURAL CONTROL

Conventionally, structures have been designed to resist natural hazards through a combination of strength, deformability (e.g. ductility) and energy absorption (e.g. damping). Structures may deform well beyond their elastic limit in severe earthquakes. Such a deformation behavior results in increased flexibility and energy absorption. Unfortunately this is directly associated with local damages to the structure.

3.1 Passive Structural Control

To ensure structural safety in strong earthquakes the integration of nonlinear elements in the structures, with enhanced energy dissipation capabilities has proven to be an effective control alternative ([3.13]). The structural performance can be improved, if a portion of the input energy is absorbed, not by the structure itself, but the supplemental device, i.e. passive structural control (Figure 3.1), ([3.33]). The term "control" denotes energy dissipation, whereas the term "passive", the fact that no external energy supply is required for the operability of the device ([3.34]). The energy dissipation devices are activated through the deformations of the primary system.

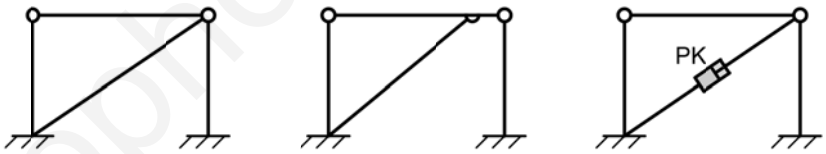

Figure 3.1 Passive structural control in frame structures.

Passive energy dissipation systems encompass a range of materials and devices for enhancing damping, stiffness and strength and can be used for both seismic hazard mitigation and rehabilitation of structures ([3.31]). In general, such systems are characterized by their capability to enhance energy dissipation in the structural systems, in which they are installed ([3.32]).

3.2 Damping Devices for Passive Seismic Control

A large number of passive control devices has been developed and installed in structures for performance enhancement under earthquake loads. Damping devices generally operate on the principles of deformation of viscoelastic materials, i.e. VE-solids, or fluids and fluid orificing, i.e. velocity or rate dependent dampers, or frictional sliding, or yielding of metals, i.e. hysteretic dampers ([3.12]).

Significant advances in research and development of viscoelastic materials, i.e. VE-dampers, particularly for seismic applications, have been made in recent years through analyses and experimental tests ([3.3]). Viscoelastic materials used in structural applications are usually copolymers or glassy substances that dissipate energy through shear deformation ([3.18]). A typical VE-damper consists of VE-layers bonded with steel plates ([3.29]). When mounted in a structure with chevron or diagonal bracing, shear deformation and hence energy dissipation takes place through the induced relative displacement between the outer steel flanges and the centre plates (Figure 3.2).

Viscoelastic dampers exhibit both elasticity and viscosity, i.e. they are displacement- and velocity-dependent. The elastic force is proportional to the displacement, the damping force, to the velocity and the total force is related to both displacement and velocity. For viscoelastic materials the behavior is typically presented in terms of stresses (τ) and strains (γ), rather than forces and displacements (Figure 3.3).

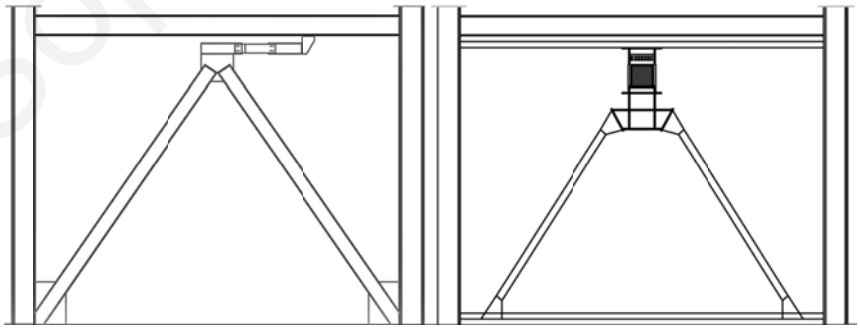

Figure 3.2 Viscoelastic dampers on chevron bracings.

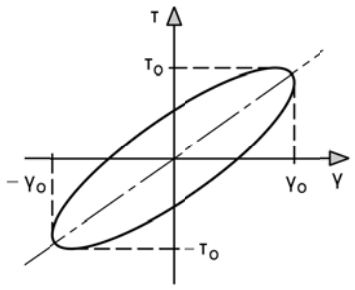

Figure 3.3 Hysteretic behavior of VE-damper.

The viscous fluids, i.e. VF-devices, developed recently include viscous walls and VF-dampers. The viscous wall consists of a plate moving in a thin steel case filled with VF. The VF-damper, widely used in military and aerospace industry for many years, has recently been adapted for structural applications in civil engineering. A VF-damper generally consists of a piston within a cylinder housing filled with a compound of silicone or similar type of oil. The piston may contain a number of small orifices through which the fluid may pass from one side of the element to the other ([3.5], [3.6]).

In recent years viscous fluid dampers have been incorporated into a large number of civil engineering structures following common bracings' configuration (Figure 3.4). In Japan, the most recent development for VE-dampers is the VE-walls, in which solid thermoplastic rubber sheets are usually sandwiched between steel plates. The term viscous fluid damper comes from the macroscopic behavior of the damper, which is essentially the same as an ideal viscous dashpot, i.e. the force output is directly related to the velocity, whereas the force-displacement diagram follows the elliptical shape (Figure 3.5).

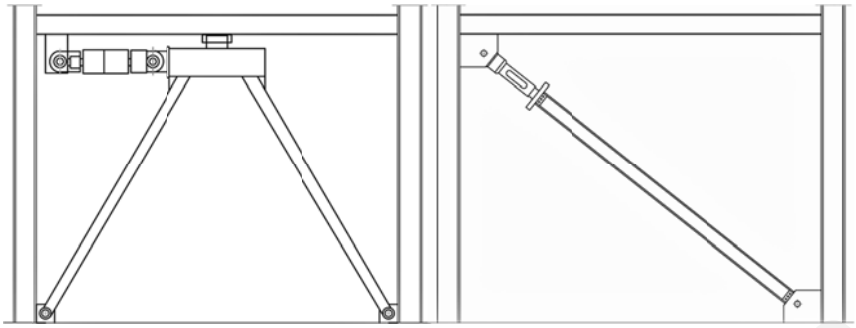

Figure 3.4 Viscous damper on chevron and diagonal bracing.

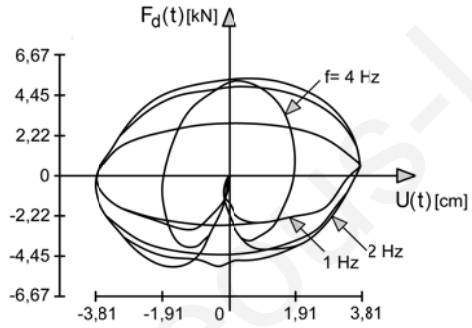

Figure 3.5 Hysteretic behavior of VF-damper ([3.6]).

In recent years, there have been a number of structural applications of friction dampers aiming at enhanced seismic protection of new and retrofitted structures. This activity is primarily associated with the use of Pall friction devices and slotted-bolted connections ([3.11], [3.25]). Friction dampers utilize the mechanism of solid friction that develops between two solid bodies sliding relative to one another, in order to provide the desired energy dissipation. Configurations of moment resisting frames with friction dampers involve commonly X- or diagonal- and sometimes chevron-bracing (Figure 3.6).

Several types of friction dampers have been developed for improving the seismic response of structures utilizing lining pads, Teflon and brass materials ([3.10], [3.40]). An example of such a device, the Pall cross-bracing friction damper, consists of a cross-bracing that connects in the center, to a rectangular damper. The damper is bolted to the cross-bracing. Under lateral load, the structural frame deforms and two of the braces are

subjected to tension, the other two, to compression. The kinetic system causes the rectangular damper to deform into a parallelogram dissipating energy at the bolted joints through sliding friction. During cyclic loading the mechanism enforces slippage in both tensile and compressive directions. Generally friction devices generate rectangular hysteretic loops indicating that significant energy can be dissipated beyond a certain force, per cycle of motion and that the cyclic behavior of friction dampers is ideal plastic (Figure 3.7).

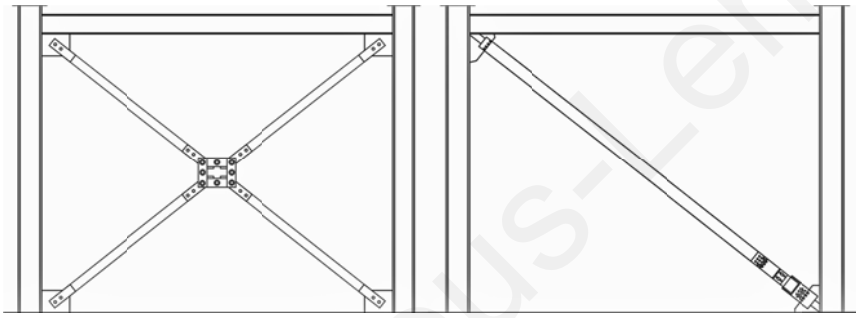

Figure 3.6 Friction dampers on cross and diagonal bracings.

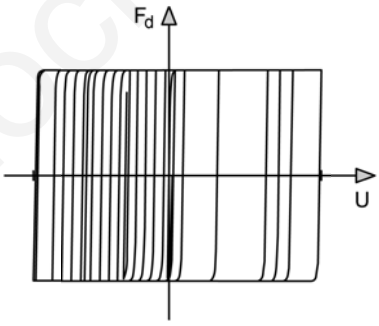

Figure 3.7 Hysteretic behavior of friction damper.

One of the most effective mechanisms for the dissipation of energy input to a structure from an earthquake may be achieved through inelastic deformation of metals. Many of these devices use mild steel plates with triangular or X-shapes, so that yielding is spread almost uniformly throughout the section's height. Other types of steel yielding devices, used mostly in Japan, include bending types of honeycomb and slit dampers and shear

panel types. Some particularly desirable features of these devices are their stable hysteretic behavior, low-cycle fatigue property, long term reliability and relative insensitivity to environmental temperature changes. A typical X-shaped plate damper or Added Damping and Stiffness device, i.e. ADAS was originally developed in the 1980's for retrofitting purposes ([3.8]). Usually ADAS and triangular shaped steel plate dampers, i.e. TADAS, are installed within chevron bracings (Figure 3.8).

Numerous analytical and experimental investigations have been conducted to determine the mechanical characteristics of individual devices ([3.35], [3.36]). The dynamic behavior was verified through experimental research studies ([3.39]). In the characteristic force-deformation diagram, the horizontal axis represents the ratio of lateral displacement to the height of the plates (Figure 3.9). The ADAS device exhibits increasing stiffness as the deformations increase. In the range of very large deformations, the respective increases become more significant ([3.41]).

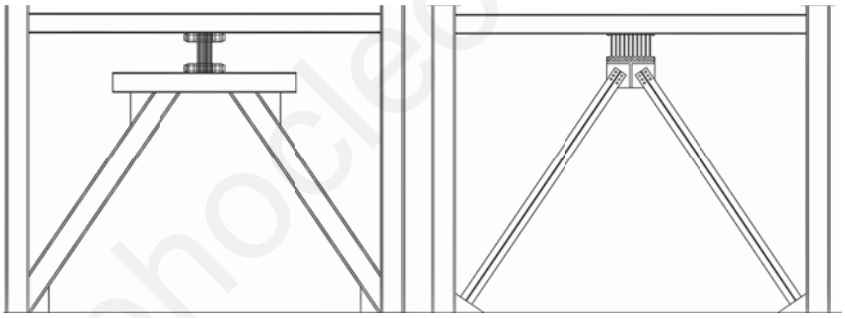

Figure 3.8 Metallic dampers on chevron bracings.

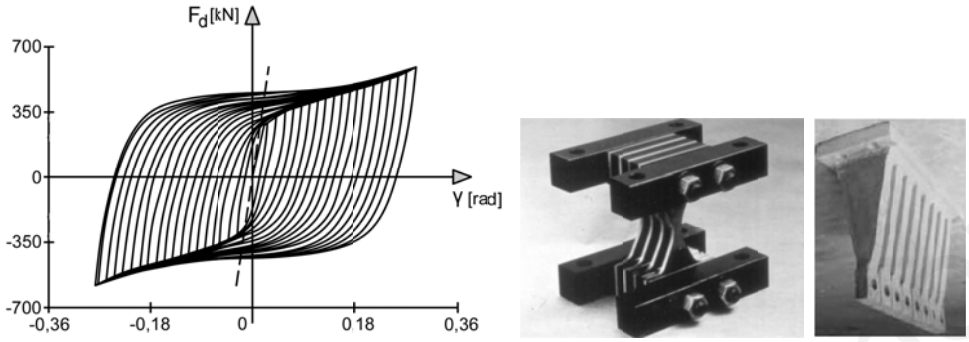

Figure 3.9 Hysteretic behavior of metallic dampers ([3.35]).

3.3 Kinetic Systems in Frame Structures

3.3.1 Eccentrically braced frames

Eccentrically braced frames, EBF, are alternatively proposed for earthquake resistance. The systems provide higher elastic stiffness than concentrically braced frames. The high ductility capacity of the system is achieved by transmitting the bracing members' force to another member, designated as "link", through shear and bending. The link is generally subjected to high shear forces at its entire length, to high bending moments at the end-points and low axial forces in the members ([3.27], [3.37]). The energy dissipation mechanism of EBF is applied following diagonal and chevron configurations (Figure 3.10).

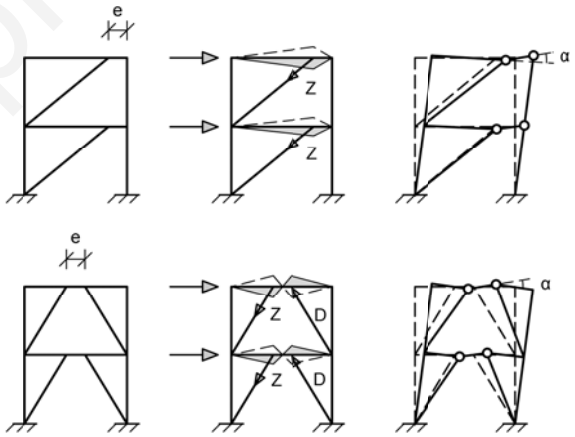

Figure 3.10 Eccentrically braced frames.

3.3.2 Buckling restraint bracing dampers

Buckling restraint bracing dampers are composed of yielding braces in tension and compression, also called unbonded braces or Buckling Restraint Bracings, BRB ([3.2]). The systems operate according to the metallic yielding principle ([3.15], [3.21], [3.38]). The unbounded braces are bracing members that consist of a steel plate core encased in a concrete-filled steel tube. A special coating is provided between the core plate and the concrete in order to reduce friction between the materials. The core steel plate provides a stable energy dissipation behavior by yielding under reversed axial loading, while the surrounding concrete-filled steel tube resists the compression by buckling. A typical bracing configuration for the BRB is shown in (Figure 3.11).

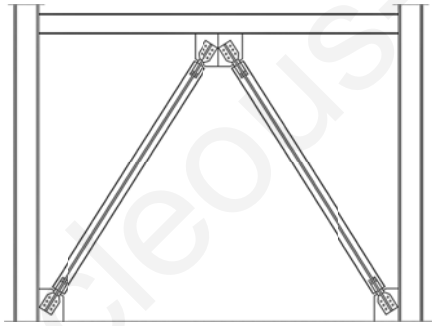

Figure 3.11 Buckling restraint bracing dampers.

3.3.3 Toggle and scissors-jack bracing configurations

Recently, the scissor-jack damper energy dissipation system and the toggle-brace-damper system configurations have been developed, in order to significantly enhance the performance of high energy dissipation using viscous fluid dampers.

The scissor-jack-damper system allows for an open space of the plane, due to its compact geometry and it is therefore architecturally desirable ([3.30]). It extends the utility of fluid viscous damping devices to structural systems that are characterized by small interstory drifts and velocities ([3.1]). The geometry of the brace and damper assembly is such that the system resembles a “jacking” mechanism (Figure 3.12).

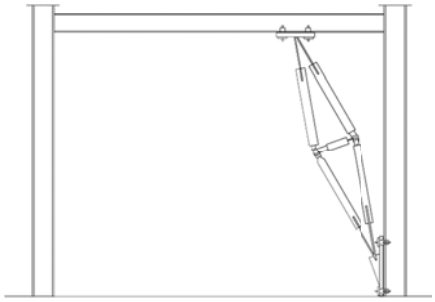

Figure 3.12 Scissor-jack system with viscous damper.

In a toggle-brace, fluid-filled dampers are employed in the frame attached on bracings that form an inverted T-shape ([3.7]). The axial displacement of the damper is amplified in respect to the lateral displacement by an Amplification Factor, AF. Such a system is not a good candidate for supplemental damping, when conventional diagonal or chevron brace configurations are used, due to the high cost of the damping system.

A toggle bracing may also be used with filled accordion metallic dampers, FAMD ([3.24]). The FAMD damper utilizes the capability of accordion thin-walled metallic tubes in buckling as a damping mechanism, which in turn increases the amount of energy absorption under axial cyclic loading. Low-density polymeric foams such as filler inside the energy absorption devices play a major role in terms of the stability of the FAMD tubular struts (Figure 3.13).

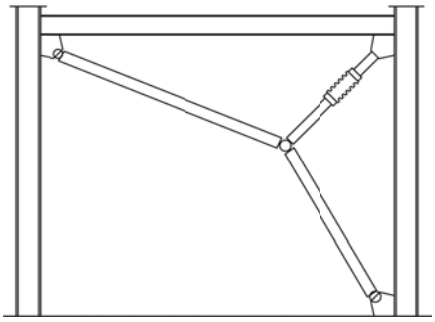

Figure 3.13 Toggle bracing with filled accordion metallic dampers.

Both systems utilize mechanisms to amplify displacements and accordingly lower force demands in the energy dissipation devices. The kinetic mechanism in turn amplifies the damper force through its shallow truss configuration and delivers it to the structural frame. Related experimental results indicate that displacement amplification factors in the range from two to five are quite practical.

3.4 Kinetic Systems with Tension-Only Members

Driven by certain advantages in architectural, aesthetic, constructability and economic context, the implementation of tension-only bracings with damping devices in frame structures may be realized through the development of suitable bracing-damper configurations, whereas all bracing members contribute during the entire load duration to the operation of the integrated damper. An optimization of the control system's operation principles for earthquake structural resistance may thus be achieved.

3.4.1 Tension-only bracings with friction dampers

The concept of tension-only bracings with friction dampers was initially followed with the Pall-Marsh friction mechanism using slender cross braces ([3.9], [3.25]). In principle the rectangular damper deforms into a parallelogram, dissipating energy at the bolted joints through sliding friction. The kinematics of the system prevents the diagonals to buckle in compression. With the completion of a loading cycle, the hysteresis loops are identical for all bracing members (Figure 3.14). The hysteretic loop of the friction damper at the cross centre follows the rectangular shape (Figure 3.15).

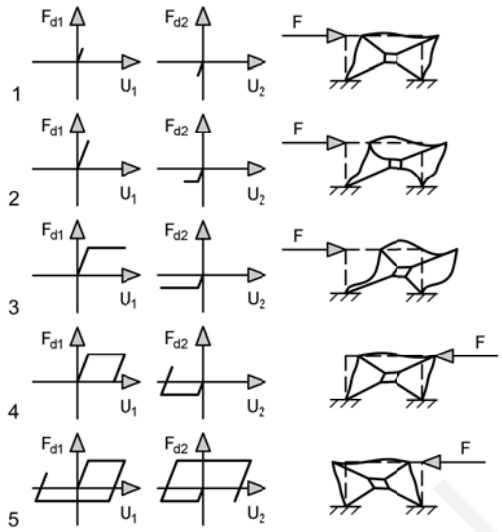

Figure 3.14 Kinematics of friction mechanism ([3.9]).

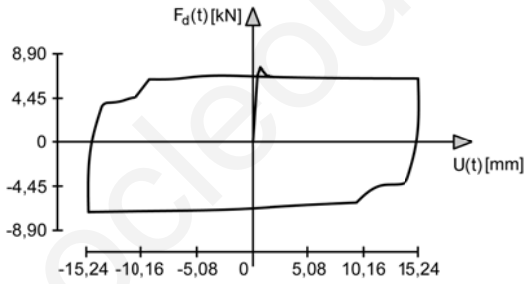

Figure 3.15 Hysteretic behavior of friction mechanism ([3.9]).

Alternatively a new damper, the rotational friction damper, which consists of two rigid plates, connected with a rotational hinge, was developed for tension-only bracings ([3.16], [3.22], [3.23]). The moment-rotation behavior in the hinge connection is elastic frictional. When the distance between the connection points changes, the angle in the hinge between the dampers changes also to adjust to new shapes. The damper dissipates energy when the elastic rotation limit is exceeded, i.e. if sliding occurs in the hinge. If another plate is connected within the viscoelastic rotational hinge between the sliding plates, then a friction-viscoelastic damper behavior is considered for energy dissipation. A special friction pad material between the damper plates in the frictional hinge is used. The

kinematics and hysteretic behavior of a rotational friction damper is shown in (Figure 3.16), (Figure 3.17).

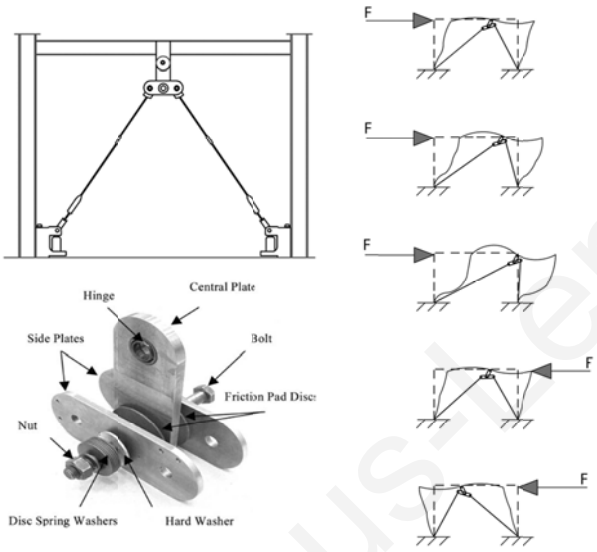

Figure 3.16 System and kinematics of rotational friction damper ([3.22]).

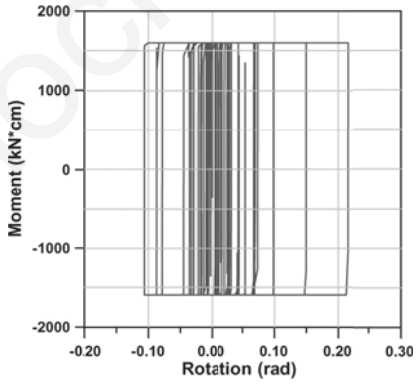

Figure 3.17 Hysteretic behavior of rotational friction damper ([3.23]).

3.4.2 Tension-only bracings with metallic dampers

Tension-only bracings with metallic dampers and cross braces configuration have been alternatively proposed in ([3.28]). The system's operation is based on the relative

displacements between the tension members, whereas hysteresis is achieved through optimization of the integrated metallic dampers plates' section. The cross braces with the articulated quadrilateral with steel dissipaters work only in tension, whereas energy dissipation develops through elasto-plastic flexure of the steel plates with varying depth (Figure 3.18). The hysteretic behavior has been identified in both experimental and analytical investigations (Figure 3.19).

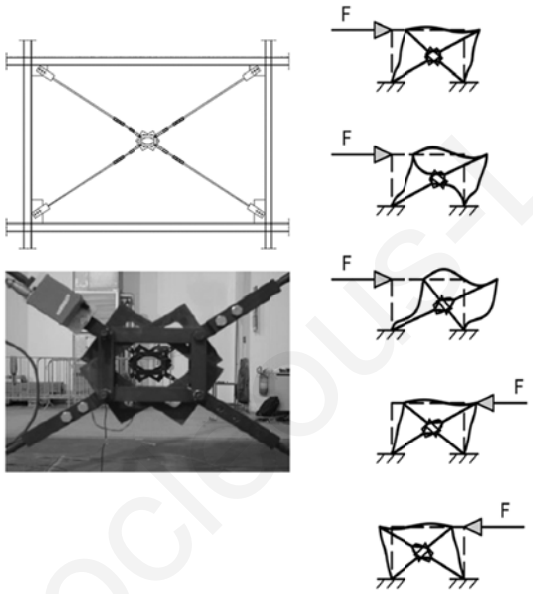

Figure 3.18 System and kinematics of light-weight dissipative bracing system ([3.28]).

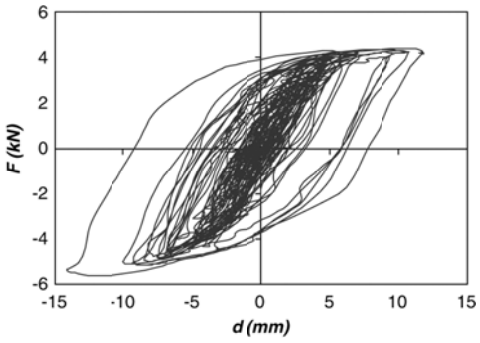

Figure 3.19 Hysteretic behavior of light-weight dissipative bracing system ([3.28]).

A similar cross cable bracing configuration has been proposed with a central energy dissipater consisting of two steel plates that are interconnected through a rotational spring ([3.17]). Under seismic excitation four cables in tension rotate the steel plates in opposite directions. The remaining cables, which connect across the shortened diagonal, are stressed elastically in compression and do not become slack, when the loading direction changes, due to the permanent rotation of the steel plates (Figure 3.20). The hysteretic behavior of the device has been identified analytically and the hysteretic loop follows an inclined rectangular shape (Figure 3.21).

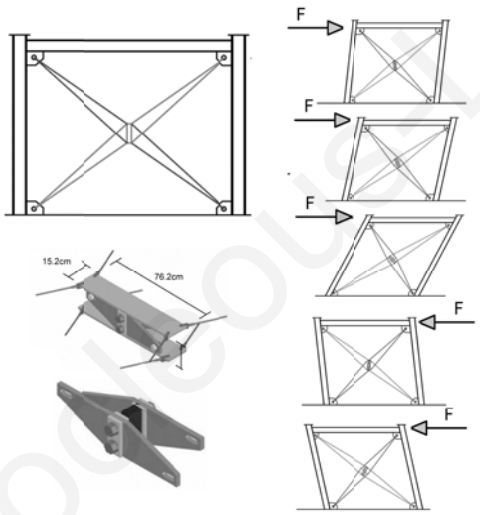

Figure 3.20 Kinematics of central energy dissipater ([3.17]).

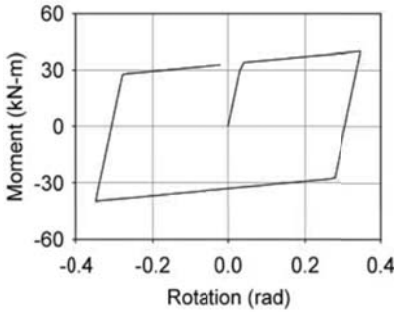

Figure 3.21 Hysteretic behavior of central energy dissipater ([3.17]).

3.5 General Remarks

The design of frame structures with additional control members for earthquake resistance refers primarily to the requirement for the primary systems to exhibit essentially a linear elastic behavior under seismic actions ([3.5]). A reduction of the energy dissipation demand on primary structural systems was successfully aimed at by a number of researchers through integration of damping devices, such as passive viscoelastic, viscous, friction and metallic yielding damping devices ([3.4]). In principle the damping devices are added in moment resisting frames attached on steel bracings that may be of accountable self-weight and stiffness ([3.14]).

The integration of energy dissipation systems to the structure results in a respective reduction of displacements and therefore, damage. Increases in force are also possible, when the energy dissipation system causes substantial increases in either the strength or stiffness of the frame. There exist ranges of the fundamental period of the controlled systems in which the damper is either ineffective or even detrimental.

The bracing components consist of steel members stressed in compression, tension and bending. The seismic control resistance of the bracings in braced frames weakens by the fact that under cyclic loading and in every half-loading cycle, the compression diagonal buckles and it therefore cannot participate in the energy dissipation process. On the other hand, a braced frame that consists only of cables or tension rods is often not suitable for earthquake resistance, due to the fact that the members become slack under their tension yielding and compression buckling.

While the energy dissipation system can achieve a considerable reduction in the systems' displacement response, it is often desirable to achieve, to a less degree, a reduction in the total forces exerted on the structure. Comparable reductions in displacements and forces of the primary system can be achieved with the development of dual systems that do not increase the strength or stiffness of the structure to which they are attached ([3.9], [3.17], [3.22], [3.23], [3.26], [3.28]).

Another related difficulty pertains to the negative impact of conventional bracing on the architectural aspects of the design ([3.19], [3.20]). Open bays are often preferred. In order to address this issue, while achieving the necessary prevention of damage through energy dissipation, alternative design configurations may be realized through the investigation of bracing mechanisms and hysteretic dampers.

CHAPTER 4 ADAPTABLE DUAL CONTROL SYSTEMS

The Adaptable Dual Control Systems, ADCS development focuses on the investigation of a new concept for structural passive seismic control that is based on a dual function of the system's components and the activation of a kinetic control mechanism. The conceptual principles followed in an original design introduced in ([4.12]) are reevaluated. New configurations that enable several important developments, i.e. the realization of improved designs, the numerical verification and the extension of the potential use of ADCS, are investigated.

The design and manufacture of the well known ADAS and TADAS mechanical metallic dampers support the development of the current investigation studies ([4.1], [4.2], [4.3], [4.5], [4.7], [4.21], [4.22], [4.23], [4.24]). In addition the SAP2000 software program is used for the analysis of the frame structures, which includes non-linear material properties, as well as real recorded earthquake ground motions for the evaluation of the structural performance ([4.4]). Finally the development of prestressed cables in structural engineering proposals encouraged their potential use as bracings in ADCS. Following the construction design of the control system's members, numerical dynamic response analyses are performed for representative seismic input records of differing frequency content. The research development contributes to the field of seismic design of moment resisting frames using seismic passive control methods that are characterized by minimal architectural impact ([4.6], [4.8], [4.9], [4.10], [4.11], [4.15]).

4.1 Systems Characteristics

ADCS performance is based on a dual function resulting from the effective synergy of its component members, which practically involves two uncoupled systems: the primary frame that consists of the columns and the beam, which is responsible for the static vertical and horizontal forces and the bracing-damper mechanism that consists of the bracing and the hysteretic damper, which is responsible for the earthquake forces and the necessary energy dissipation ([4.13][4.14][4.16][4.17][4.18][4.19][4.20]).

ADCS design enables the primary frame to respond elastically, while inelastic action due to the seismic event is handled by the hysteretic damper, which acts as a second line of protection against earthquake damage. In principle, the control concept is based on the achievement of predefined performance levels during the dynamic systems' response, through the development of deformation rather than stiffness. The ductility, i.e. ability of mild steel to dissipate energy through permanent and inelastic deformation, is used in ADCS design through integration of plate sections acting as hysteretic damper. A kinetic mechanism is activated in ADCS during the dynamic excitation by the horizontally induced motion at the base of the structure. In every half-loading cycle the respective displacement of the primary frame is followed by the connected bracing movement through rotations of the eccentric discs. The rotations result to respective axial displacements of the bracing at the connection joints, stretching the members. Since the bracing members form a kinetically closed circuit due to the configuration designs utilizing the discs, ideally the reactions on the primary frame are neutralized at the end of each cycle of movement and all members contribute to the energy dissipation mechanism. Therefore during strong ground motions, the relative displacements between the bracing and a member of the primary frame lead to yielding deformations of the damper. The kinetically closed circuit controls not only the axial displacements of the bracing, but also the relative displacements between the damper's joints, so that the energy dissipation is maximized.

4.2 ADCS Design Requirements

The optimization of the bracing-damper mechanism in all ADCS-configurations involves tuning between the stiffness, the yield force and the inelastic deformations of the hysteretic damper, so that the energy flow in terms of hysteresis by the damper and the elastic strain energy in the bracing and the primary frame is effectively managed during the earthquake induced motion.

In general, the triangulation of primary frames results in stiffness increase, which comprises an advantage in resisting wind loads and seismic loads of small amplitude. Nevertheless, such a stiffness increase is sometimes a disadvantage as regards strong

earthquakes due to the proportionally related increase in acceleration and base shear, which in some circumstances may lead to larger demands in strength upgrading and therefore larger sections for the members. Therefore the challenge of ADCS design is not only to define the effective relations between the stiffness of the members used and the load at which the damper yields but also to hold the response properties, i.e. the maximum base shear and the relative displacements of the controlled system in bounds with the respective responses of the primary system. The results of the investigation studies provide these characteristic properties in four configuration designs named after ADCS0, ADCS1, ADCS2 and ADCS3.

4.3 ADCS0 Design

4.3.1 General for ADCS0 design

The conceptual idea of ADCS0 was originally presented in a recent past study, whereas it was investigated under the simulated action of the El-Centro earthquake record. The study indicated the potential for future work of new proposals ([4.12]). The benefits of the control method are realized through the investigation as regards the performance of the original configuration under some new improved realizations. The configuration followed by ADCS0 is reevaluated for the effectiveness of its design with a different more suitable plate's section used, i.e. triangular steel plates instead of rectangular ones that were initially applied, and the controlled system's dynamic response behavior is further evaluated under the action of two additional international seismic records.

The areas of appropriate stiffness relations of the frame to the hysteretic damper and the braces when the energy dissipation of the entire system is controlled by the damper-bracing mechanism were deduced in the original study and are followed as initial estimations for the new ADCS developments.

4.3.2 Configuration design for ADCS0

ADCS0 configuration suggests a system of two cross braces and a horizontal one, which resist only in tension (Figure 4.1). The diagonals are fixed at the bottom of the columns and are capable to move at the top corners of the frame through rotations of the connecting eccentric discs. A hysteretic damper, connected between the frame and the horizontal cable member of the bracing mechanism prevents their free relative motion.

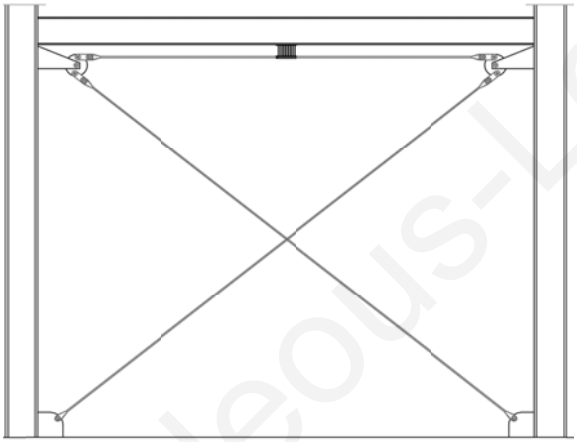

Figure 4.1 ADCS0 with cross bracing-damper mechanism.

4.3.3 Kinetic model of ADCS0

The kinetic model of the cross bracing-damper mechanism is exemplified in (Figure 4.2). The frame is laterally translating, the bracing members are kept straight and the hysteretic damper exhibits shear deformations. The increase in length of one cross-cable diagonal corresponds to the same length decrease of the other cross-cable diagonal, so that under cyclic loading both cross braces are permanently under tension. During the excitation, yielding deformations of the damper allow for relative motion between the bracing members and the frame. This comprises the source of energy dissipation since the damper plates are forced to yield in their inelastic region.

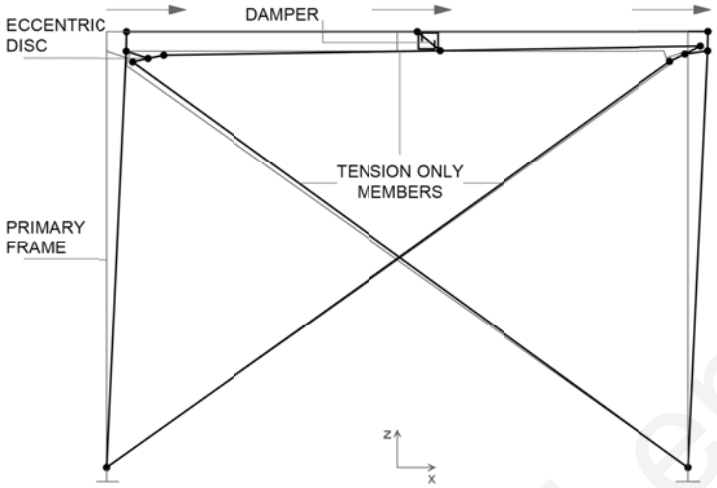

Figure 4.2 ADCS0 kinetic model.

4.3.4 Construction design of ADCS0

Construction design principles of ADCS0 refer to the use of rotating discs or slipping in saddle-shaped bearings. The mechanical rotating disc's principle of function is chosen to be followed in the new configuration designs primarily due to its benefits as regards its simplicity in construction and success in the transfer of movement without the possibly related significant losses due to friction in the saddle bearings.

4.4 ADCS1 Design

4.4.1 General for ADCS1 design

The configuration of a portal bracing for the controlled system is very attractive in its large architectural opening at the façade plane, in contrary to other configurations of braced frames, where for example the location of doors would almost be impossible to accommodate ([4.13], [4.14], [4.16]).

4.4.2 Configuration design of ADCS1

The bracing members of the proposed control system, ADCS1, are connected at the bottom of the columns and are free to move in the plane at the connecting joints of the frame (Figure 4.3). A hysteretic damper is placed between the beam and the horizontal bracing member to utilize this relative movement for energy dissipation purposes.

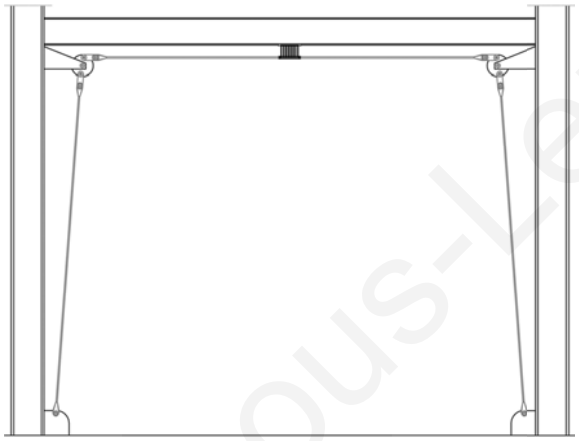

Figure 4.3 ADCS1 with portal bracing-damper mechanism.

4.4.3 Kinetic model of ADCS1

Large horizontal movements of the system at the base due to the seismic excitation activate the ADCS1 mechanism (Figure 4.4). In every half-loading cycle of excitation the eccentric discs rotate as a result of the lateral displacement of the frame. The movement is transferred through the disc to the horizontal and vertical connected bracing members. They result in stretching through development of tensile forces. The horizontal bracing's tension reacts to the shear force, which acts at one of the damper's joint. In this way all bracing members of the portal composition contribute to the energy dissipation of the damper. The damper deforms due to this shear force and dissipates energy in the form of heating due to inelastic yielding of the mild steel plates.

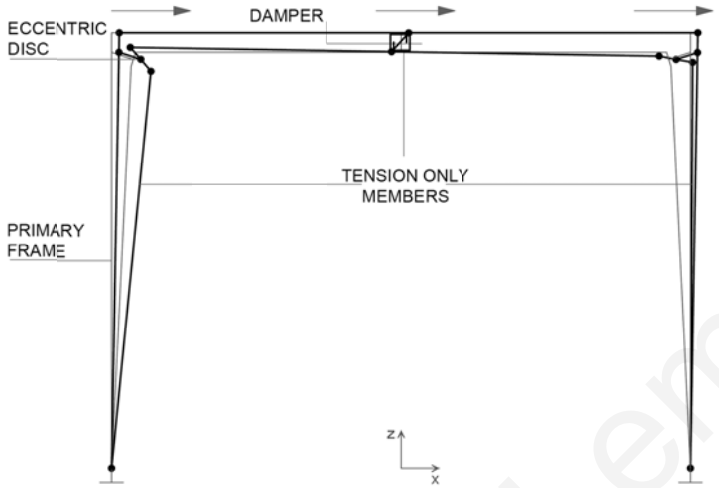

Figure 4.4 ADCS1 kinetic model.

4.4.4 Construction design of ADCS1

ADCS1 has the same number of joints as ADCS0, but the composed bracing members are the shortest possible to eliminate any buckling under compression as much as possible. Due to its high sensitivity in respect to out of plane deformations, the controlled system is assumed to comprise part of a complete 3D-structure, whereas the frame is expected to accommodate respective stability requirements through a rigid diaphragm in the perpendicular plane direction at the primary beam level.

The mechanical disc provides the anchor for the socket connection of the tension rods used for the bracing members in ADCS1. Both open and closed sockets are suitable for ADCS1's tension rods, which are fixed-fitted.

The hysteretic damper consists of a series of triangular shaped steel plates, which are welded on two horizontal gusset plates (Figure 4.5). The plate-dampers´ characteristic shape enables uniform deformation curvatures over the sections' height. Therefore all section lines reach their maximum yielding potential at the same time under the developed shear forces.

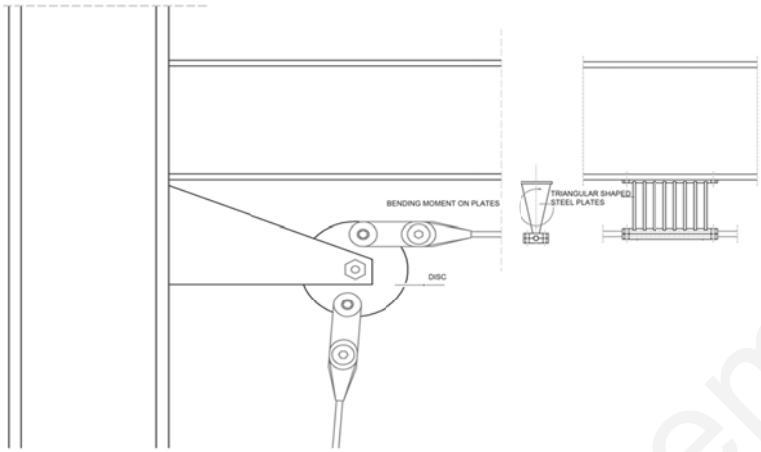

Figure 4.5 Connection principle of ADCS1 with rotating disc and hysteretic damper.

4.5 ADCS2 Design

4.5.1 General for ADCS2 design

In order to improve the performance through the activation of the bracing-damper mechanism in ADCS1 and maximize the seismic input energy dissipation potential through hysteresis of the damper, a chevron bracing is added to the portal bracing to form ADCS2 design ([4.13], [4.17], [4.19], [4.20]).

4.5.2 Configuration design of ADCS2

ADCS2 configuration design enables a more stable behavior of the controlled system for a larger population of changing design parameters, compared to ADCS1, primarily because of the use of diagonal bracings, i.e. chevron braces, additionally to the vertical and horizontal ones. The configuration design of ADCS2 still remains attractive for its available opening at the façade planes, although more joints are needed for the connecting elements to effectively transfer the movement internally and lead to the necessary energy dissipation (Figure 4.6).

All cable-braces of the proposed control system are hinge-connected through fixed cable fittings at the bottom of the columns and are free to move horizontally at the

connecting joints of the frame. The hysteretic damper is placed between the beam and the horizontal member of the portal cables. The latter are connected to the eccentric discs of the primary frame´s joints and the adjacent columns at the supports. An additional pair of chevron braces is connected to an eccentric disc at midpoint fixed at the lower horizontal connecting plate of the damper.

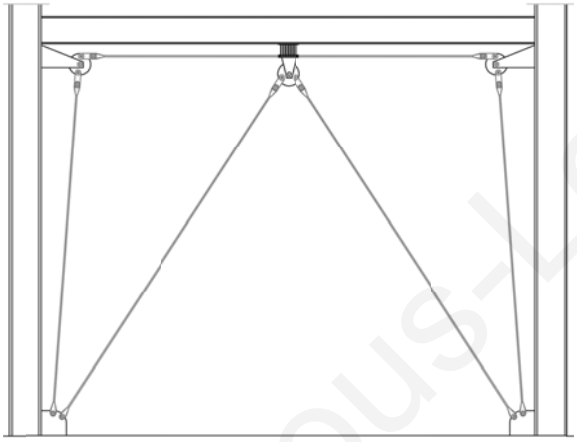

Figure 4.6 ADCS2 with portal and chevron bracing-damper mechanism.

4.5.3 Kinetic model of ADCS2

The portal bracing is primarily responsible for the relative displacements of the bracing to the primary system leading to deformations of the interconnected hysteretic damper, whereas the chevron bracing through its rotating action is responsible not only for further increase of the damper's deformations and in extend the resulting energy dissipation, but also for the decrease of the sensitivity of the control mechanism to the earthquake loading (Figure 4.7).

The hysteretic damper is positioned at the midpoint between the horizontal bracing member and the beam as in ADCS1 and ADCS0. The intention is to support the development of deformations due to shear action in the damper, which results from the lateral displacements of the primary frame at the beam's level and the resultant from both

the horizontal and inclined bracings' axial deformation, to reach maximum values. Thus, all members participate in the energy dissipation process.

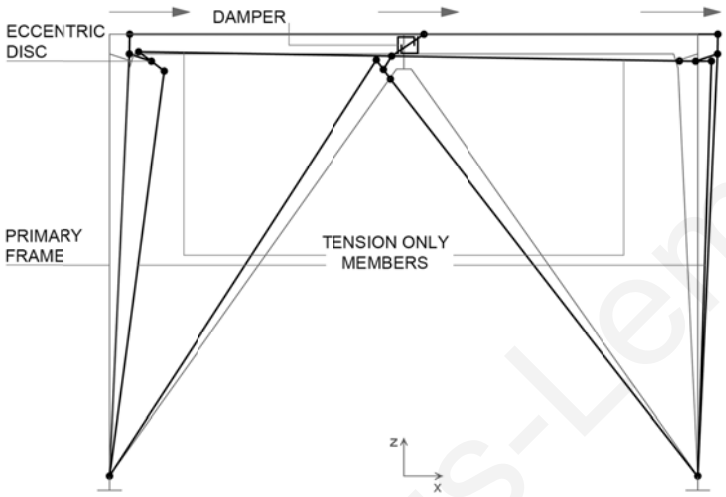

Figure 4.7 ADCS2 kinetic model.

4.5.4 Construction design of ADCS2

The number of joints in ADCS2 is larger than in ADCS1 and ADCS0, due to the added members, but the effective use of the diagonals' contribution is possible to balance this expense.

The benefits of the triangular section shape characteristics used in ADCS0 and ADCS1 are considered for the choice of the hysteretic damper in ADCS2 design and the same damper is chosen for uniform deformation curvatures and maximized yielding over the section's height. Also the use of mechanical discs is chosen for ADCS2 design, which utilizes an additional third device to connect the concurrent chevron with the horizontal bracing at the optimum place of the damper installation (Figure 4.8).

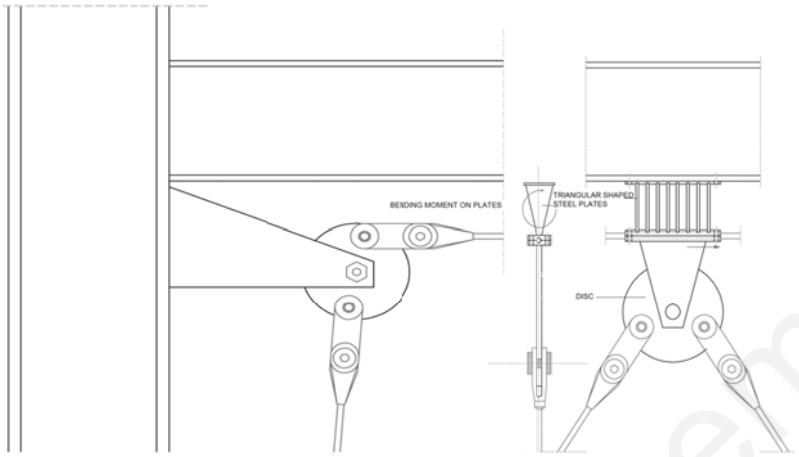

Figure 4.8 Connection principle of ADCS2 with rotating discs and hysteretic damper.

4.6 ADCS3 Design

4.6.1 General for ADCS3 design

In ADCS3 three secondary members are used to form a triangular kinetically closed configuration of the bracing system. The intention is to investigate the differences, when the damper utilizes the resultant from a horizontal, a vertical and a diagonal bracing member ([4.13], [4.14], [4.17], [4.21]).

4.6.2 Configuration design of ADCS3

The cables are connected at the bottom of the column and are free to move at both joints of the frame (Figure 4.9). At the frame's joint, on the side of the column base connection, the cables are interconnected through a rotating circular shaped disc. At the opposite frame's joint, they are connected through a rotating U-shaped disc that is linked to the frame's joint through a secondary diagonal cable. A hysteretic damper is placed perpendicularly, between the secondary bracing member and gusset plates that are welded to the column.

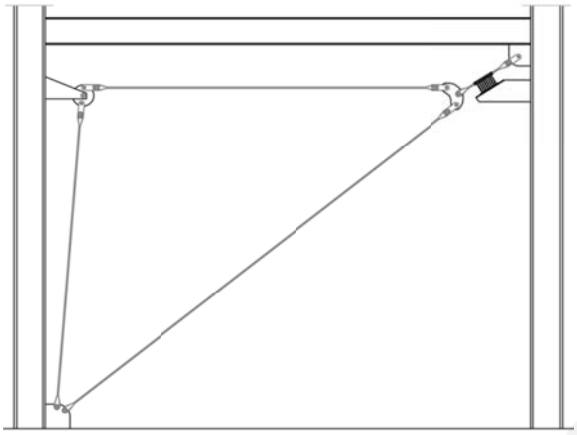

Figure 4.9 ADCS3 with diagonal bracing-damper mechanism.

4.6.3 Kinetic model of ADCS3

As in all ADCS, the kinetic mechanism in ADCS3 is initiated when the lateral displacement due to the seismic events at the base of the structure takes place (Figure 4.10). In every half-loading cycle the respective displacement of the primary frame is followed by the cables through rotations of the eccentric discs. For either sense of lateral displacement the discs rotate, stretching the members. Principally the bracing members form a kinetic closed circuit and therefore the reactions on the primary frame are neutralized and the members remain under tension. When the system moves to the opposite direction, one of the two connected cables goes into tension, while the other one tends to be subjected to compression. Due to the closed circuit arrangement, the tensioned cable stretches through the rotating disc the other one. In any case the rotating discs and the prestress of the cables ensure a smooth transition of forces in the tension-only members in each half-loading cycle change. Relative displacements between the secondary bracing member and the column lead to yielding deformations of the damper's steel plates for the necessary energy dissipation.

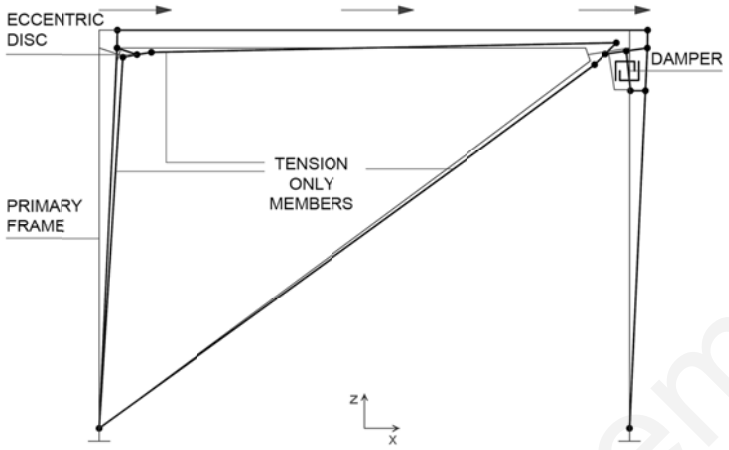

Figure 4.10 ADCS3 kinetic model.

4.6.4 Construction design of ADCS3

The construction principle with rotating discs is followed for the triangular configuration ADCS3 as well (Figure 4.11).

The hysteretic damper is placed perpendicularly, between the secondary bracing member and gusset plates that are welded to the column. In the case when cables are used in ADCS3, then they may end to sockets with threaded studs for customizing adjustments when prestress is to be introduced. The type of hysteretic damper-plates used is identical for all ADCS, since the benefits of uniformly distributed deformations over the sections' height proved to be very effective for the range of the present study.

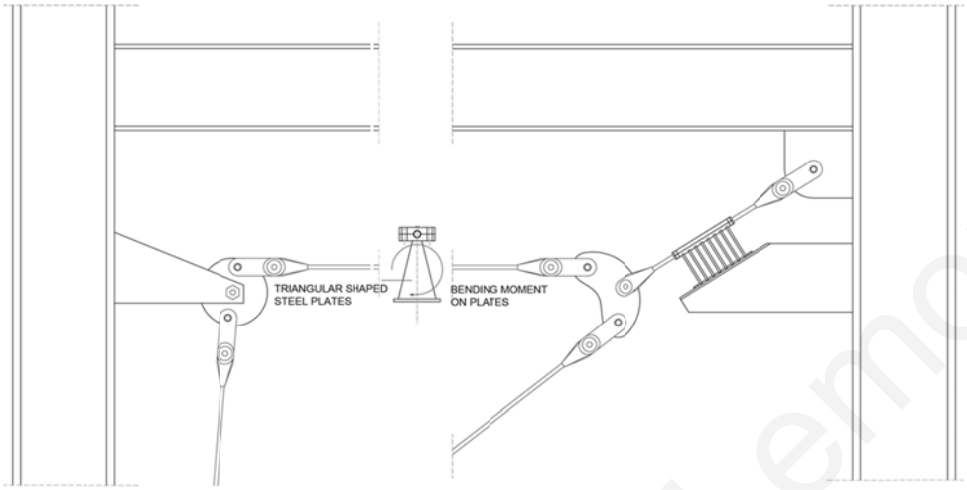

Figure 4.11 Connection principle of ADCS3 with rotating discs and hysteretic damper.

CHAPTER 5 ADCS MODELS AND MECHANICAL PROPERTIES

The Finite-Element analysis of ADCS relies on a simplified single-degree-of-freedom, SDOF, 2D-model, ([5.1], [5.3]). The resulting mechanical behavior of the systems is based on the following assumptions: the primary structural- and bracing members are designed to remain in the elastic region, while non-linearity is only addressed to the hysteretic damper ([5.10], [5.11], [5.12], [5.13], [5.14], [5.15], [5.16]). The software program SAP2000 was used for the evaluation of the dynamic behavior of the controlled SDOF system ([5.5]). The behavior examined is derived from the horizontal lateral displacement, being the single free movement of the controlled frame, and the response is compared with the primary frame's dynamic behavior.

5.1 Primary System

A typical geometry was assigned for the ideal 2D-model of a steel moment resisting frame of 6.0 m long beam and 4.5 m high column members. IPBl550 section was selected for the beam and IPBv500 for the columns ($S235$, E = 2.1x10^4 kN/cm^2, ρ = 78.5 kN/m^3). The dimensioning of the members fulfilled Eurocode 3 design requirements, for a static vertical load of 1200 kN, a horizontal wind load of 15 kN and 25 % of the vertical load as static equivalent seismic load. The primary frame's fundamental period results to T = 0.34 s and its stiffness to k = 41717.37 kN/m.

5.2 ADCS Model

The basic principles in modeling considerations followed in ADCS0 are adopted at first step in order to compare the resulting behavior of the new alternatives with the reference one ([5.9]). Though, for the purposes of the current study, i.e. preliminary investigation of the dynamic performance of all ADCS, the model of hysteresis of the damper is simulated based on the wen-plasticity model and the nature of tension-only bracings is captured. In ADCS1 design, tension rods are suggested, whereas for ADCS2 and ADCS3 cable

members may be used as bracings ([5.12], [5.14], [5.16]). The bracing elements in all ADCS design configurations were modeled as frame objects with zero compression limits. In addition, for avoiding any compression force in the cables, they are assigned a suitable pretension stress through a target force. The resulting maximum forces in the bracing under the seismic loadings of the analysis, considering the prestress load, enable the members' deformations to be kept within the elastic range. For the range of the developed stresses and strains in the bracing members the material's mechanical behavior is assumed to be linear.

The implementation of cable members in ADCS1 was avoided due to high prestress values that would be required for the members. In ADCS2 and ADCS3, the magnitude of the prestress target force is slightly higher than the maximum resulting force in the bracing when subjected under the selected seismic excitations. Each bracing of ADCS2 and ADCS3 was assigned a suitable prestress, identified through a trial and error procedure, at the level of 25 and 10 % of the maximum allowable stress of $f_{allowable}$ = 140 kN/cm^2, respectively. The members are kept straight and taut when they are deformed.

The rotating disc is modeled as a composition of three short-length frame objects, each assigned with suitably large stiffness values to represent the real property of a mechanical disc's shaft.

The hysteretic damper is modeled as a two joints non-linear link element, NLINK. The ideal model assumes that the stiffness coefficient of the hysteresis of the damper corresponds to the initial elastic values of the yielding element. The NLINK follows the wen-plasticity model of hysteresis.

5.3 Seismic Input Records

The primary frame and the controlled systems are evaluated in their dynamic behavior under the action of three selected international earthquakes (Table 5.1). The earthquake records represent "moderately long, extremely irregular motions", while the predominant periods of the selected ground motions range in their respective displacement response

spectra between 1.5 – 3.0 s ([5.3]). In the analysis no critical damping was considered for the model or the dynamic loading motions. The time history of their base acceleration due to the selected seismic records indicates the differences in frequency content, time duration and peak ground acceleration (Figure 5.1).

Table 5.1 International seismic input records.

Seismic case	Record	Station	Mw	PGA [g]	Duration [s]
A	El Centro 1940	Imperial valley, component 180	6.9	0.348	53.76
B	Kobe 1995	JMA, component 0	6.9	0.810	48.00
C	Northridge 1994	Olive view, component 90	6.7	0.604	30.00

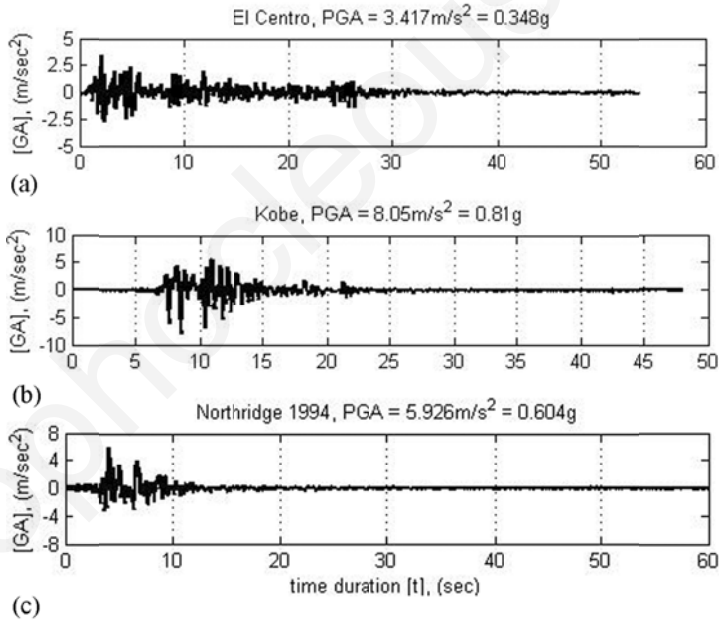

Figure 5.1 International seismic input records.

5.4 ADCS Mechanical Properties

5.4.1 General

Buildings incorporating hysteretic damping devices may be designed for an optimum strength and stiffness ratio of the hysteretic damper over the frame's respective properties, to provide significant measurements of seismic input energy dissipation ([5.2], [5.4], [5.7], [5.8], [5.20]). ADCS may result to significant energy dissipation for the selected earthquake cases of the analysis, provided that the geometrical and mechanical parameters of the hysteretic element are predefined accordingly. The hysteretic element selected in ADCS has been modeled and tested both analytically and experimentally by other researchers in the last years ([5.6], [5.18], [5.18]).

The hysteretic damper's force-deformation relationship that governs its behavior is considered through an independent spring hinge that connects the primary members, i.e. beam or column, with the added secondary members, i.e. slender tension elements. The internal deformation in the damper is the plastic deformation that causes the damper to dissipate energy through heating.

5.4.2 Mechanical properties of hysteretic damper

The seismic response of the controlled systems for the desirable level of seismic protection depends primarily on two main properties:

a. The effective values of the relative stiffness of the primary frame, the bracing and the hysteretic device at the target displacement that leads to the selection of the design elastic stiffness of the damper, k_d, given by the following Equation:

$$k_d = \frac{nEbt^3}{6h^3} \tag{5.1}$$

where h is the steel plate's height, b is the width (fixed to the beam or column), t is the -thickness and n is the number of steel plates ($S235$, E = 2.1x10^4 kN/cm^2, ρ =

78.5 kN/m^3).

b. The load, at which the damper yields and dissipates energy through its inelastic yielding deformation, P_y, given by the following Equation:

$$P_y = \frac{nf_y bt^2}{6h} \tag{5.2}$$

where f_y is the yield stress ($S235$, f_y = 24 kN/cm^2).

Hysteretic dampers may exhibit a bilinear or trilinear hysteresis, an elasto-plastic or rigid-plastic behavior. The analytical modeling of the damper's stiffness properties followed in the present study is based on the linear equivalent assumption (tangent stiffness model). The damper's force-deformation relationship, for the respective degree of freedom that corresponds to shear, is assumed to follow the hysteretic model defined as "wen-plasticity property type of uniaxial deformation" ([5.5]). The results are calculated based on this characteristic hysteresis model, which is mathematically described as follows:

$$f = ratio \cdot k \cdot d + (1 - ratio) \cdot yield \cdot z \tag{5.3}$$

where f is the force, d is the induced displacement, k is the elastic spring constant, i.e. initial stiffness, "yield" is the yield force, "ratio" is the specified ratio of the post-yield stiffness to the elastic stiffness, i.e. secondary stiffness ratio, and z is an internal hysteretic variable that evolves according to the following differential Equation:

$$\dot{z} = \frac{k}{yield} \begin{cases} \dot{d}\left(1 - |z|^{\exp}\right) & if\ \dot{d}\, z > 0 \\ \dot{d} & otherwise \end{cases} \tag{5.4}$$

where "exp" is an exponent greater than or equal to unity (practically about 20) and z is a path dependency parameter. SAP2000 provides the analytical model described in Equation (5.3), which represents the hysteretic behavior of the device.

During the dynamic motion, inertia forces are activated by all lumped masses, including the mass distributed on the rigid plates' section. The inertia forces contributed by the damper are expressed through the resistance to the angular acceleration. The related resistance is given as the integral of the "second moment" about an axis of all the elements of mass d_m, which compose the body of the steel plate used for added damping, MMI, as follows:

$$MMI = \rho \int r^2 dV \equiv RI \tag{5.5}$$

where MMI is the mass moment of inertia (RI in SAP2000 software), ρ is the density of the material used, V is the volume of the section shape and r is the perpendicular distance from the axis to the arbitrary element d_m.

The damper provides energy dissipation through its hysteretic behavior. A design parameter, the Damper Ratio, DR, that describes the response of ADCS as a function of the damper's stiffness and yield force, may be introduced as follows:

$$DR = \frac{k_d}{P_y} \tag{5.6}$$

By substituting Equations (5.1) and (5.2) in Equation (5.6), DR may be written in the following form:

$$DR = \frac{Et}{f_y h^2} \tag{5.7}$$

The controlled systems may be tuned to perform in such a way that a specific earthquake hazard protection level is reached. The performance level is possible to be predefined by the designer in quantifiable energy measures of deformation. Thus, ADCS may be designed for a target performance level. In the present study the performance index for structural safety is defined as Effective Energy Deformation Index, EEDI, which physically represents the amount (e.g. area) of input seismic energy dissipated by the hysteretic device over the entire seismic time duration.

5.4.3 ADCS mechanical properties investigation

Mechanical and geometrical properties for the investigation of ADCS vary in a wide range of values (Table 5.2). The respective values of the Damper Ratio vary between a minimum value of DR = 64.29 1/m and a maximum value of DR = 784.25 1/m for ADCS1, between a minimum value of DR = 84.22 1/m and a maximum value of DR = 481.3 1/m for ADCS2, whereas DR for the proposed ADCS3 varies between a minimum value of DR = 44 1/m and a maximum value of DR = 700 1/m. These ranges of DR values are considered adequate to clearly distinguish the trend and guide the selection of the respective characteristic value for the damper in each configuration design that leads to an optimum EEDI.

Table 5.2 ADCS's mechanical properties investigation values.

ADCS	Stiffness k_d [kN/m]	Yield force P_y [kN]	Number of plates n	Thickness t [cm]	Height h [cm]	Width b [cm]
ADCS1	423.18 – 15748	4.94 – 55.13	1 – 11	0.9 – 3.6	5 – 40	4 – 20
ADCS2	150 – 5250	1.75 – 17.5	2 – 6	1.0 – 2.4	20 – 40	5
ADCS3	112 – 24192	2.60 – 42.66	6 – 10	0.8 – 2.0	15 – 40	4 – 6

CHAPTER 6 **DYNAMIC RESPONSE**

The results from the numerical simulations and parametric studies presented in this chapter demonstrate the effects of the bracing-damper mechanisms within the dual systems for passive seismic control. In parallel to the investigation of the energy dissipated by the hysteretic damper over the seismic input energy, the related base shear and relative displacements of the controlled systems for different stiffness- and yield force values of the damper are further investigated ([6.6], [6.8], [6.10], [6.11]).

A number of numerical simulations have been conducted considering different combinations of assigned values of the parameters that govern the response of the ADCS proposals. ADCS1 was analytically investigated for 366, ADCS2 for 397 and ADCS3 for 342 cases, in order to identify the dynamic behavior of the three different configuration designs. The results from the simulations are presented to identify the energy dissipation over the seismic input energy through a defined ratio, as well as the maximum values of base shear and the relative displacements of the controlled systems ([6.5], [6.7], [6.9]).

6.1 ADCS0 Dynamic Response

6.1.1 General for ADCS0 design

The potentials of using the conceptual idea of the adaptable mechanisms in frame structures were indicated and the stiffness properties of the composed system's members are followed as initial estimations in the new ADCS designs ([6.4]). ADCS0 reference configuration is reevaluated following the new adjustments, which concern new sections of damper and additional seismic records ([6.6], [6.8]). The intention is to reevaluate and compare the dynamic responses with the ones of the alternative control configurations.

6.1.2 Energy dissipation results for ADCS0

ADCS0 inherits the suggested values of damper's stiffness of k_d = 3910 kN/m and yield force of P_y = 14.73 kN. These are derived for the present analysis by using ten triangular-shaped steel plates, instead of rectangular ones that have been originally considered, with t = 1.2 cm, h = 20 cm and b = 5 cm (damper: 1012205).

ADCS0 is implemented in the respective primary system and analyzed for its energy dissipation performance under the three international seismic loading cases (Figure 6.1). For the selected design value of a Damper Ratio of DR = 265.45 1/m, the respective energy dissipation accounts to 92.43 % in seismic case A and 90.61 % in case C. In seismic case B with highest peak ground acceleration the controlled system's effective energy deformation index, EEDI, remains comparatively poor with a value of 58.86 %.

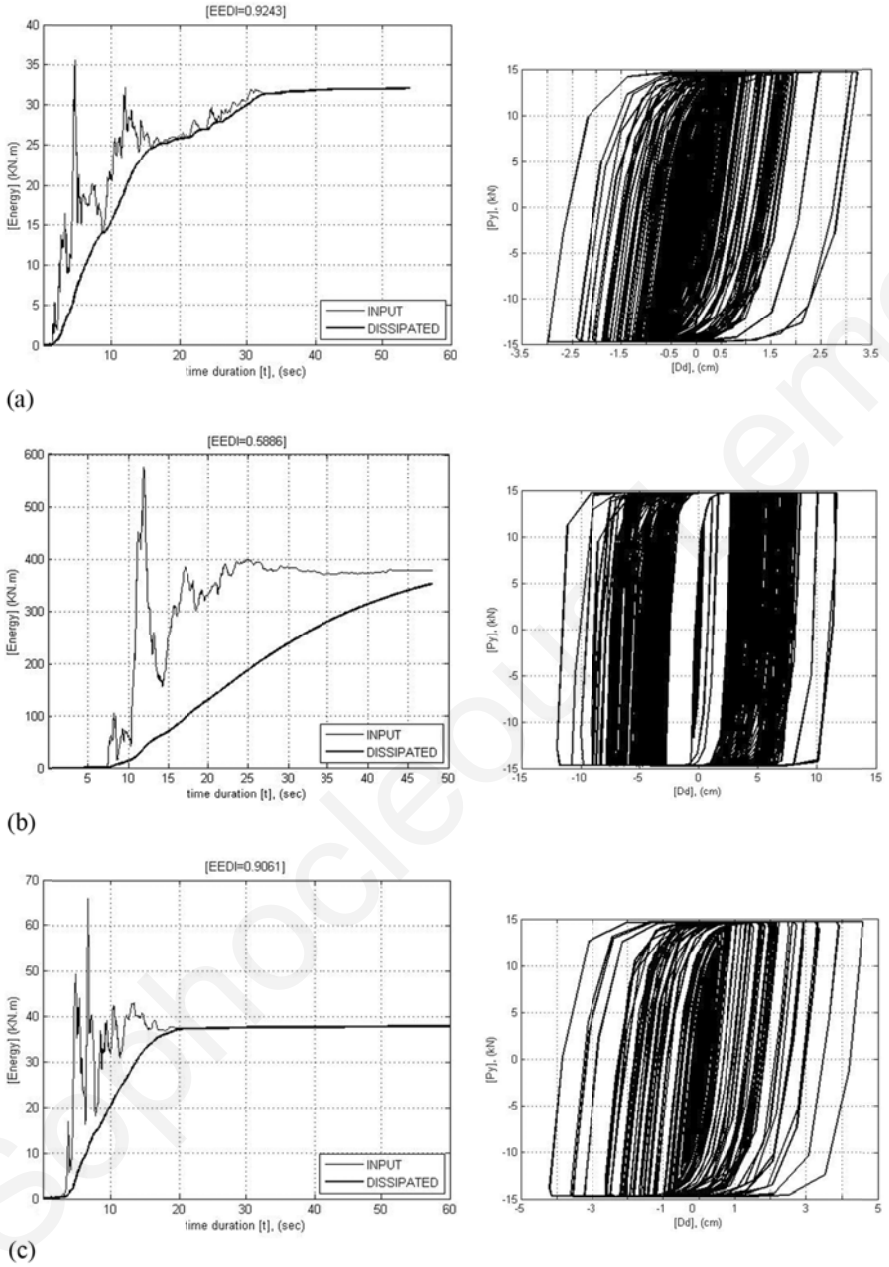

Figure 6.1 ADCS0 hysteretic damper's energy dissipation and force-deformation behavior (damper: 1012205): (a) seismic case A; (b) seismic case B; (c) seismic case C.

6.1.3 Base shear results for ADCS0

The maximum base shear of ADCS0 for a *DR* value of 265.45 1/m (damper: 1012205) compared to the primary frame's response, yields to a respective decrease of 23 % in seismic case A and 2 % in case C. In seismic case B the maximum base shear increases by almost 24 % (Table 6.1).

Table 6.1 Primary frame's and ADCS0 (damper: 1012205) maximum base shear BS and effective energy dissipation index EEDI.

Seismic case	Max. base shear [kN]		Effective energy dissipation index [%]
	Primary frame	ADCS1	
A	2102	1619	92.43
B	5570	6880	58.86
C	2304	2253	90.61

The time history response for the first 25 s of the primary frame's base shear to the controlled system's base shear is shown in (Figure 6.2).

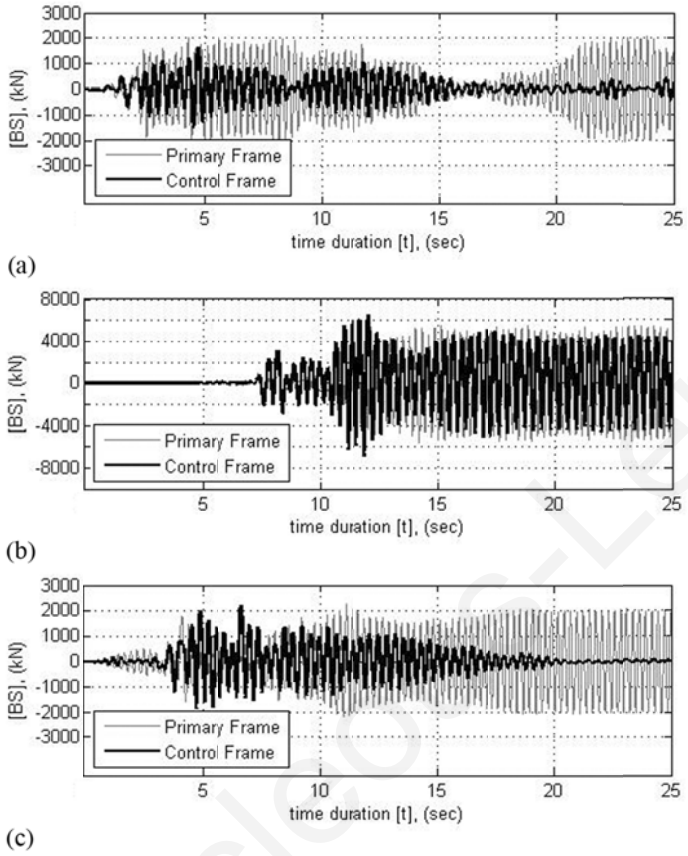

Figure 6.2 Primary frame's and ADCS0 base shear BS time history (damper: 1012205): (a) seismic case A; (b) seismic case B; (c) seismic case C.

6.1.4 Relative displacement results for ADCS0

In all seismic loading cases ADCS0 induces an increase of the maximum relative displacements compared to the primary frame's response. In particular, the increase accounts to 42 % in seismic case A, 129 % in case B and 77 % in case C (Table 6.2). The controlled system's respective average increase with the optimum hysteretic device (damper: 1012205) accounts to 83 %.

Table 6.2 Primary frame's and ADCS0 (damper: 1012205) maximum relative displacements U_x.

Seismic case	Max. relative displacement [cm]	
	Primary frame	ADCS0
A	2.561	3.625
B	6.779	15.490
C	2.805	4.959

The system's relative displacements response, when the optimum hysteretic device (damper: 1012205) is used in ADCS0 for the seismic cases A, B and C, is illustrated in (Figure 6.3).

It may be concluded that, for the previously suggested ADCS0 design, the good results in energy dissipation performance achieved take place at the cost of respective increased relative displacements.

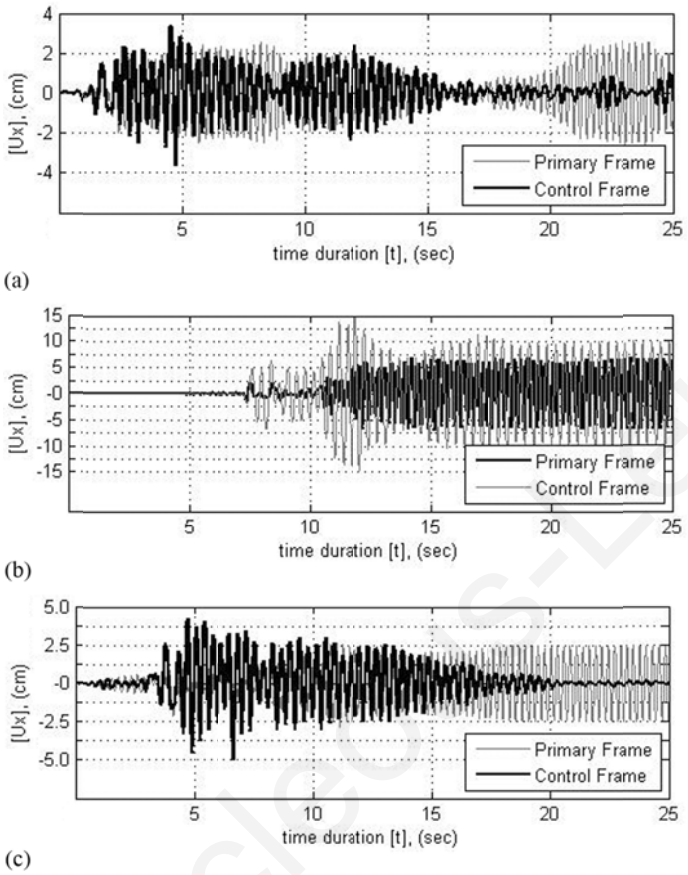

Figure 6.3 Primary frame's and ADCS0 relative displacement U_x time history (damper: 1012205): (a) seismic case A; (b) seismic case B; (c) seismic case C.

6.1.5 Damper deformations in ADCS0

The deformation of ADCS0 optimum hysteretic device (damper: 1012205) due to shear for the non-linear link element is shown in the time history range for the first 25 s (Figure 6.4). In seismic case A the peak for its time duration is equal to 3.212 cm, in case B, to 12.030 cm and in case C, to 4.577 cm. In respect to the controlled system's relative displacements the respective maximum values equal to 88.60 % for case A, 77.66 % for case B and 92.30 % for case C.

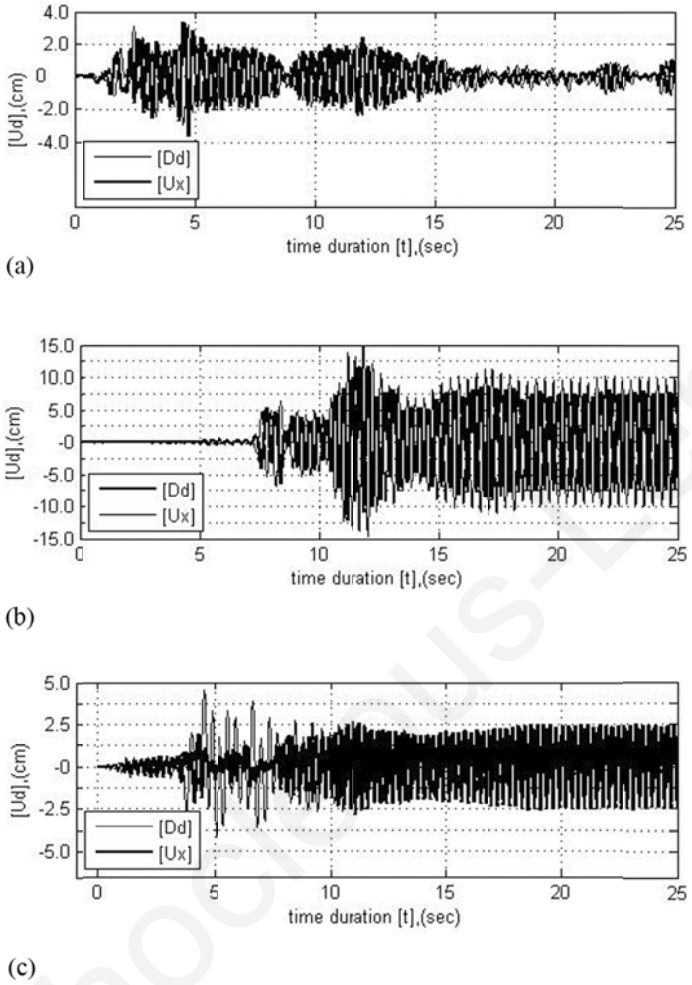

Figure 6.4 Damper's shear deformation D_d and ADCS0 relative displacement U_x time history (damper: 1012205): (a) seismic case A; (b) seismic case B; (c) seismic case C.

6.2 ADCS1 Dynamic Response

6.2.1 Natural period identification for ADCS1

Earthquake resistant systems are characterized at first place by their fundamental period. Since the controlled system's period is only associated to the behavior of the system in its linear elastic range, it depends only on the two components' stiffness, i.e. the primary

frame's, k , and the damper's stiffness, k_d that are linked in parallel, while remaining independent of P_y, which represents the nonlinear behavior of the damper. Compared to the primary frame's fundamental period of T = 0.34 s the controlled system's period decreases slightly in the range of 0.278 < T < 0.288 s. This fact results from the constraints imposed to the controlled system, considering a rigid diaphragm in the perpendicular plane direction for the implementation of the portal bracing. Furthermore the resulting fundamental period for the controlled system, that considers the inelastic nature of the incorporated damper, may provide first indications in respect to possible stiffness-, base shear- and related input energy variations through the integration of ADCS1 within the primary frame. For verification purposes the relation of the controlled system's period in respect to all damper's characteristic parameters k_d, P_y and DR is included in (Figure 6.5).

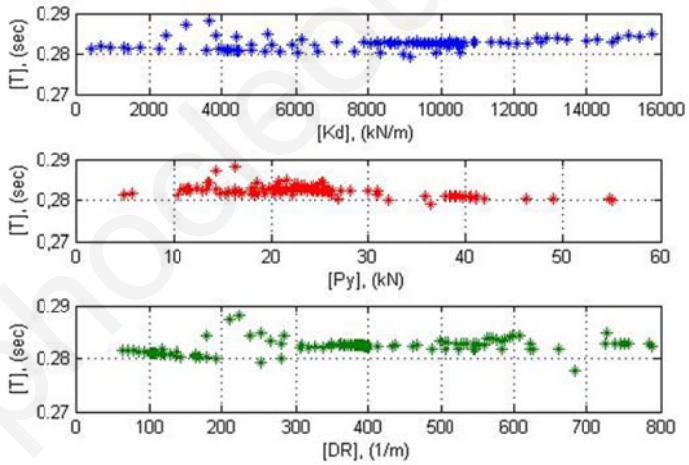

Figure 6.5 ADCS1 fundamental period T to damper's stiffness k_d, yield force P_y and damper ratio DR values.

6.2.2 Energy dissipation results for ADCS1

A number of 366 combinations of assigned values for the predominant parameters of the design, i.e. the damper's stiffness and yield force, are used in ADCS1 parametric analyses for all seismic cases. The ratio values of the hysteretic energy to the input energy of the

system, calculated for each value of DR, are presented in (Figure 6.6). The energy ratio variation, which is used to measure the effectiveness of ADCS1, is marked on the y-axis, whereas the x-axis contains the DR-values.

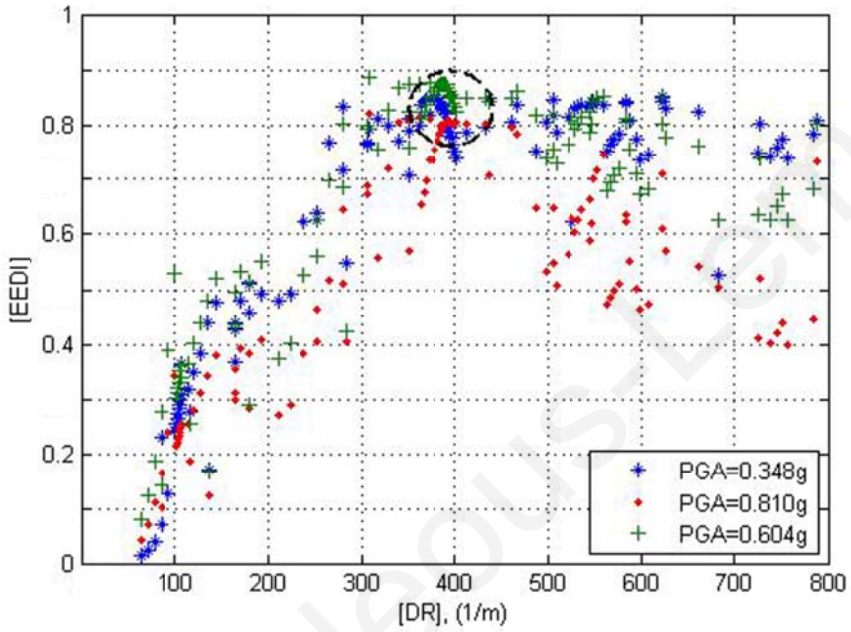

Figure 6.6 ADCS1 effective energy deformation index EEDI to damper ratio DR.

In ADCS1, DR varies between a minimum value of 64.29 1/m and a maximum value of 784.25 1/m. The limit range of favorite DR values is clearly distinguished within this range. The time variations of the system's input and dissipated energy that may lead to high energy dissipation performance by ADCS1 for all three seismic loading cases considered are shown in (Figure 6.7). High energy dissipation by the controlled system, for example exceeding 70 % of the input energy, may be achieved for the seismic loading cases A and C for values of DR > 350 1/m. For the same range of DR values and in seismic case B the control system dissipates in some cases only more than 60 % of the input energy. The results show that the maximum energy dissipation for all three seismic cases is favored with values of DR within the range 350 < DR < 466.7 1/m. On the contrary, ADCS1 energy dissipation is in particular less successful for low values of DR, i.e. DR < 350 1/m. For the entire DR range of input data the results indicate that ADCS1

performance is less satisfactory for the seismic case B, which is the loading case characterized by the highest peak ground acceleration.

The selected geometry of the damper's steel plates accounts to n = 2, t = 2.8 cm, h = 25 cm and b = 10 cm (damper: 2282510). The respective optimum DR value accounts to 392 1/m, which results from the selected parameters for the damper stiffness, i.e. k_d = 9835 kN/m, and the characteristic yield force of P_y = 25.09 kN. The Effective Energy Deformation Index, EEDI, reaches 82.40 % in seismic case A, 80.90 % in case B and 87.15 % in case C.

In the parametric study the damper's plates' height h, proves to influence stronger the system's behavior than the other geometric parameters, i.e. b, t and n. The form of the respective hysteresis curves depends primarily on the level of the plastic hysteretic damping. The selected hysteretic damper develops in seismic case A primarily hysteresis curves of the elasto-plastic type model, whereas in the cases B and C, of the rigid-plastic type model. Especially in the latter cases the damper determines the dynamic behavior of the system.

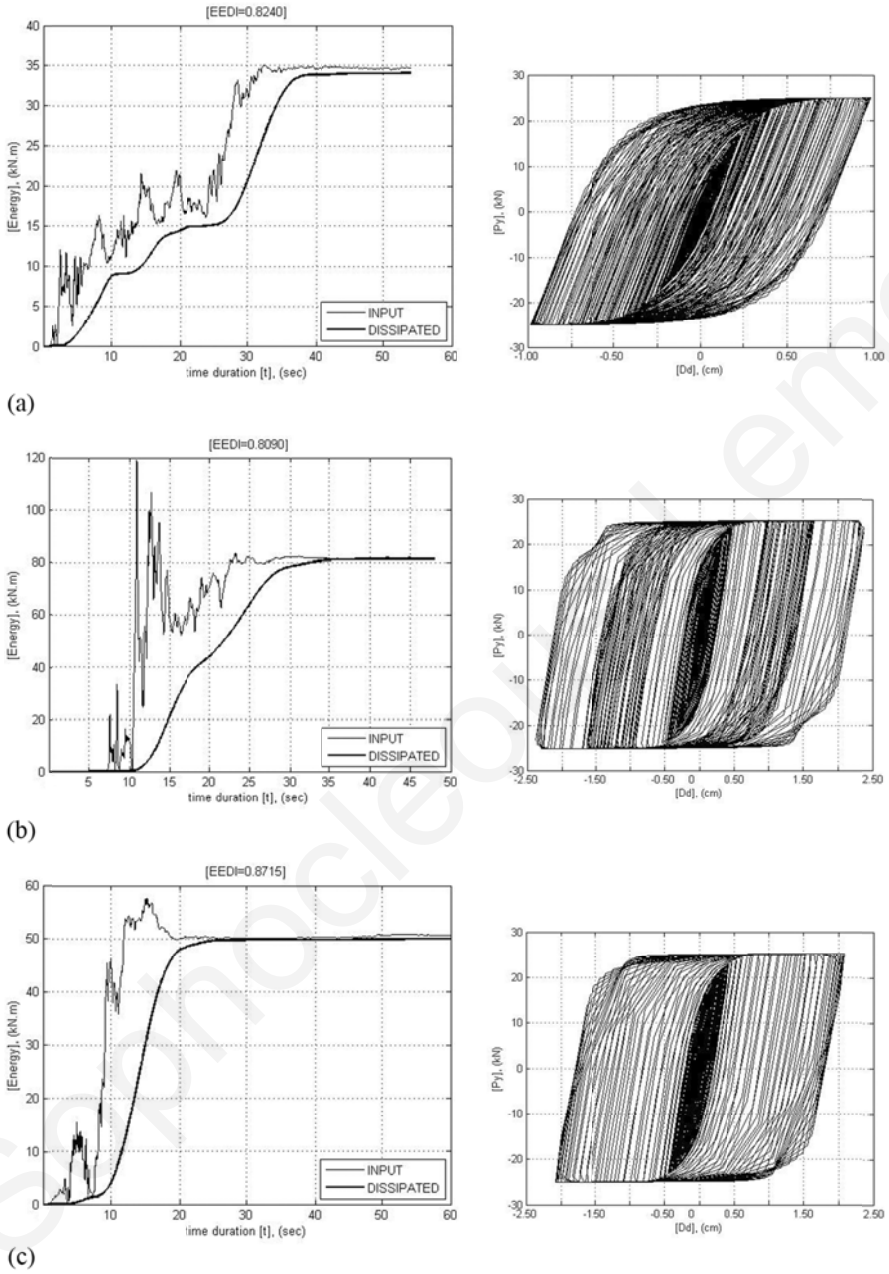

Figure 6.7 ADCS1 hysteretic damper's energy dissipation and force-deformation behavior (damper: 2282510): (a) seismic case A; (b) seismic case B; (c) seismic case C.

6.2.3 Base shear results for ADCS1

ADCS1 base shear responses under the three strong ground motions used in the analysis indicate some basic characteristics of the controlled system's performance. The magnitudes of base shear peaks are presented in absolute values as a function of both the Damper Ratio *DR* and period *T* (Figure 6.8), (Figure 6.9), (Figure 6.10). The parallel presentation of the results in relation to *T* is pursued for verification of the response relations derived as to the *DR* design parameter. The comparison is indicative for the fact that *DR* may also be selected as a characteristic property, whereas in parallel consideration of *T* is used to characterize ADCS1 dynamic behavior.

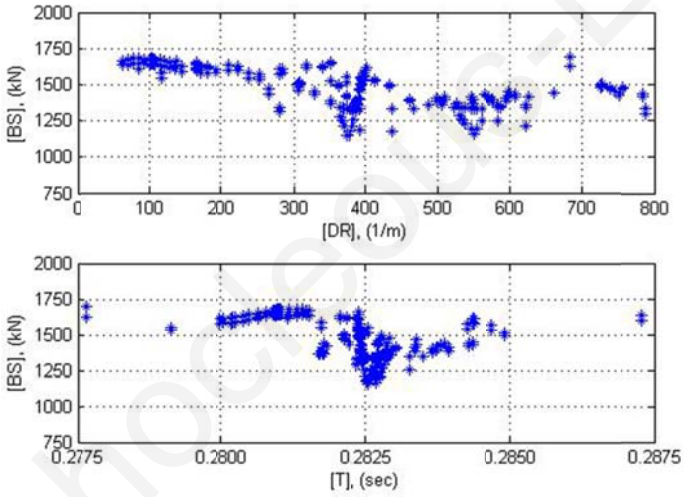

Figure 6.8 ADCS1 maximum base shear BS to damper ratio *DR* and fundamental period *T* for seismic case A.

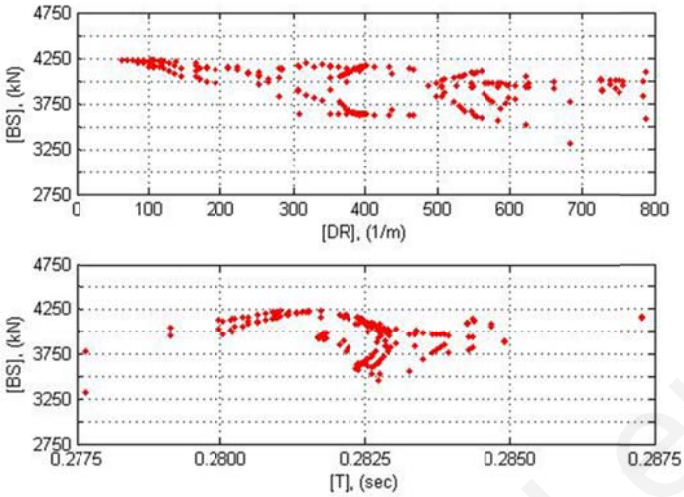

Figure 6.9 ADCS1 maximum base shear BS to damper ratio DR and fundamental period T for seismic case B.

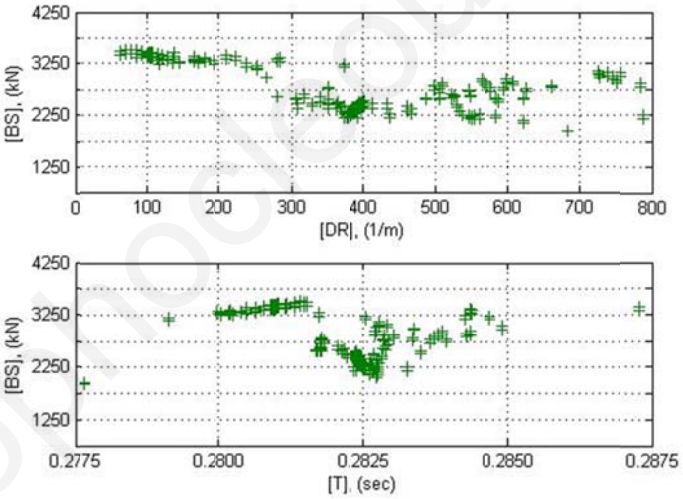

Figure 6.10 ADCS1 maximum base shear BS to damper ratio DR and fundamental period T for seismic case C.

ADCS1 maximum base shear response does not increase significantly in any analysis case. For the selected DR values of $350 < DR < 466.7$ 1/m the lowest values of the controlled system's base shear may be obtained. Compared to the primary frame's base shear, ADCS1 maximum base shear decreases for a DR value of 392 1/m (damper:

2282510) by 35 % in seismic case A and by 26 % in case B, whereas in case C it increases slightly by almost 0.05 % (Table 6.3). The average decrease of the maximum base shear accounts to 20 %, whereas the energy dissipation exceeds in all cases a benchmark of 80 % of the input seismic energy. The time history for the first 30 s of the primary frame's base shear (light line) to the ADCS1 base shear (bright line) under the three loading cases for the DR value of 392 1/m (damper: 2282510) is shown in (Figure 6.11).

Table 6.3 Primary frame's and ADCS1 (damper: 2282510) maximum base shear BS and effective energy dissipation index EEDI.

Seismic case	Max. base shear [kN]		Effective energy dissipation index [%]
	Primary frame	ADCS1	
A	2102	1374	82.40
B	5570	4139	80.90
C	2304	2413	87.15

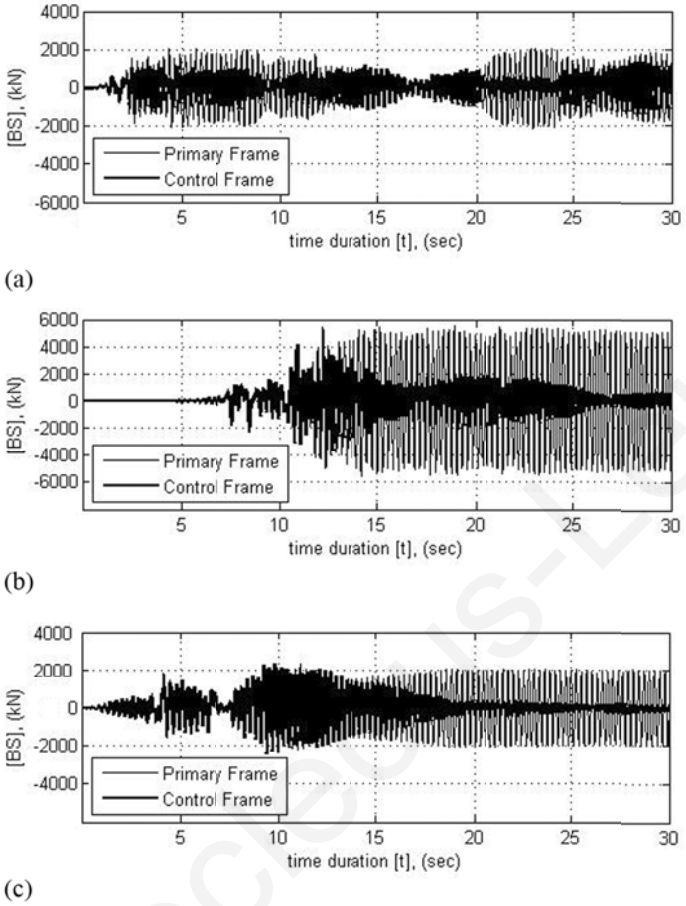

Figure 6.11 Primary frame's and ADCS1 base shear BS time history (damper: 2282510): (a) seismic case A; (b) seismic case B; (c) seismic case C.

6.2.4 Relative displacement results for ADCS1

ADCS1 relative displacements response was investigated to reveal the major respective trend characteristics. ADCS1 relative displacements are presented in absolute peak values as a function of *DR* and *T* . The minimum response values occur for *DR* values within the range of 350 < *DR* < 466.7 1/m. For all seismic loading cases considered, ADCS1 relative displacements are in agreement with the respective base shear responses. They decrease significantly for the entire *DR* range of values, compared to the respective primary frame's response, in the seismic loading cases A and -B, which are characterized by the lowest and highest peak ground acceleration respectively. In case C an increase of

the controlled system's maximum relative displacement takes place with a respective decrease of *DR* attaining an upper value of 5.503 cm. In relation to this the respective most unfavorable responses for seismic case A and -B account to 2.332 and 5.794 cm respectively.

The system's relative displacement response as to the period T and the Damper Ratio DR is shown in (Figure 6.12), (Figure 6.13), (Figure 6.14). Only slight variations in the displacements magnitudes appear in respect to the period T . The slight increase of T is due to a decrease of k_d and therefore to the respective increase of the system's relative displacements.

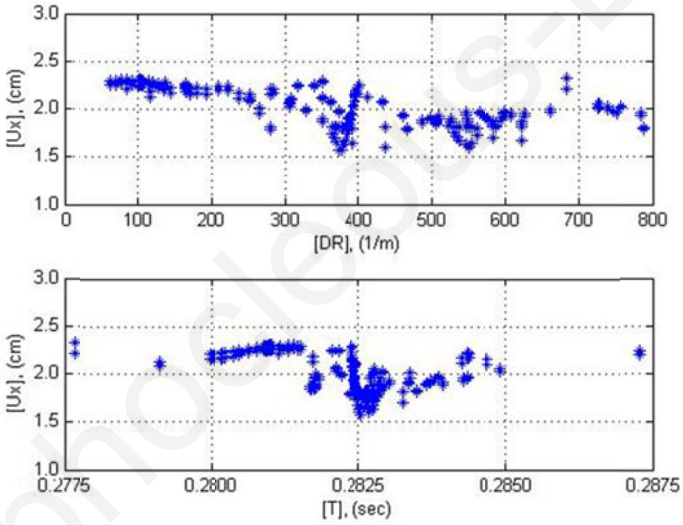

Figure 6.12 ADCS1 maximum relative displacement U_x to damper ratio DR and fundamental period T for seismic case A.

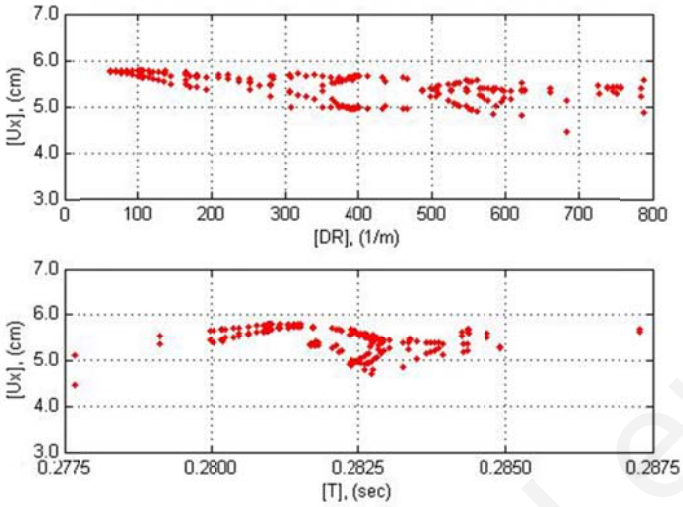

Figure 6.13 ADCS1 maximum relative displacement U_x to damper ratio *DR* and fundamental period T for seismic case B.

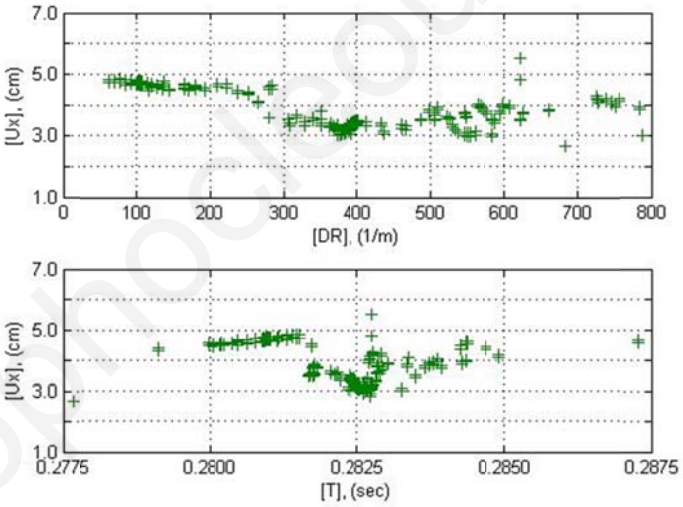

Figure 6.14 ADSC1 maximum relative displacement U_x to damper ratio *DR* and fundamental period T for seismic case C.

The reduction of the controlled system's maximum relative displacements compared to the respective values of the primary frame for a *DR* value of 392 1/m (damper: 2282510) accounts to approximately 26 % for seismic case A and 17 % for case B. In case C the controlled system's maximum relative displacement increases by 19 % compared to the

maximum value of the primary frame (Table 6.4). The relative displacements of the controlled system reduce thus on average by 8 %.

Table 6.4 Primary frame's and ADCS1 (damper: 2282510) maximum relative displacements U_x.

Seismic Case	Max. relative displacement [cm]	
	Primary frame	ADCS1
A	2.561	1.906
B	6.779	5.628
C	2.805	3.330

The time history variation for the first 30 s of the primary frame's relative displacements (light line) to the controlled system's relative displacements (bright line) under the three loading cases for the *DR* value of 392 1/m (damper: 2282510) is shown in (Figure 6.15).

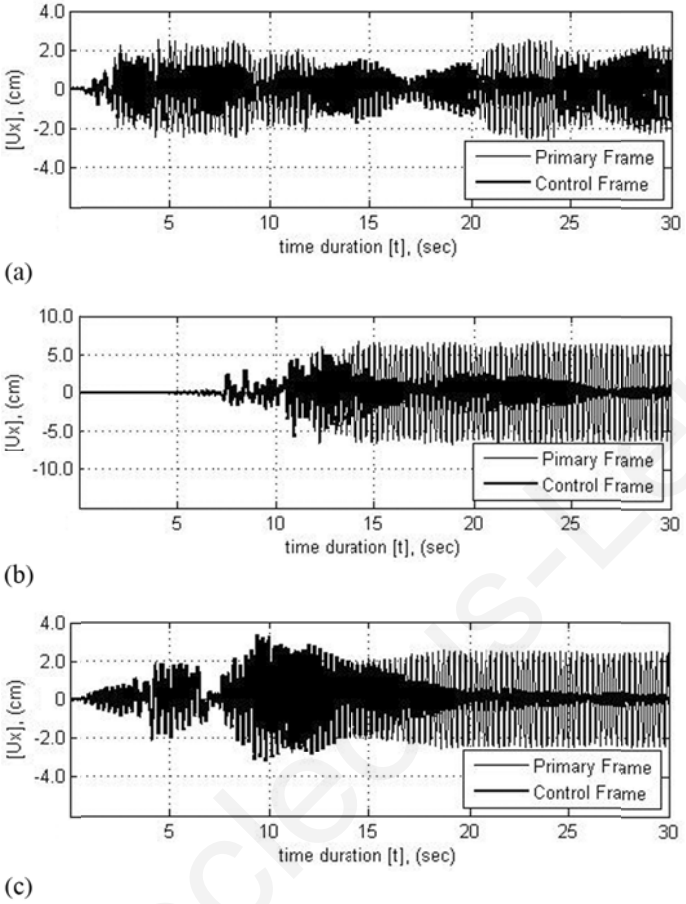

Figure 6.15 Primary frame's and ADCS1 relative displacement U_x time history (damper: 2282510): (a) seismic case A; (b) seismic case B; (c) seismic case C.

6.2.5 Damper deformations in ADCS1

Within the available range of investigation the selected hysteretic device (damper: 2282510) is characterized by a *DR* value of 392 1/m. The optimum selection is successful in terms of the maximum shear deformations of the element that account to 0.983 cm for seismic case A, 2.377 cm for case B and 2.080 cm for case C. These values comprise 52, 42 and 63 % of the controlled system's maximum relative displacements in the three seismic cases respectively. The time history response for the first 30 s of the damper's shear deformations for the three loading cases is shown in (Figure 6.16). The bright

colored lines represent the damper's shear deformations and the light colored lines the controlled system's relative displacements.

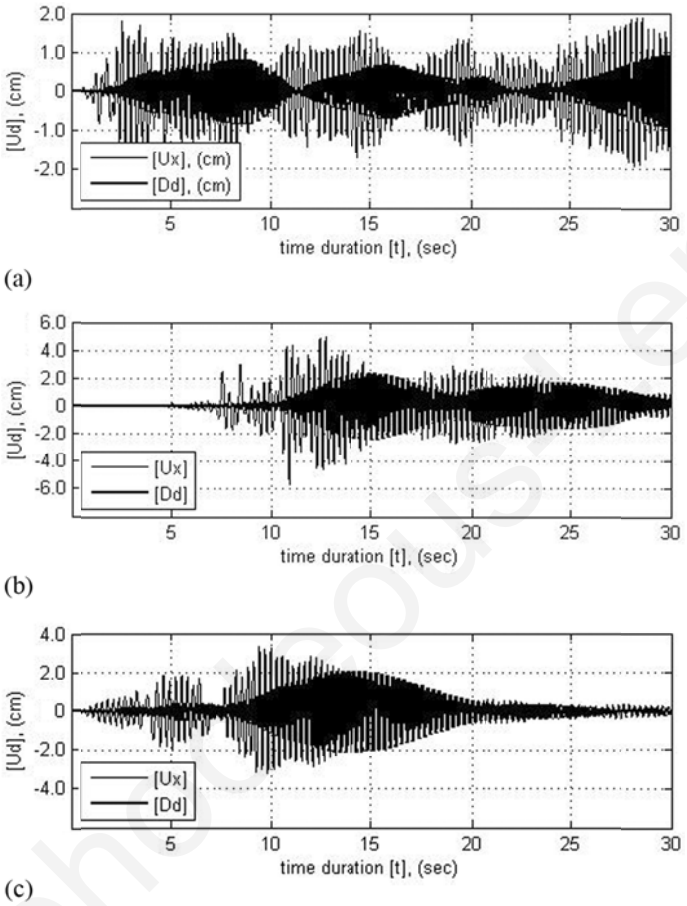

Figure 6.16 Damper's shear deformation D_d and ADCS1 relative displacement U_x time history (damper: 2282510): (a) seismic case A; (b) seismic case B; (c) seismic case C.

6.2.6 Bracings axial forces identification for ADCS1

ADCS1 bracing members were modeled as frame objects with zero compression limits. The static vertical and horizontal loading of the frame causes tension-only to the bracing rods, although under seismic loading also compression is developed in the members. The resulting maximum axial tension and compression forces of the members under the seismic

loadings of the analysis were kept in all cases within the elastic range of deformations (Table 6.5). The implementation of cable members in ADCS1 is avoided due to high prestress values that would be required for the members. Tension rods are considered instead.

Table 6.5 ADCS1 bracing members' axial forces (damper: 2282510).

Seismic case	Max. tension force [kN]	
	Horizontal member	Side members
A	20.39	75.20
B	44.75	164.95
C	36.17	133.36

6.3 ADCS2 Dynamic Response

6.3.1 Natural period identification for ADCS2

Compared to the primary frame's fundamental period of T = 0.34 s the controlled system's period decreases to the range of T = 0.27 s. This may provide first indications in respect to possible stiffness-, base shear- and related input energy variations through the integration of ADCS2 within the primary frame. For verification purposes the relation of the controlled system's period in respect to all damper's characteristic parameters, k_d, P_y and DR, is shown in (Figure 6.17).

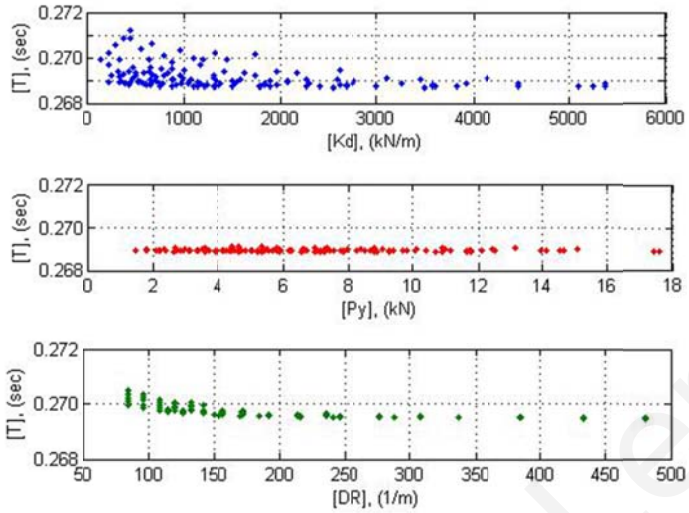

Figure 6.17 ADCS2 fundamental period T to damper's stiffness k_d, yield force P_y and damper ratio DR values.

6.3.2 Energy dissipation results for ADCS2

397 combinations of assigned values of the damper's stiffness and yield force in terms of DR have been used in the parametric analysis for all seismic cases to project the potentials for energy dissipation by ADCS2. The ratio values of the hysteretic energy to the input energy of the system, defined as EEDI, are presented for each value of DR in (Figure 6.18). The effectiveness' index EEDI is marked on the y-axis, while on the x-axis the variation of the design parameter DR is marked.

The investigation for ADCS2 energy deformation narrows to a range of $100 < DR < 150$ 1/m for maximum energy dissipation. ADCS2 energy dissipation effectiveness is in particular unsuccessful for high values of DR, i.e. $DR > 200$ 1/m, especially for the low peak ground acceleration, i.e. PGA < 0.60g. ADCS2 performed comparatively better under the seismic case B with high peak ground acceleration, i.e. PGA > 0.80g. The high values of DR result from respective high values of k_d that lead to an almost rigid-plastic behavior of the damper and cause a certain time delay in the initiation of the energy dissipation process.

The selected hysteretic device for ADCS2 (damper: 616355) with a geometry of n = 6, t = 1.6 cm, h = 35 cm and b = 5 cm, yields at P_y = 8.78 kN for highest energy dissipation performance and limitation of the system's base shear- and relative displacement responses. The respective optimum DR value accounts to 114.3 1/m (k_d = 1003.10 kN/m). ADCS2 effectiveness in deformation measurement of EEDI reaches 86.38 % in seismic case A, 81.64 % in case B and 85.13 % in case C (Figure 6.19).

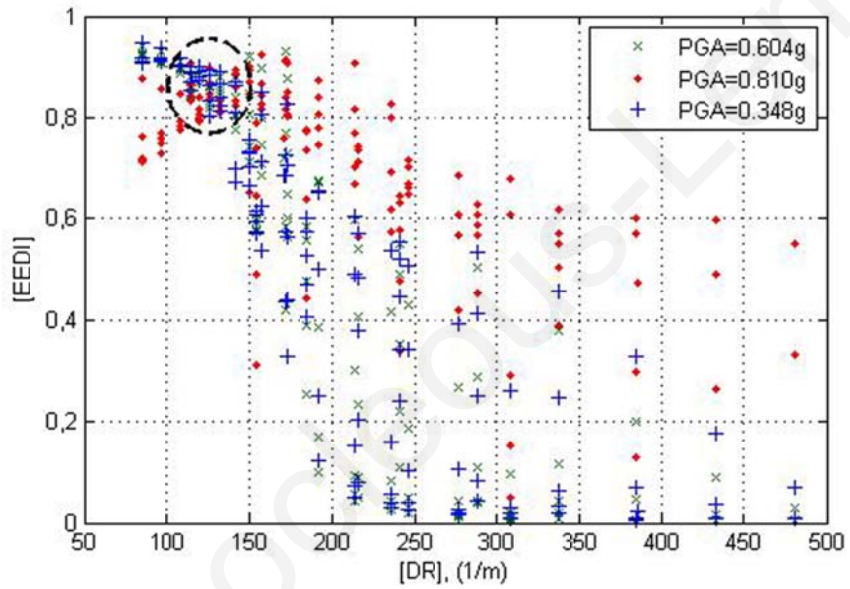

Figure 6.18 ADCS2 effective energy deformation index EEDI to damper ratio DR.

As shown in the parametric study, the damper's plates' height h proved to influence stronger the system's behavior than the other geometric parameters. This is also indicated by Equation (5.7).

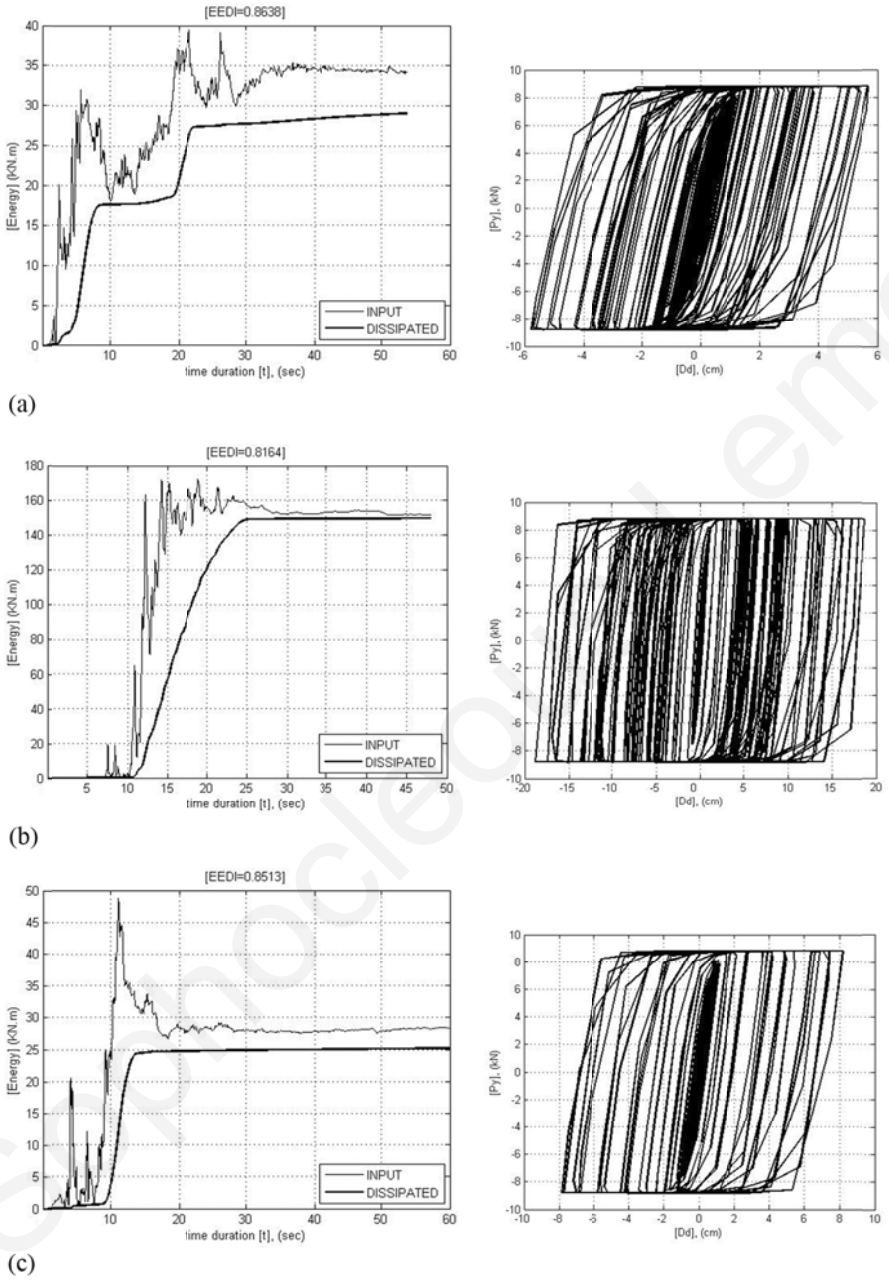

Figure 6.19 ADCS2 hysteretic damper's energy dissipation and force-deformation behavior (damper: 616355): (a) seismic case A; (b) seismic case B; (c) seismic case C.

6.3.3 Base shear results for ADCS2

ADCS2 base shear response performance reveals some promising trends. The magnitudes of base shear are presented in absolute values as a function of DR and T in (Figure 6.20), (Figure 6.21), (Figure 6.22). Within the selected DR values for optimum energy dissipation performance by ADCS2, i.e. $100 < DR < 150$ 1/m, the base shear of the controlled systems obtains the lowest values.

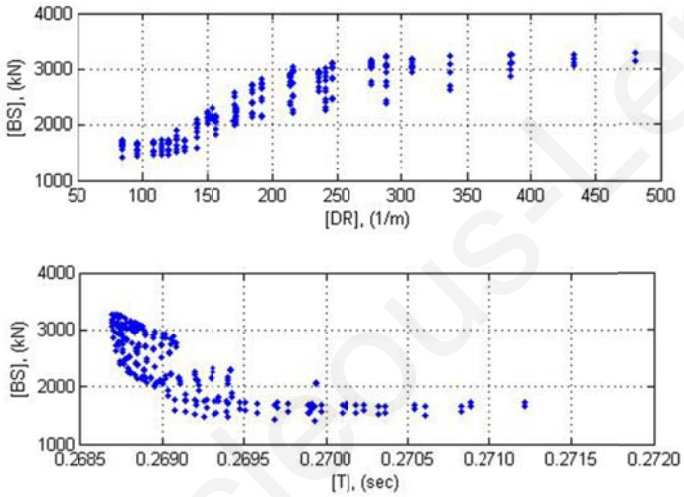

Figure 6.20 ADCS2 maximum base shear BS to damper ratio DR and fundamental period T for seismic case A.

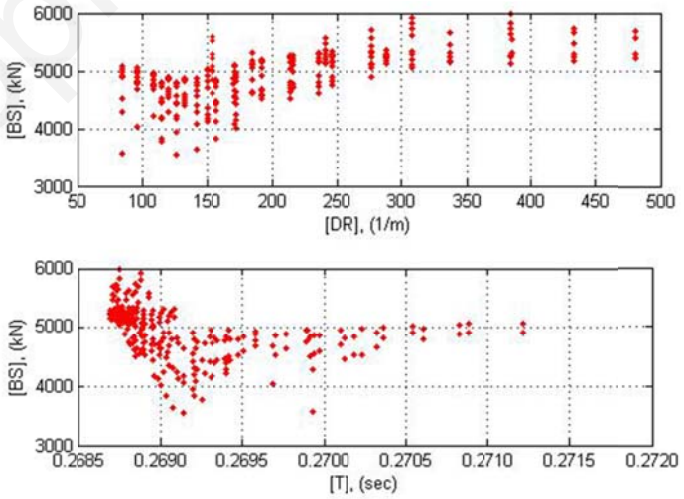

Figure 6.21 ADCS2 maximum base shear BS to damper ratio *DR* and fundamental period *T* for seismic case B.

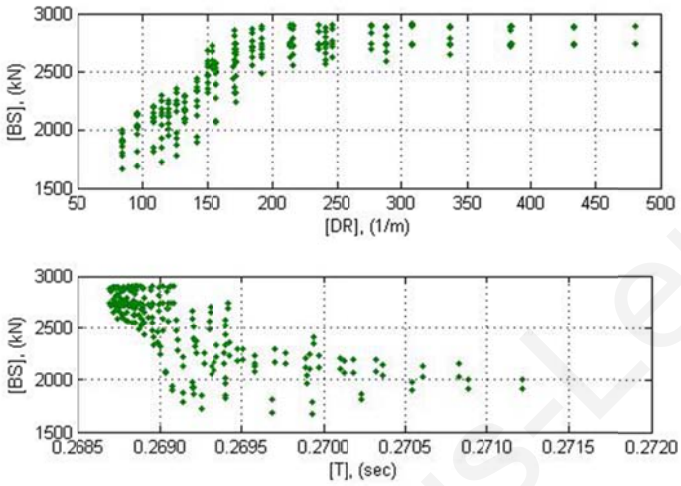

Figure 6.22 ADCS2 maximum base shear BS to damper ratio *DR* and fundamental period *T* for seismic case C.

Compared to the primary frame's base shear, ADCS2 maximum base shear decreases for the optimum selected value of *DR* of 114.3 1/m (damper: 616355) by 8 % in seismic case A and 13 % in case B, whereas in case C it increases by almost 2 %. The numerical comparisons of the maximum system's responses are presented in (Table 6.6). The average decrease of the maximum base shear accounts to 6.3 %, whereas the energy dissipation exceeds in all cases a benchmark of 80 % of the input seismic energy.

Table 6.6 Primary frame's and ADCS2 (damper: 616355) maximum base shear BS and effective energy dissipation index EEDI.

Seismic case	Max. base shear [kN]		Effective energy dissipation index [%]
	Primary frame	ADCS2	
A	2102	1932	86.38
B	5570	4830	81.64
C	2304	2340	85.13

On average for all seismic cases considered no significant variation of the maximum base shear can thus be registered for ADCS2. The time history for the first 25 s of the primary frame's base shear to the controlled systems' base shear under the three earthquake cases is shown in (Figure 6.23).

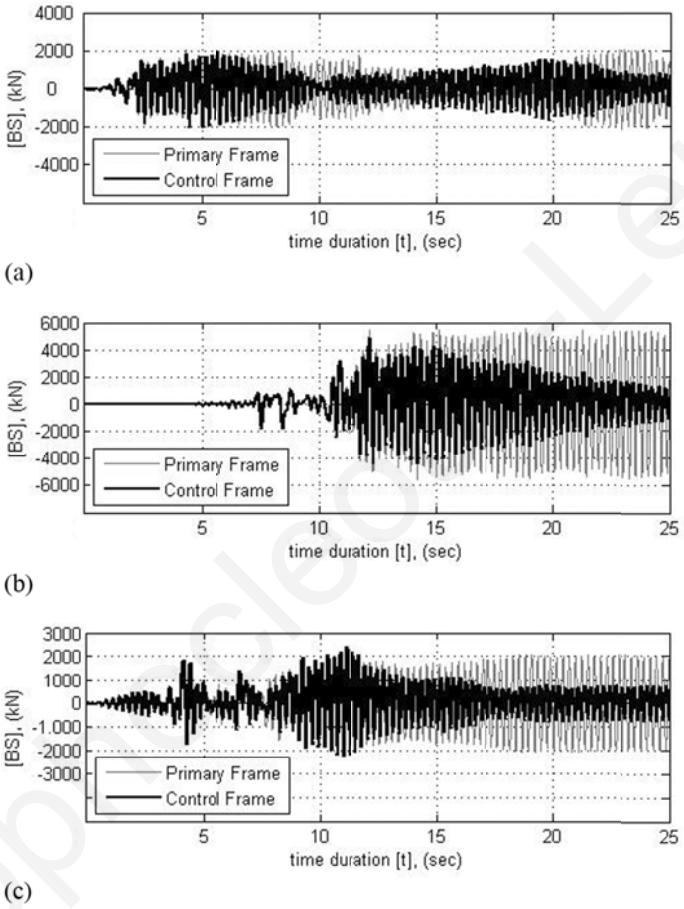

Figure 6.23 Primary frame's and ADCS2 base shear BS time history (damper: 616355): (a) seismic case A; (b) seismic case B; (c) seismic case C.

6.3.4 Relative displacement results for ADCS2

The relative displacement magnitudes of ADCS2 are presented in absolute values as a function of *DR* and *T* in (Figure 6.24), (Figure 6.25), (Figure 6.26). The minimum response values occur within the range of $100 < DR < 150$ 1/m. The highest responses

increase develops within the range of 150 < *DR* < 250 1/m, while maximum response values are obtained without major differences for *DR* > 400 1/m. In the range of *DR* > 400 1/m the maximum relative displacements of the controlled system reach 4.0 cm for low peak ground accelerations, i.e. PGA < 0.60g, and 7.0 cm in seismic case B with high peak ground acceleration, i.e. PGA > 0.80g.

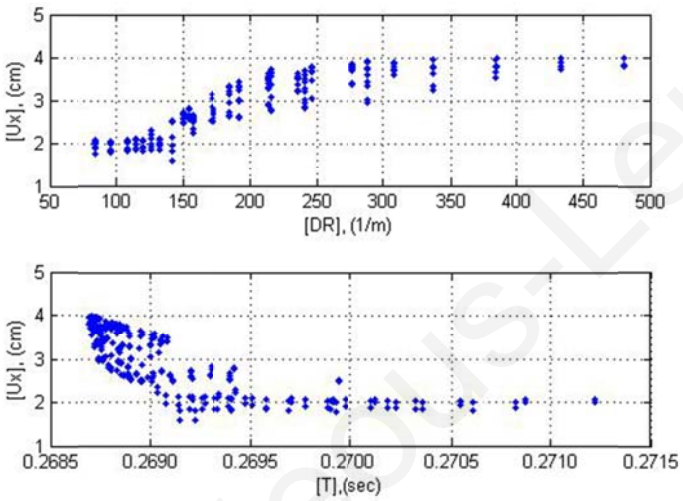

Figure 6.24 ADCS2 maximum relative displacement U_x to damper ratio *DR* and fundamental period T for seismic case A.

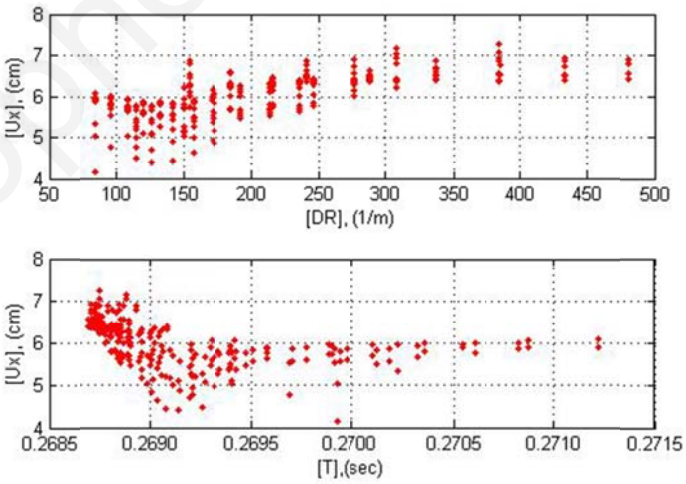

Figure 6.25 ADCS2 maximum relative displacement U_x to damper ratio *DR* and

fundamental period T for seismic case B.

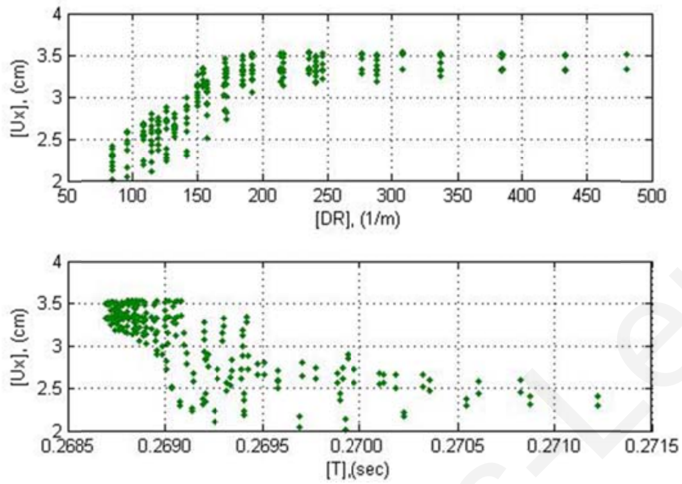

Figure 6.26 ADCS2 maximum relative displacement U_x to damper ratio DR and fundamental period T for seismic case C.

The relative displacements of the system are primarily influenced by the values of the damper's stiffness k_d. In particular, for relatively low values of k_d, the relative displacements of ADCS2 are kept low. This implies that the damper initiates the energy dissipation due to its permanent deformations from an early loading stage. The respective values of P_y are high enough so that maximum possible resistance is obtained and thus sufficient effective cumulative plastic deformation is exhibited by the damper. The system's relative displacement responses, as reported in their variation with period T, comply also with this observation.

For the selected DR value of 114.3 1/m (damper: 616355) the controlled system's maximum relative displacement reduces by almost 9 % for seismic case A and 15 % for case B, although for case C it increases insignificantly by almost 1 % (Table 6.7). The relative displacements of the controlled system reduce thus on average by almost 8 %. The time history for the first 25 s of the primary frame's relative displacements to the controlled systems' relative displacements is shown in (Figure 6.27).

Table 6.7 Primary frame's and ADCS2 (damper: 616355) maximum relative displacements U_x.

Seismic Case	Max. relative displacement [cm]	
	Primary frame	ADCS2
A	2.561	2.336
B	6.779	5.759
C	2.805	2.828

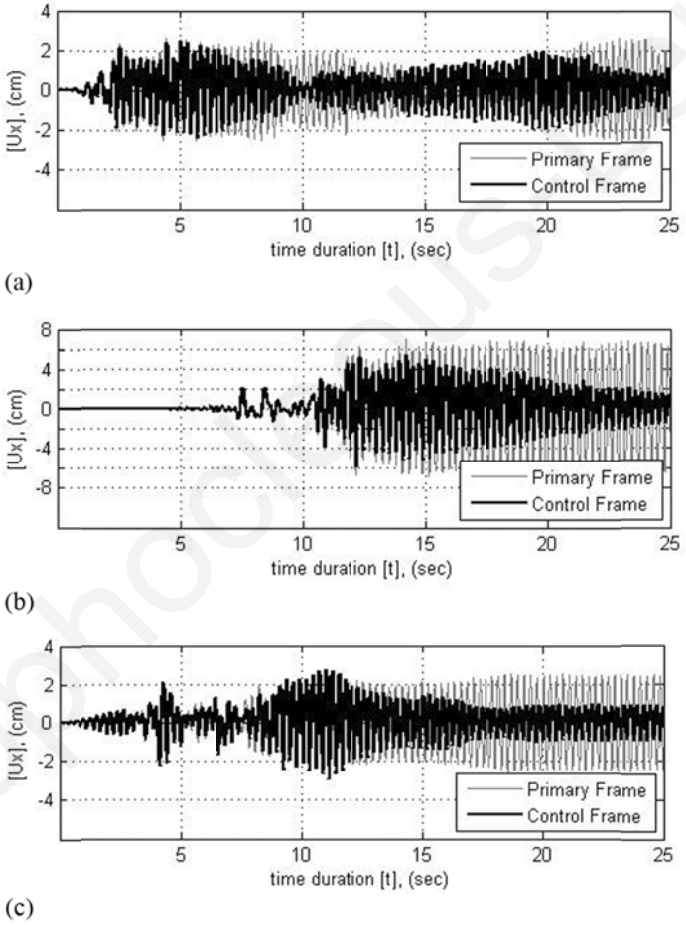

Figure 6.27 Primary frame's and ADCS2 relative displacement U_x time history (damper: 616355): (a) seismic case A; (b) seismic case B; (c) seismic case C.

6.3.5 Damper deformations in ADCS2

For a *DR* value of 114.3 1/m (damper: 616355) the maximum shear deformations of the damper account to 5.626 cm for seismic case A, 18.650 cm for case B and 8.109 cm for case C. Compared to the controlled system's relative displacements the deformation increase of the element accounts to 141, 224 and 187 % for the three seismic cases respectively.

The time history for the first 25 s of the ADCS2's damper's shear deformations for the three loading cases with a *DR* value of 114.3 1/m (damper: 616355) is shown in (Figure 6.28). The light colored lines represent the damper's shear deformations and the bright colored lines the controlled system's relative displacements.

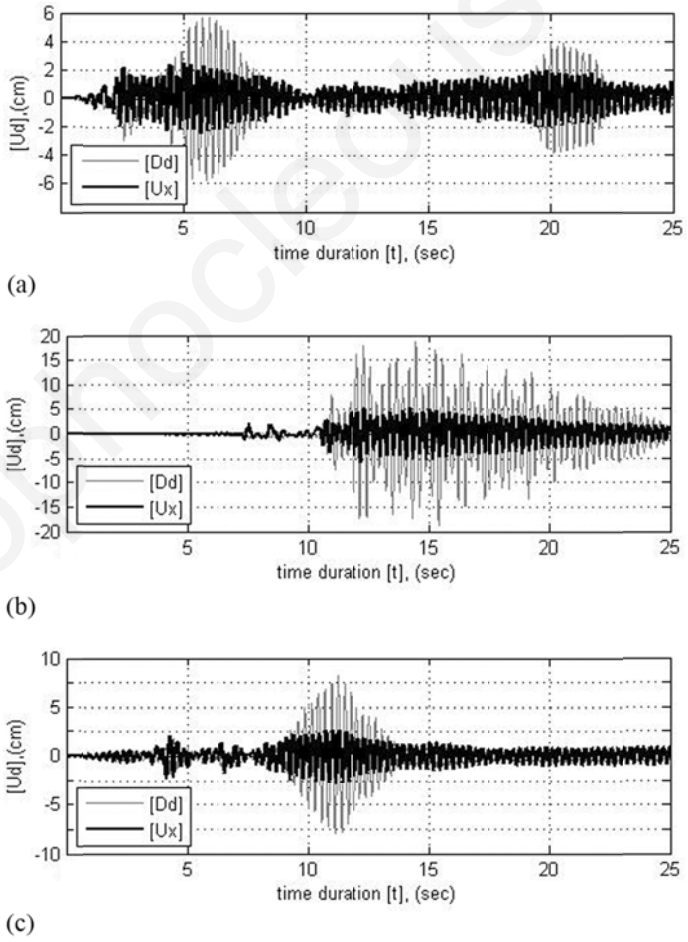

Figure 6.28 Damper's shear deformation D_d and ADCS2 relative displacement U_x time history (damper: 616355): (a) seismic case A; (b) seismic case B; (c) seismic case C.

6.3.6 Bracings axial forces identification for ADCS2

In the selected controlled system the cables are modeled as frame objects with zero compression limits. To avoid any related modification of the resulting members' axial forces, these are assigned with a suitable pretension stress through a target force. For the range of the developed stresses and strains in the bracing members the material's mechanical behavior is assumed to be linear.

The static vertical and horizontal loading of the frame causes tension-only to the bracing although under seismic loading compression has also been developed in the members. The magnitude of the prestress target force is slightly higher than the maximum resulting force in the bracing under the selected seismic excitations. In seismic case B a maximum compression force of 107.35 kN was developed in the side diagonal of ADCS2 portal bracing. To prevent this a prestress of 25 % of the maximum allowable stress of $f_{allowable}$ = 140 kN/cm^2 was applied at the end of a trial and error procedure. The prestress force leads to a linear elastic resistance by the bracings in all seismic loading cases (Table 6.8).

Table 6.8 ADCS2 bracing members' axial forces (damper: 616355).

Seismic case	Max. tension force [kN]		
	Horizontal member	Side members	Chevron members
A	46.23	190.37	103.22
B	56.49	244.94	121.05
C	42.64	173.43	98.46

6.4 ADCS3 Dynamic Response

6.4.1 Natural period identification for ADCS3

The slight difference within the entire range of the controlled systems' period of 0.275 s < T < 0.280 s allows for the design considerations to be based on the characteristic parameter DR rather than T. The population of the different properties used in the parametric analyses in relation to the determined properties of the non-linear link, i.e. k_d, P_y and DR, is included in (Figure 6.29).

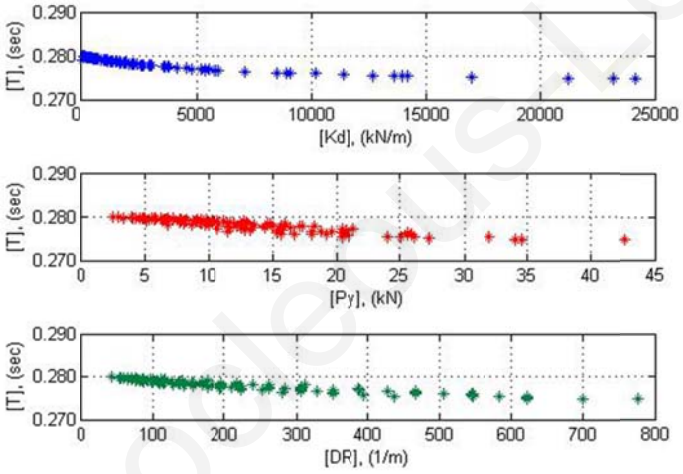

Figure 6.29 ADCS3 fundamental period T to damper's stiffness k_d, yield force P_y and damper ratio DR values.

6.4.2 Energy Dissipation results for ADCS3

EEDI measures the capability of ADCS3 for energy dissipation. The challenge of implementing the hysteretic damper at the optimal point in ADCS3 triangle is successfully managed as the results from the 342 analytical trials reveal in terms of EEDI measures. EEDI is marked on the y-axis and DR on the x- axis (Figure 6.30).

Although high energy dissipation by the controlled system, for example exceeding 60 % of the input energy, may be achieved for the seismic loading case A, with values of DR >

284 1/m, for seismic case B the respective values of DR account to DR > 168 1/m. In seismic case C the control system may dissipate in only some cases more than 60 % of the input energy when DR > 200 1/m.

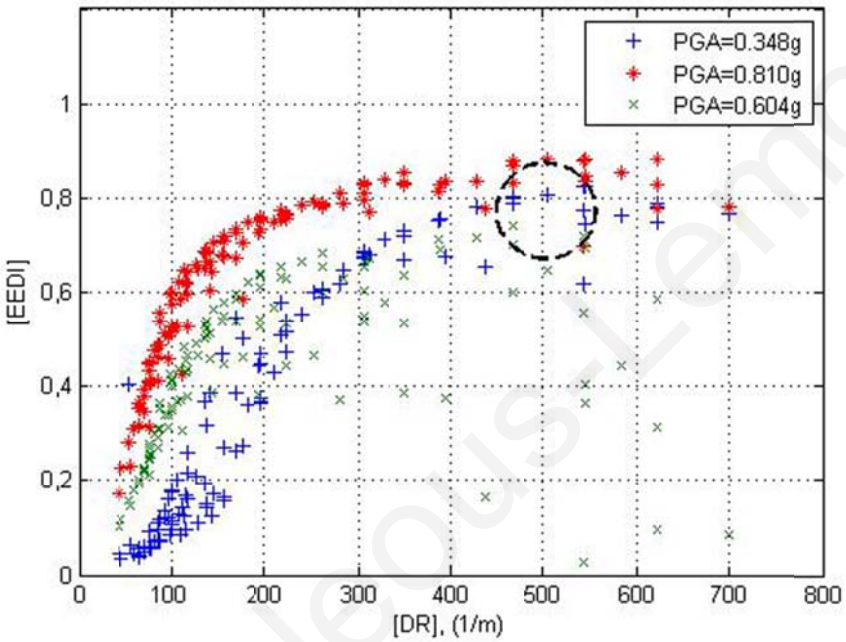

Figure 6.30 ADCS3 effective energy deformation index EEDI to damper ratio DR.

Maximum energy dissipation for all three seismic cases is favored by values of 437 < DR < 544 1/m considering in parallel the reduction of the controlled system's maximum base shear and relative displacements. ADCS3 energy dissipation is in particular less successful for low values of DR, i.e. DR < 240 1/m, especially under the action of low peak ground accelerations, as in seismic case A. For the entire DR range of analysis ADCS3 performed comparatively better in seismic case B with highest peak ground acceleration.

The optimum DR value accounts to 466.67 1/m (damper: 612155). The damper with a geometry of n = 6, t = 1.2 cm, h = 15 cm and b = 5 cm, has a stiffness value of k_d =

5376 kN/m and yields at P_y = 11.52 kN. EEDI reaches 79.93 % in seismic case A, 83.19 % in case B and 74.16 % in case C (Figure 6.31).

The parametric study for ADCS3 dynamic responses shows high variations in EEDI, when different heights of the plates are used, whereas when the width and number of plates change, the variations are minimal and almost with no practical meaning. The form of the corresponding hysteresis curves depends primarily on the grade of the plastic hysteretic damping. The selected hysteretic damper develops in all three seismic cases exclusively hysteresis curves of the rigid-plastic type model. In these cases the damper determines the dynamic behavior of the system.

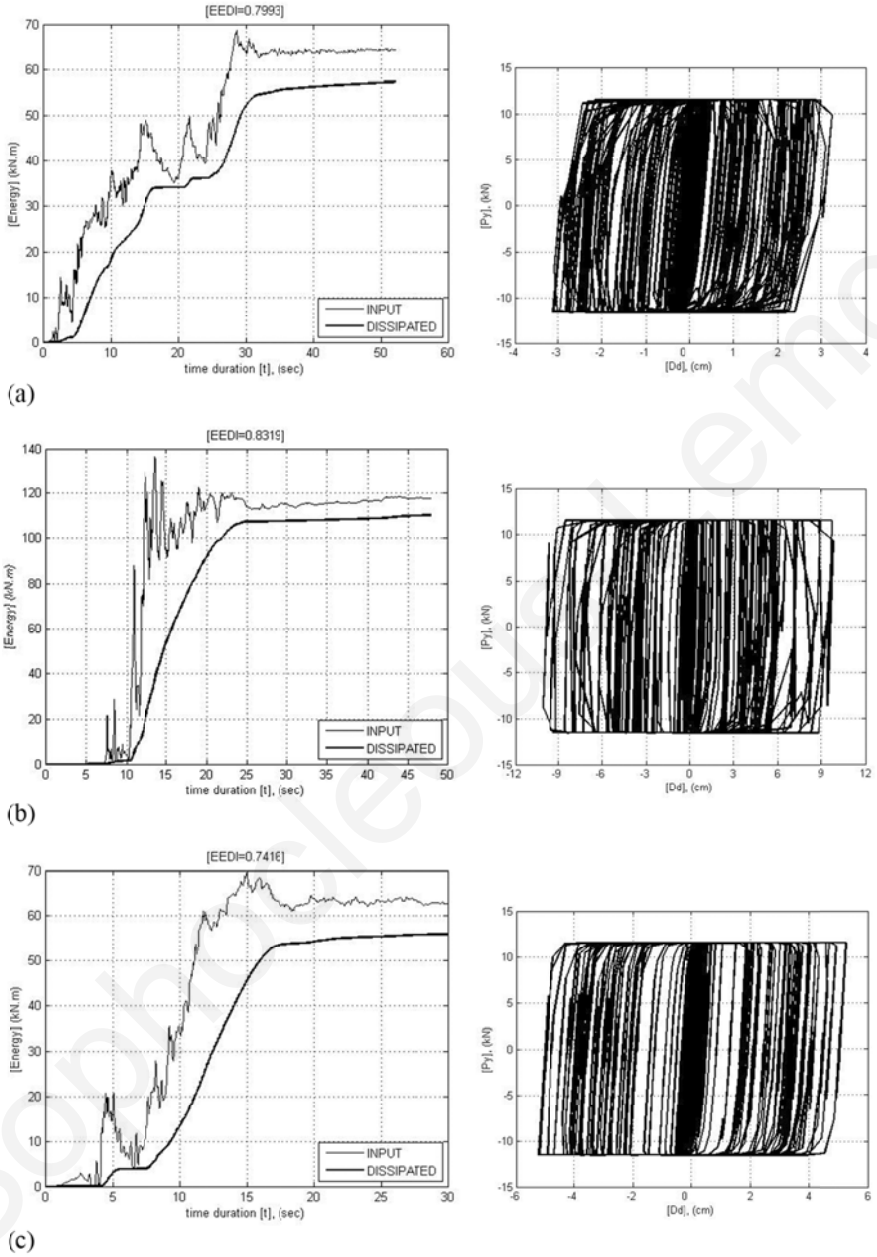

Figure 6.31 ADCS3 hysteretic damper's energy dissipation and force-deformation behavior (damper: 612155): (a) seismic case A; (b) seismic case B; (c) seismic case C.

6.4.3 Base shear results for ADCS3

ADCS3 base shear responses magnitudes are presented in absolute values as a function of DR and T in (Figure 6.32), (Figure 6.33), (Figure 6.34). The two parallel illustrations for DR and T present a similar trend. The peak values of the base shear of the controlled system decrease significantly for the entire DR range, compared to the respective primary frame's response, in the seismic loading case B with highest peak ground acceleration. In case A with lowest peak ground acceleration small reductions of the maximum base shear of the controlled system are observed, especially for low values of DR, i.e. $DR < 240$ 1/m. In case C a considerable increase of the maximum base shear takes place with a respective decrease of DR. Even in such cases ADCS3 responses do not exceed the limits imposed by the elastic frame design according to the Eurocode 3 guidelines.

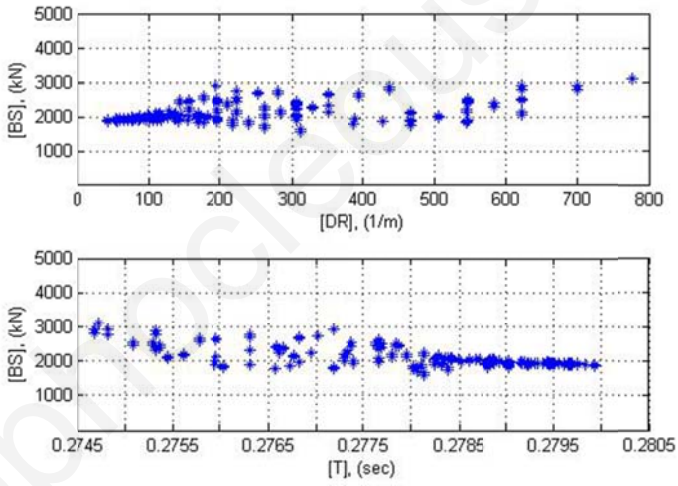

Figure 6.32 ADCS3 maximum base shear BS to damper ratio DR and fundamental period T for seismic case A.

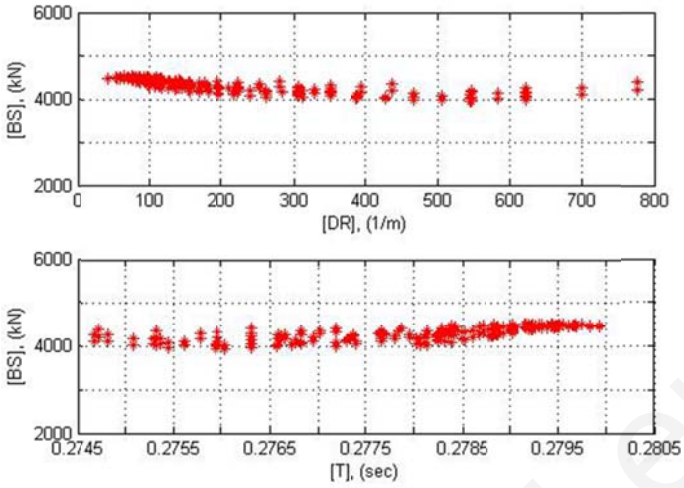

Figure 6.33 ADCS3 maximum base shear BS to damper ratio DR and fundamental period T for seismic case B.

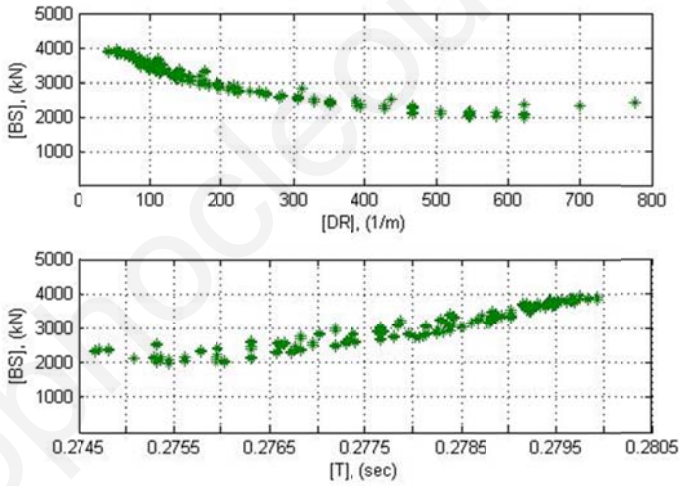

Figure 6.34 ADCS3 maximum base shear BS to damper ratio DR and fundamental period T for seismic case C.

Within the selected DR values for high energy dissipation performance of ADCS3, i.e. $437 < DR < 544$ 1/m, the base shear of the controlled systems obtains the lowest values. Compared to the primary frame's base shear, ADCS3 maximum base shear decreases for a DR value of 466.67 1/m (damper: 612155) by 16 % in seismic case A, by almost 28 % in

case B, whereas in case C it increases slightly by 1 % (Table 6.9). On average it decreases by 14.33 %. In all three cases the energy dissipation effected by ADCS exceeds 74 % of the input seismic energy.

Table 6.9 Primary frame's and ADCS3 (damper: 612155) maximum base shear BS and effective energy dissipation index EEDI.

Seismic case	Max. base shear [kN]		Effective energy dissipation index [%]
	Primary frame	ADCS3	
A	2102	1764	79.93
B	5570	4031	83.19
C	2304	2321	74.16

The time history for the first 30 s of the primary frame's base shear (light line) to the controlled system's base shear (bright line) under the three loading cases for the DR value of 466.67 1/m (damper: 612155) is shown in (Figure 6.35).

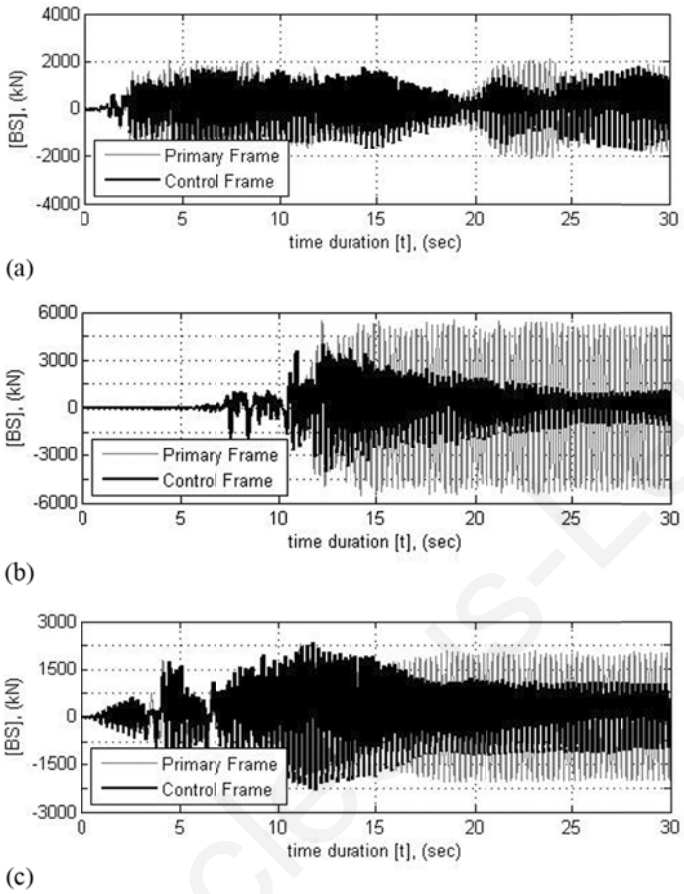

Figure 6.35 Primary frame's and ADCS3 base shear BS time history (damper: 612155) (a) seismic case A; (b) seismic case B; (c) seismic case C.

6.4.4 Relative displacement results for ADCS3

ADCS3 relative displacements absolute values are presented as a function of DR and T in (Figure 6.36), (Figure 6.37), (Figure 6.38). The minimum response values occur within the range of 437 < DR < 544 1/m. The highest responses increases develop with decrease of DR, i.e. DR < 240 1/m. For all seismic loading cases the trend for the system's relative displacements are in agreement with the respective trend for the base shear responses. The controlled system's maximum relative displacement decreased significantly for the entire DR range of values, compared to the respective primary frame's response, in seismic loading case B with highest peak ground acceleration, whereas in case C a considerable

increase of the maximum relative displacement takes place with a respective decrease of DR, attaining an upper value of 5.348 cm. The respective most unfavorable responses for seismic case A and B account to 4.100 and 6.131 cm respectively.

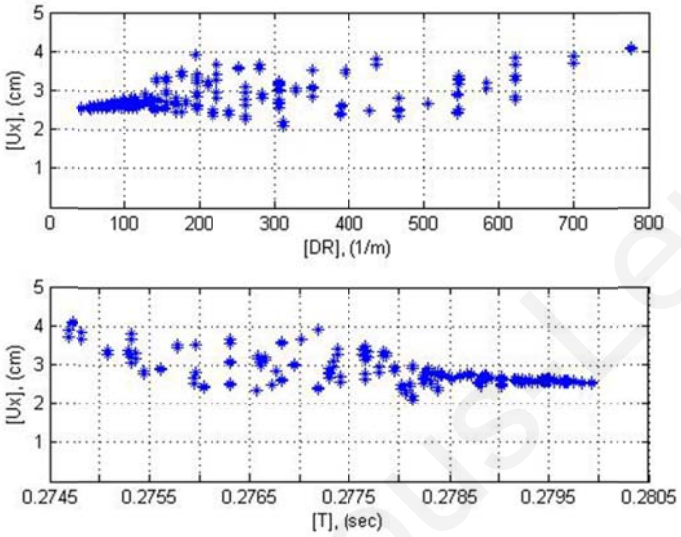

Figure 6.36 ADCS3 maximum relative displacement U_x to damper ratio DR and fundamental period T for seismic case A.

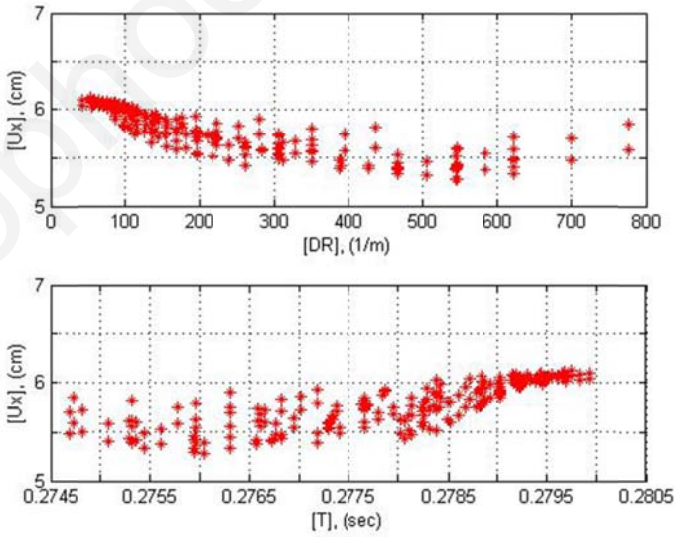

Figure 6.37 ADCS3 maximum relative displacement U_x to damper ratio DR and fundamental period T for seismic case B.

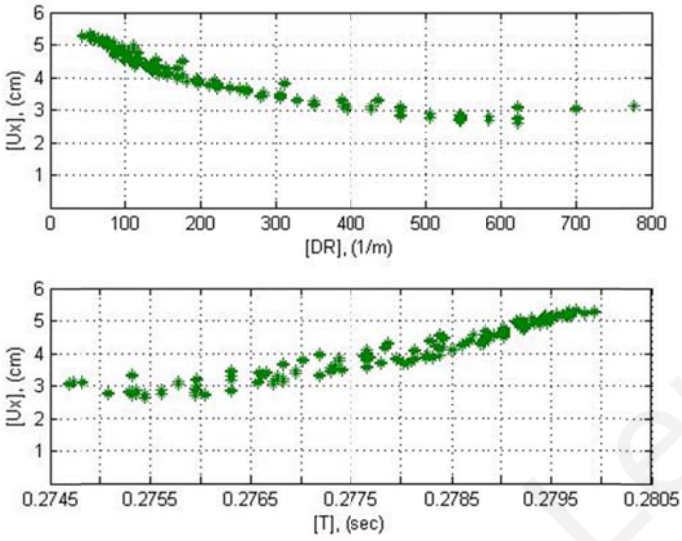

Figure 6.38 ADCS3 maximum relative displacement U_x to damper ratio DR and fundamental period T for seismic case C.

The relative displacements of ADCS3 increase when the damper's stiffness k_d is low while the respective values of P_y are high. In this context it may be concluded that maximum resistance and sufficient cumulative plastic deformation capacity of the damper utilized for this optimum case of ADCS3 is obtained with k_d = 5378 kN/m and P_y = 11.52 kN. This explanation conforms to the system's relative displacement responses as to their period T, which is most clearly indicated in the respective results for seismic case B and C. The reduction of the controlled system's maximum relative displacements compared to the respective values of the primary frame for a DR value of 466.67 1/m (damper: 612155) accounts to approximately 7 % in seismic case A and 20 % in case B. In seismic case C the controlled system's maximum relative displacement increases by almost 12 % compared to the maximum value of the primary frame (Table 6.10). On average, the relative displacement of the controlled system increases by 5 %.

Table 6.10 Primary frame's and ADCS3 (damper: 612155) maximum relative displacements U_x.

Seismic Case	Max. relative displacement [cm]	
	Primary frame	ADCS3
A	2.561	2.372
B	6.779	5.409
C	2.805	3.129

The time history for the first 30 s of the primary frame's relative displacements (light line) to the controlled system's relative displacements (bright line) under the three loading cases for the DR value of 466.67 1/m (damper: 612155) is shown in (Figure 6.39).

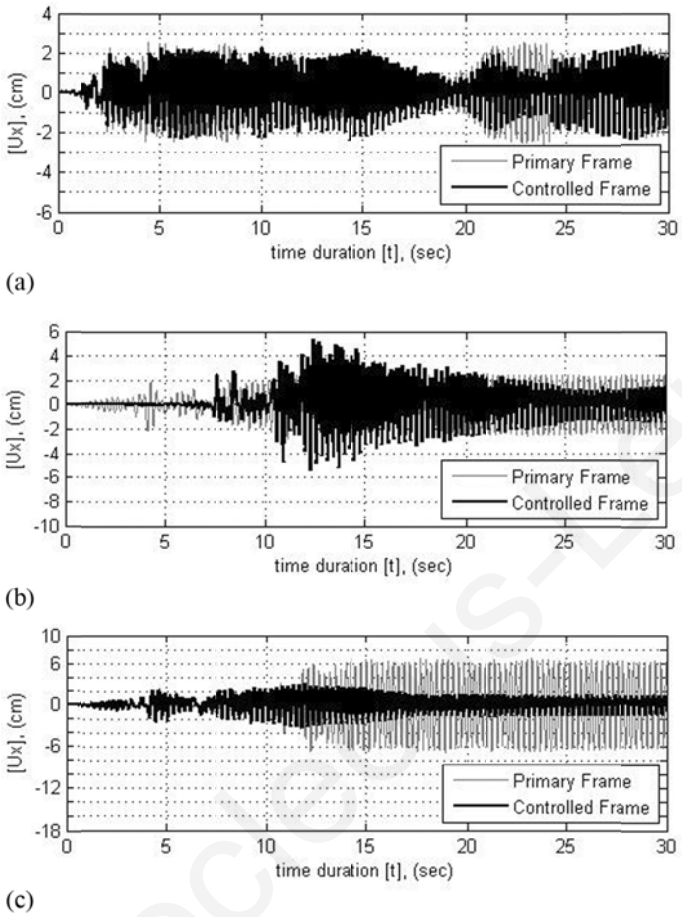

Figure 6.39 Primary frame's and ADCS3 relative displacement U_x time history (damper: 612155): (a) seismic case A; (b) seismic case B; (c) seismic case C.

6.4.5 Damper deformations in ADCS3

The hysteretic damper is positioned at the frame's joint area between the secondary bracing member and the column. Shear deformations of the device are activated through relative displacements of the primary system to the bracing mechanism. For a *DR* value of 466.67 1/m (damper: 612155) the maximum shear deformations of the damper account to 3.233 cm for seismic case A, 10.250 cm for case B and 5.244 cm for case C. Compared to the controlled system's relative displacements the deformation increase of the element accounts to 36.30, 89.50 and 67.59 % for the three seismic cases respectively. The time

history for the first 30 s of the damper's shear deformations for the three loading cases with a *DR* value of 466.67 1/m (damper: 612155) is shown for the first 30 s in (Figure 6.40). The light colored lines represent the damper's shear deformations and the bright colored lines the controlled system's relative displacements.

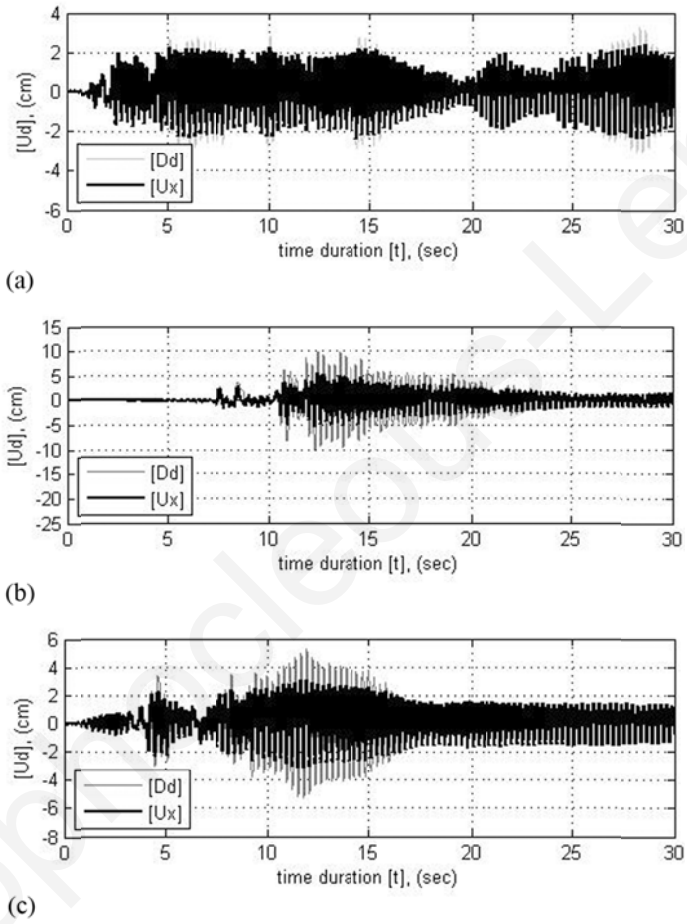

Figure 6.40 Damper's shear deformation D_d and ADCS3 displacement U_x time history (damper: 612155): (a) seismic case A; (b) seismic case B; (c) seismic case C.

6.4.6 Bracings axial forces identification for ACDS3

A maximum compression force of 63.68 kN is developed in seismic case B in the diagonal bracing member when a *DR* value of 466.67 1/m (damper: 612155) is assigned to the

controlled system. For this reason, following a trial and error procedure, a prestress of 10 % of the maximum allowable stress of the cables' section, of $f_{allowable}$ = 140 kN/cm^2, was applied to the bracing members. In the case of the cables' diameter of d_c = 20 mm their respective pretension was set equal to the target force of P_y = 43.98 kN. The resulting maximum axial tension forces of the members under the seismic loading cases of the analysis were kept minimum and within the elastic range of deformations (Table 6.11).

Table 6.11 ADCS3 bracing members' axial forces (damper: 612155).

Seismic case	Max. tension force [kN]		
	Horizontal member	Diagonal member	Vertical member
A	46.05	72.32	50.46
B	48.56	104.69	59.04
C	47.67	85.84	55.93

6.5 ADCS selected effective stiffness ratios

ADCS optimum effective stiffness ratios considered in the analyses refer to the following: k' denotes the ratio of the damper's stiffness, k_d, over the stiffness of the primary frame k. k'' denotes the ratio of the equivalent effective stiffness of the bracing, as it results from the weakest connected bracing-link, k_b, over the damper's stiffness k_d.They result from the weakest bracing in the chain-connected members (Table 6.12).

Table 6.12 Controlled systems optimum effective stiffness ratios.

System	P_y [kN]	DR $[\frac{1}{m}]$	$k' = \frac{k_d}{k}$	$k'' = \frac{k_b}{k_d}$
ADCS0	14.73	265.45	0.1062	1.65
ADCS1	25.09	392.00	0.2360	0.42
ADCS2	8.78	114.30	0.0240	4.10
ADCS3	11.52	466.67	0.1290	0.77

CHAPTER 7 DYNAMIC RESPONSE VERIFICATION

7.1 Dynamic Response Verification

ADCS designs are verified based on a wider range of seismic input records from the Mediterranean earthquake prone area. The optimum damper that was selected based on the parametric studies conducted is employed for each one of the three systems. The dynamic response verification studies aim at providing both validation and reliability of ADCS potential for ensuring earthquake safety of the primary system ([7.1], [7.2], [7.4]).

7.1.1 Seismic records of the Greek-Mediterranean area

The dynamic performance of the three ADCS systems was examined under ten selected seismic events recorded in the Greek-Mediterranean region (Table 7.1). Both the peak ground acceleration and the frequency content are different for each of the selected records, while the time duration varied in the range between 13.91 and 46.01 s (Figure 7.1).

Table 7.1 Seismic records of the Greek Mediterranean area.

Seismic case	Record	Station	PGA [g]	Duration [s]
1	Aigio 95	Aigio, 0^0	0.50	30.04
2	Athens 99	Sepolia, 0^0	0.33	46.01
3	Ionian 83	Argostoli, 90^o	0.24	32.33
4	Kalamata 86	Kalamata, 0^0	0.22	59.63
5	Heraklio 84	Heraklio, 90^0	0.21	16.67
6	Aigio 90	Aigio, 90^0	0.20	16.13
7	Etolia 88	Valsamata, 90^0	0.18	25.43
8	Killini 88	Zakinthos, 90^0	0.15	27.83
9	Preveza 81	Preveza, 0^0	0.14	18.35
10	Gulf of Corinth	Nafpaktos, 90^0	0.10	13.91

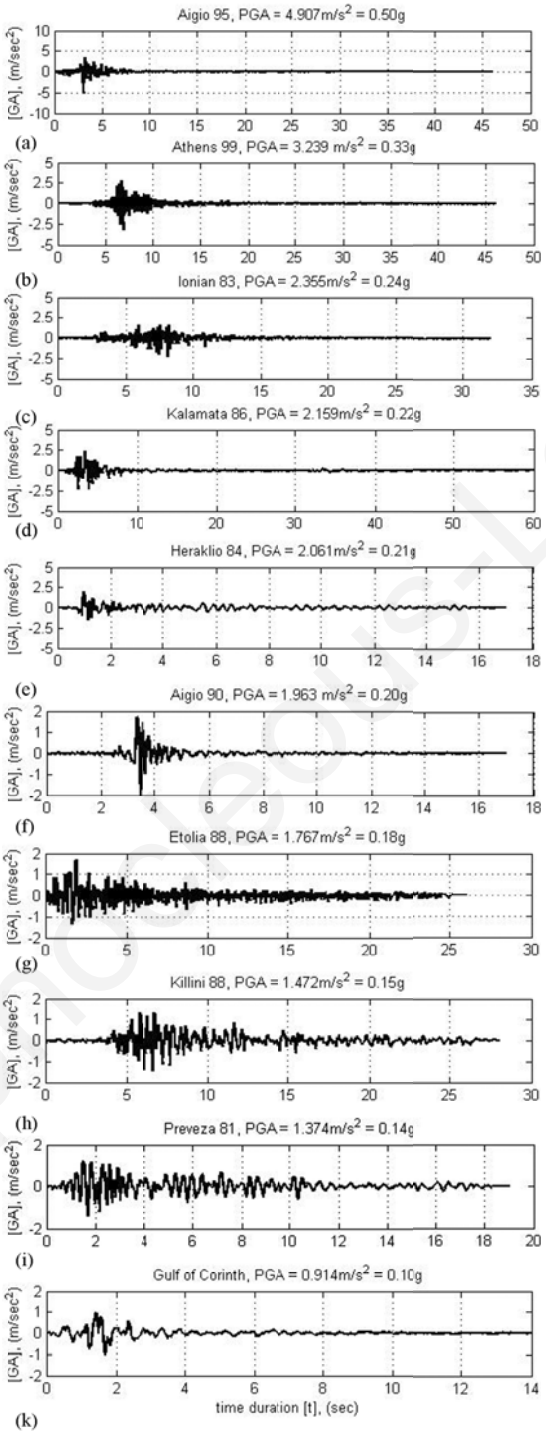

Figure 7.1 Greek Mediterranean seismic input records.

7.2 ADCS1 Dynamic Response Verification

7.2.1 Energy dissipation verification for ADCS1

The capability of ADCS1 design configuration to enhance energy dissipation in the system under the action of the ten selected seismic records was verified for the selected damper's steel plates of n = 2, t = 2.8 cm, h = 25 cm and b = 10 cm (damper: 2282510, DR = 392 1/m, k_d = 9835 kN/m, P_y = 25.09 kN). EEDI reaches 73.98 % in seismic case 1, 88.36 % in case 2, 27.90 % in case 3, 79.00 % in case 4, 28.82 % in case 5, 56.82 % in case 6, 70.20 % in case 7, 52.45 % in case 8, 67.23 % in case 9, whereas practically no energy dissipation is succeeded in case 10 (Figure 7.2).

ADCS1 resistance to the different seismic events in terms of energy dissipation depends strongly on the dynamic properties of each seismic excitation ([7.3]). The configuration design is tuned to mitigate the relative sensitivity to each ground motion and in 30 % of the cases the system performs unsatisfactorily, i.e. in seismic cases 2, 4 and 10, whereas in 20 % of the cases the system's performance is on average, i.e. in seismic cases 6 and 8 and in half of the cases the system performs successfully with an energy dissipation of over 67.00 % of the input energy. On average, EEDI accounts for all ten earthquake excitations to 54.48 %.

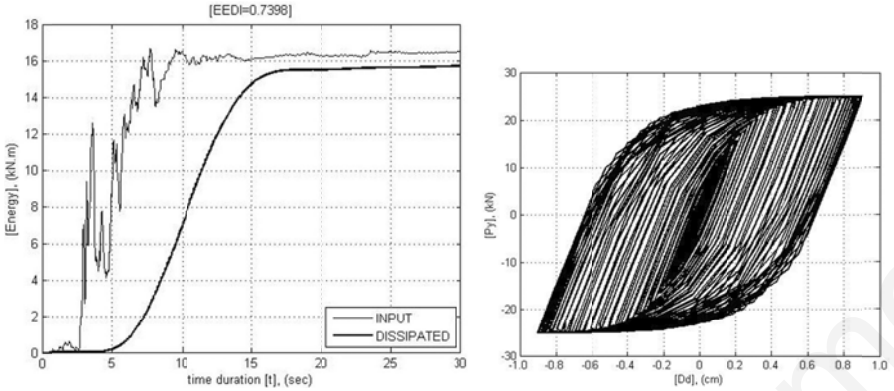

(a)

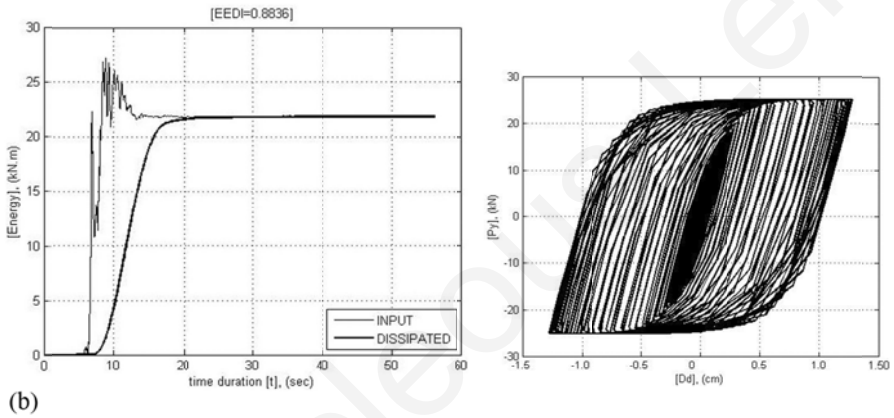

(b)

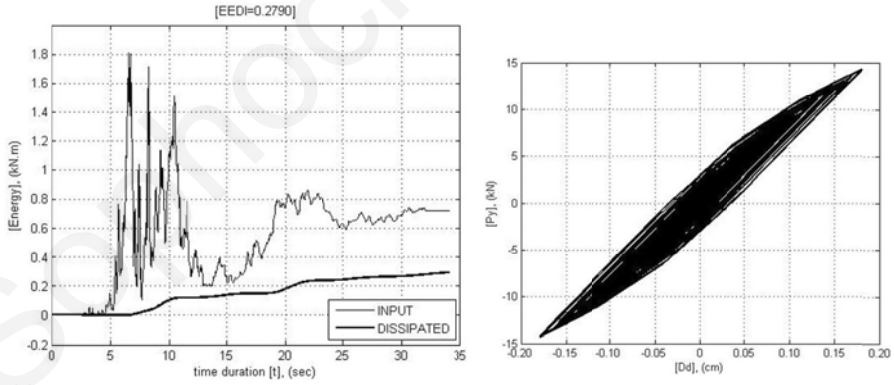

(c)

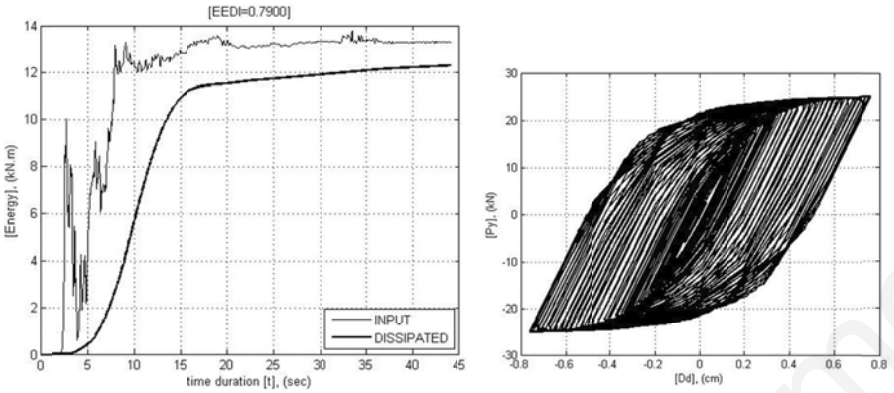

(d)

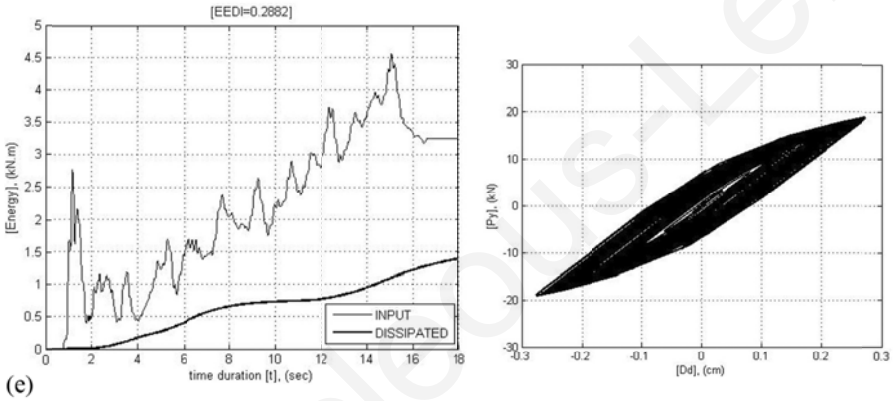

(e)

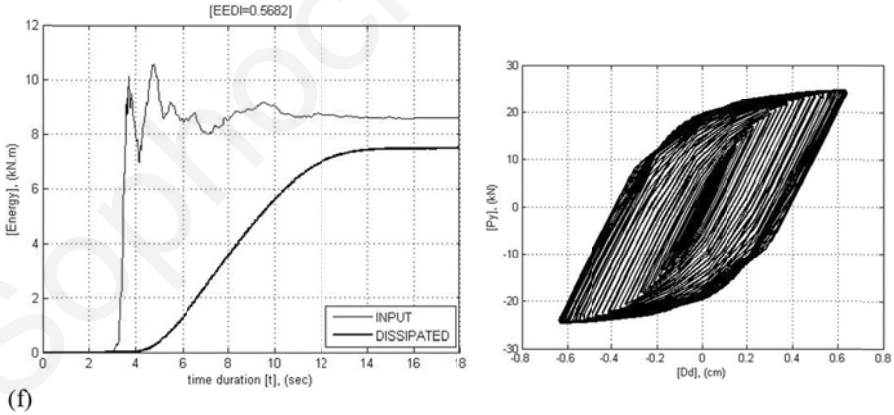

(f)

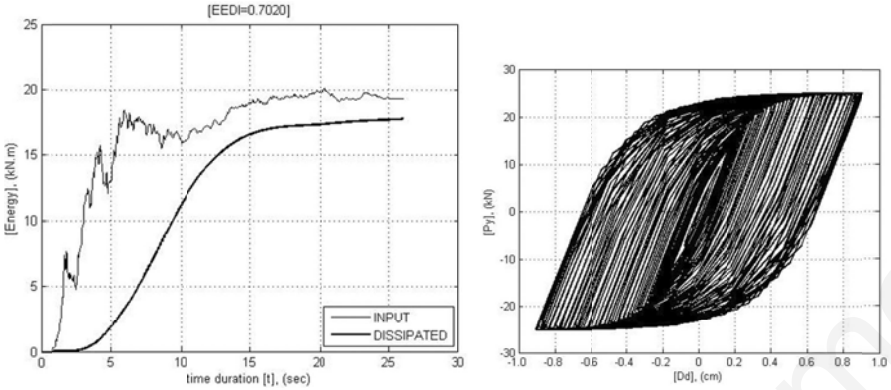

(g)

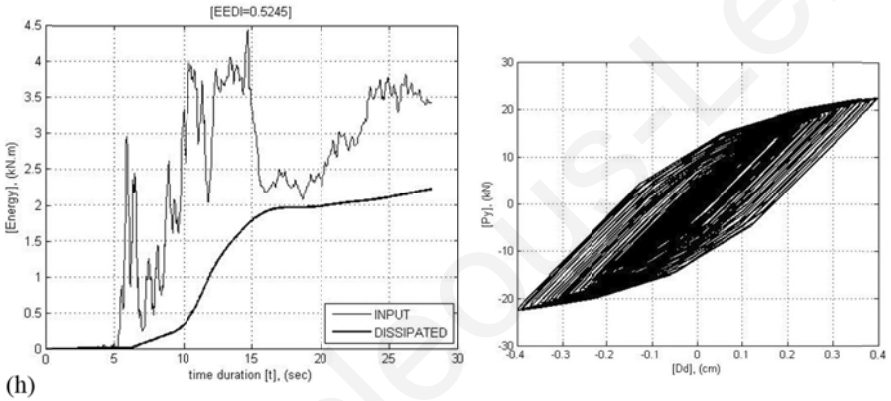

(h)

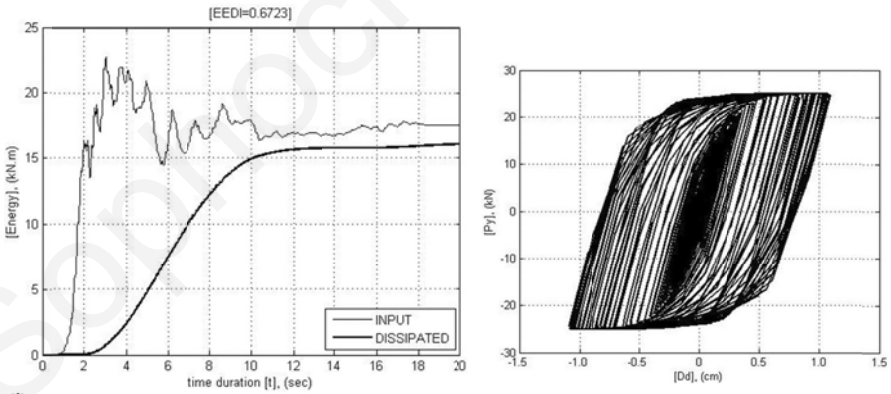

(i)

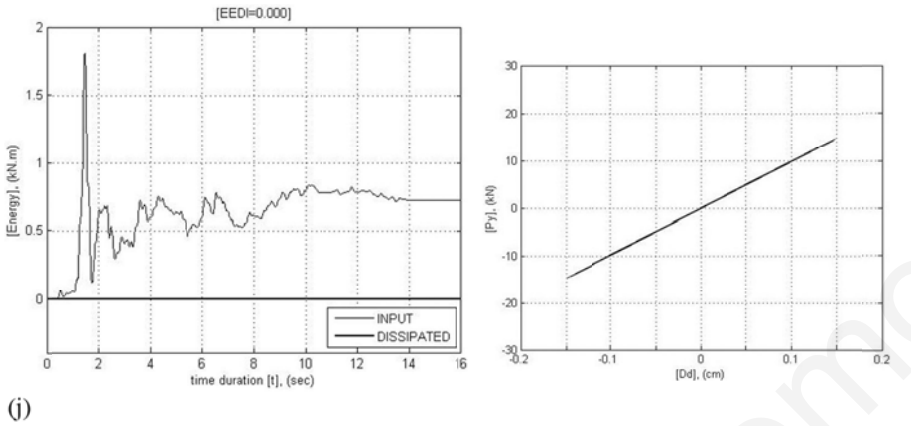

Figure 7.2 ADCS1 hysteretic damper's energy dissipation and force-deformation behavior (damper: 2282510): (a) seismic case 1; (b) seismic case 2; (c) seismic case 3; (d) seismic case 4; (e) seismic case 5; (f) seismic case 6; (g) seismic case 7; (h) seismic case 8; (i) seismic case 9; (j) seismic case 10.

7.2.2 Base shear verification for ADCS1

The maximum base shear responses of the controlled system obtained in the ten seismic cases are compared to the primary frame's respective responses (Table 7.2). In 10 % of the cases (seismic case 7) the maximum base shear is increased by 59.37 %, whereas in all other cases there is a considerable respective decrease as follows: 14.00 % in case 1, 12.00 % in case 2, 5.80 % in case 3, 4.69 % in case 4, 57.97 % in case 5, 13.86 % in case 6, 73.91 % in case 8, 32.68 % in case 9 and 3.59 % in case 10. On average ADCS1 causes 15.91 % decrease of the controlled system's base shear.

Table 7.2 Primary frame's and ADCS1 (damper: 2282510) maximum base shear BS.

Seismic Case	Max. base shear [kN]	
	Primary frame	ADCS1
1	1577.00	1355.27
2	2048.00	1798.69
3	500.30	471.28
4	1278.00	1218.54
5	1738.00	730.50
6	1361.00	1172.43
7	882.90	1407.06
8	2516.00	656.47
9	2445.00	1646.02
10	519.10	500.47

7.2.3 Relative displacements verification for ADCS1

The absolute values of the relative displacements of ADCS1 under the ten seismic records of the Mediterranean are compared to the respective responses of the primary frame. The results verify that in 60 % of the cases the relative displacements responses of the controlled system are not increased, whereas a slight increase is obtained in 40 % of the cases as follows: 0.27 % in seismic case 3, 0.77 % in case 4, 0.84 % in case 7 and 0.97 % in case 10. The respective responses decrease accounts to 2.50 % in case 1, 0.56 % in case 2, 52.34 % in case 5, 2.47 % in case 6, 70.00 % in case 8 and 23.41 % in case 9 (Table 7.3). On average ADCS1 causes 14.84 % decrease of the system's maximum relative displacements.

Table 7.3 Primary frame's and ADCS1 (damper: 2282510) maximum relative displacements U_x.

Seismic Case	Max. relative displacement [cm]	
	Primary frame	ADCS1
1	1.918	1.87
2	2.494	2.48
3	0.633	0.65
4	1.542	1.66
5	2.119	1.01
6	1.661	1.62
7	1.067	1.96
8	3.066	0.91
9	2.977	2.28
10	0.629	0.69

7.3 ADCS2 Dynamic Response Verification

7.3.1 Energy dissipation verification for ADCS2

ADCS2 (damper: 616355, DR = 114.3 1/m, k_d = 1003.10 kN/m, P_y = 8.78 kN) for the selected damper's geometry of n = 6, t = 1.6 cm, h = 35 cm and b = 5 cm, was verified under the action of the ten selected seismic records of the Mediterranean region ([7.6], [7.7]). The following EEDI values are obtained (Figure 7.3): 92.36 % in seismic case 1, 88.96 % in case 2, 92.04 % in case 3, 95.39 % in case 4, 81.57 % in case 5, 76.41 % in case 6, 91.52 % in case 7, 79.50 % in case 8, 70.03 % in case 9 and 86.82 % in case 10. In all the events ADCS2 dissipates on average 85.46 % of the input energy.

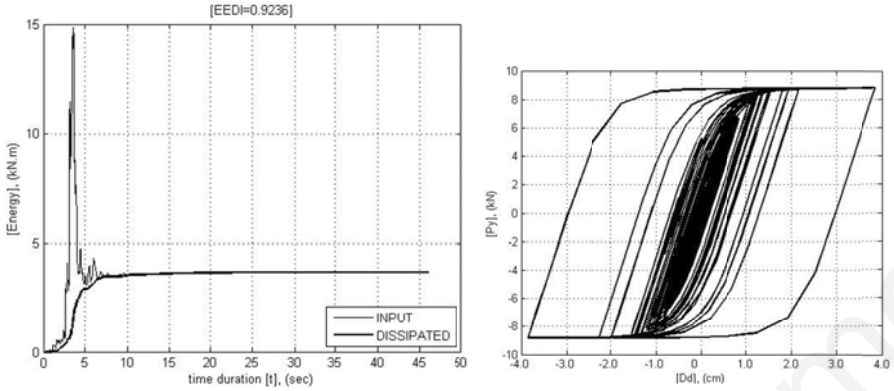

(a)

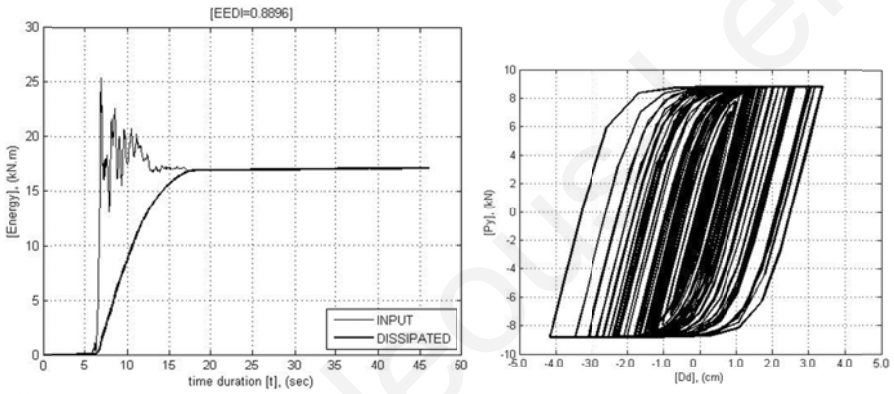

(b)

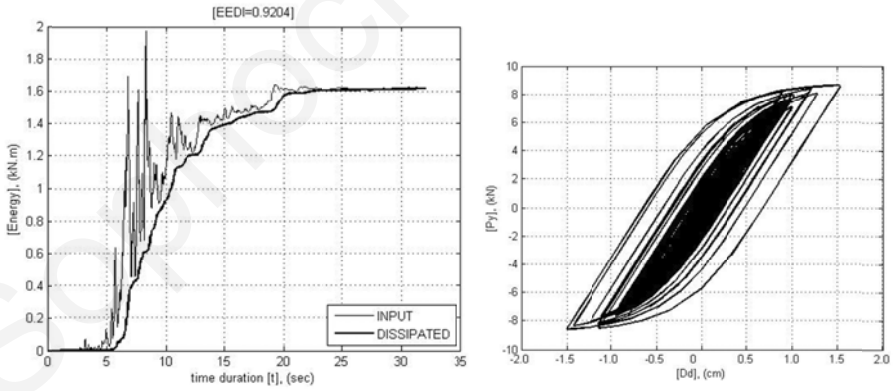

(c)

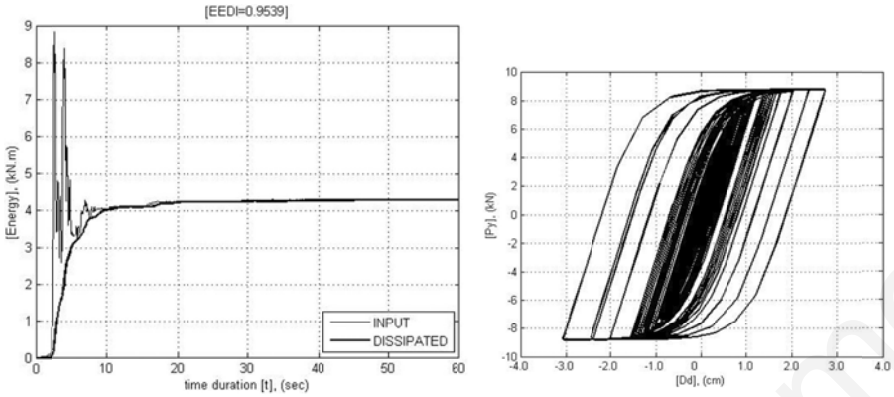

(d)

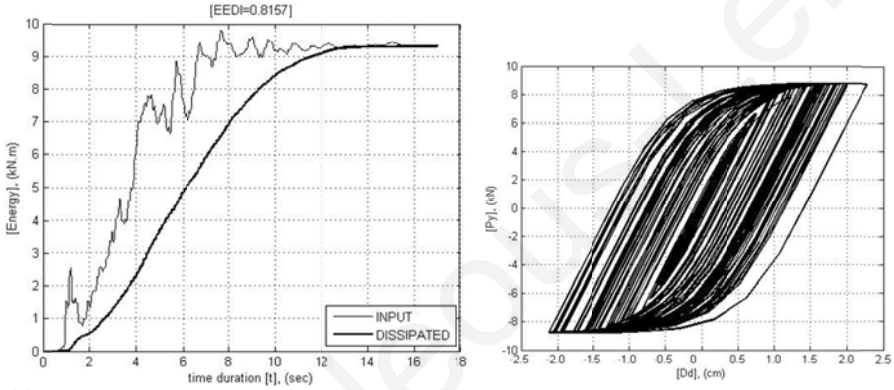

(e)

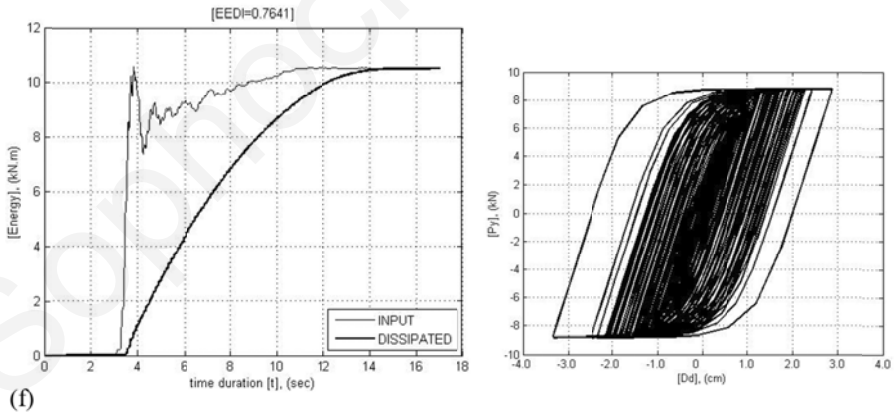

(f)

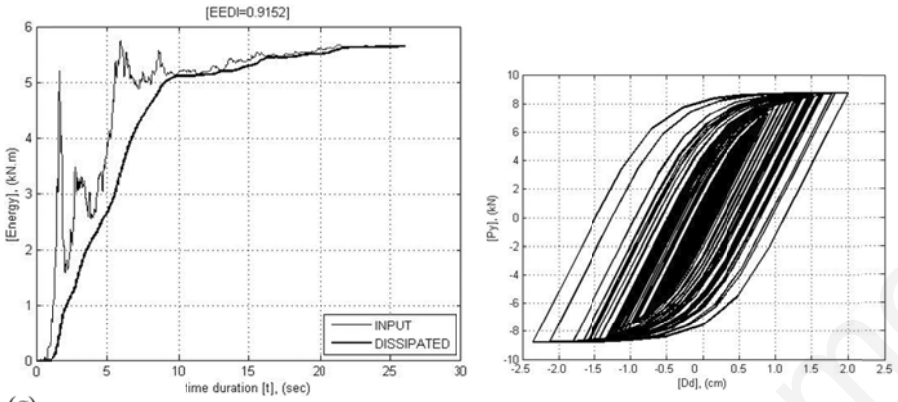

(g)

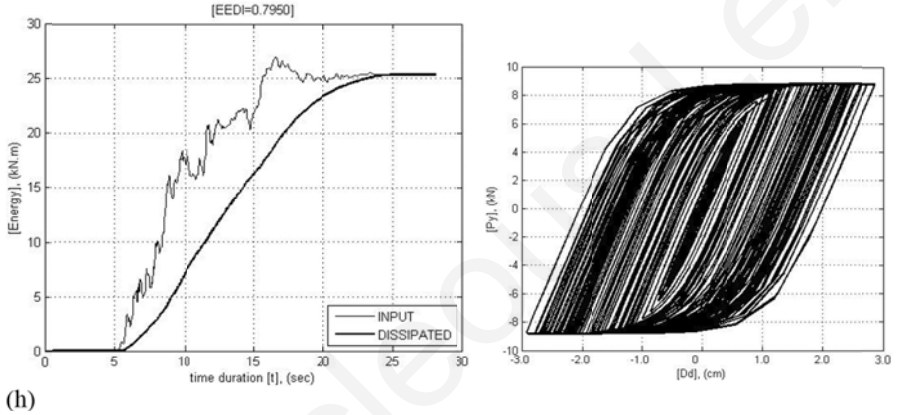

(h)

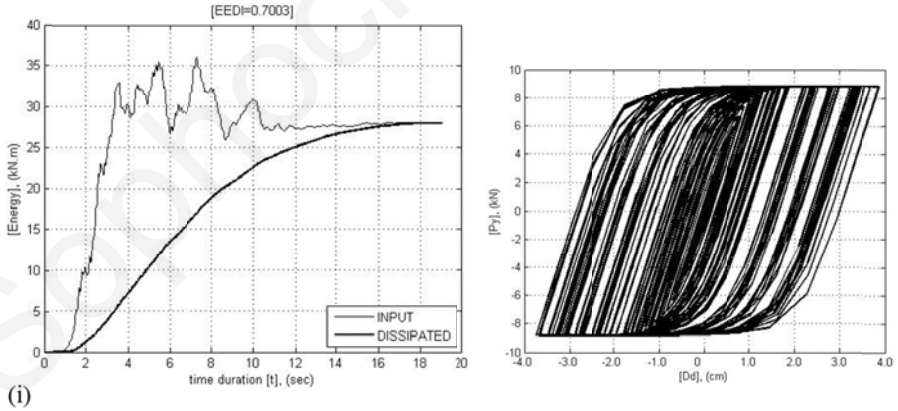

(i)

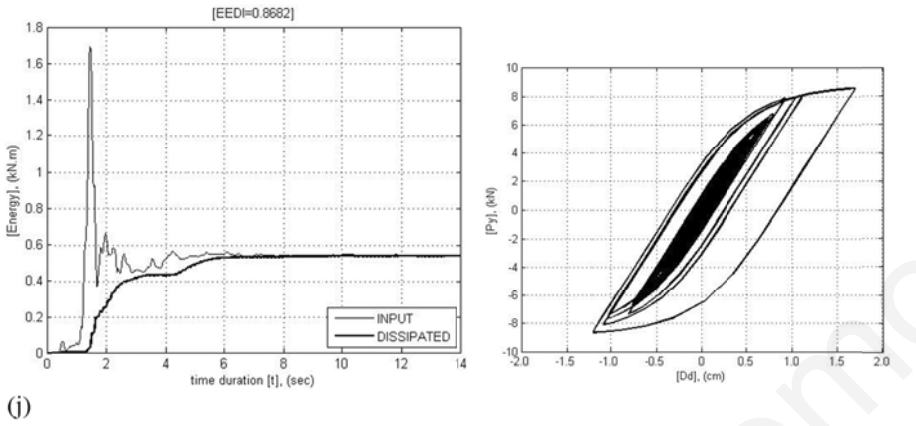

Figure 7.3 ADCS2 hysteretic damper's energy dissipation and force-deformation behavior (damper: 616355): (a) seismic case 1; (b) seismic case 2; (c) seismic case 3; (d) seismic case 4; (e) seismic case 5; (f) seismic case 6; (g) seismic case 7; (h) seismic case 8; (i) seismic case 9; (j) seismic case 10.

7.3.2 Base shear verification for ADCS2

In 30 % of the cases examined the maximum base shear of the controlled system increases: By 29.00 % in seismic case 3, 18.00 % in case 7 and 0.50 % in case 10 (Table 7.4). The respective response decreases by 11.52 % in case 1, by 7.50 % in case 2, by 6.70 % in case 4, by 27.39 % in case 5 and by 11.35 % in case 6. On average ADCS2 causes 1.70 % decrease of the controlled systems base shear.

Table 7.4 Primary frame's and ADCS2 (damper: 616355) maximum base shear BS.

Seismic Case	Max. base shear [kN]	
	Primary Frame	ADCS2
1	1577.00	1395.31
2	2048.00	1894.39
3	500.30	645.57
4	1278.00	1192.3
5	1738.00	1261.95
6	1361.00	1206.59
7	882.90	1042.11
8	2516.00	1389.42
9	2445.00	2094.37
10	519.10	521.68

7.3.3 Relative displacements verification for ADCS2

Favorite results are obtained in 70 % of the cases. In seismic cases 2, 3 and 6 an increase of the relative displacements is registered, by 0.38 %, 0.36 % and 0.25 % respectively. The respective decrease accounts to 29.60 % in case 1, 31.25 % in case 4, 31.00 % in case 5, 0.90 % in case 7, 38.35 % in case 8, 0.23 % in case 9 and 62.90 % in case 10 (Table 7.5). On average ADCS2 causes 19.32 % decrease of the system's maximum relative displacements.

Table 7.5 Primary frame's and ADCS2 (damper: 616355) maximum relative displacements U_x.

Seismic Case	Max. relative displacement [cm]	
	Primary frame	ADCS2
1	1.918	1.35
2	2.494	2.59
3	0.633	0.86
4	1.542	1.06
5	2.119	1.46
6	1.661	1.62
7	1.067	0.97
8	3.066	1.89
9	2.977	2.91
10	0.629	0.45

7.4 ADCS3 Dynamic Response Verification

7.4.1 Energy dissipation verification for ADCS3

ADCS3 system with an optimum damper of n = 6, t = 1.2 cm, h = 15 cm and b = 5 cm (damper: 612155, DR = 466.67 1/m, k_d = 5376 kN/m, P_y = 11.52 kN) is validated for its energy dissipation under the ten seismic records of reference [(7.5)]. EEDI accounts to 86.00 % in seismic case 1, 60.82 % in case 2, 86.35 % in case 3, 76.57 % in case 4, 86.45 % in case 5, 74.61 % in case 6, 89.57 % in case 7, 84.28 % in case 8, 62.80 % in case 9 and 53.32 % in case 10. On average ADCS3 reaches an EEDI of 76.08 % (Figure 7.4).

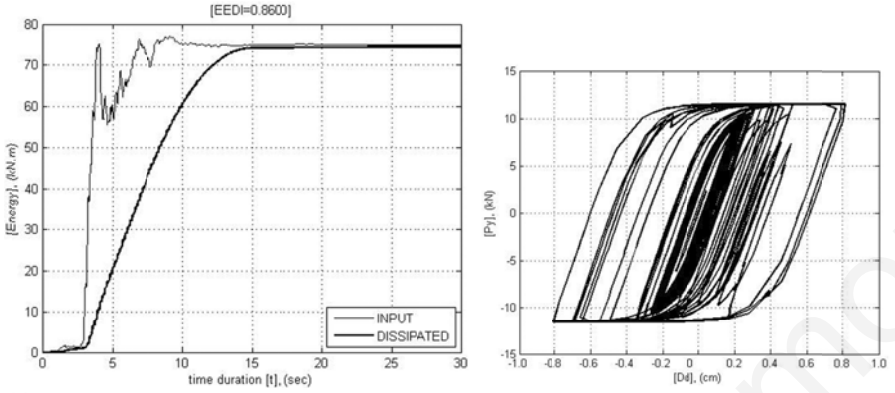

(a)

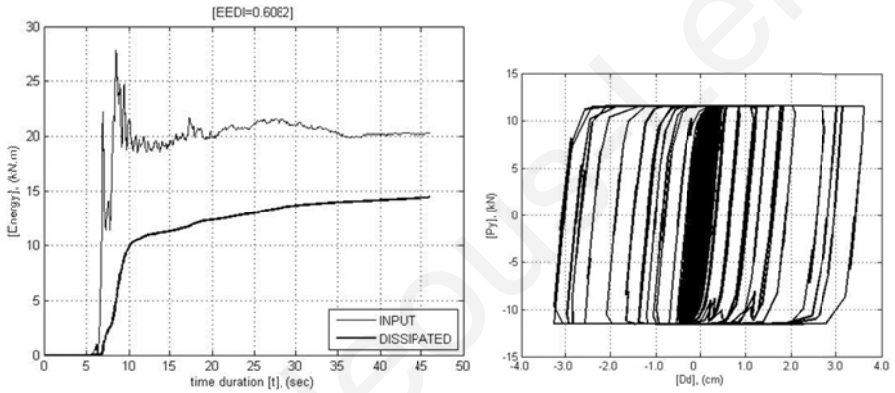

(b)

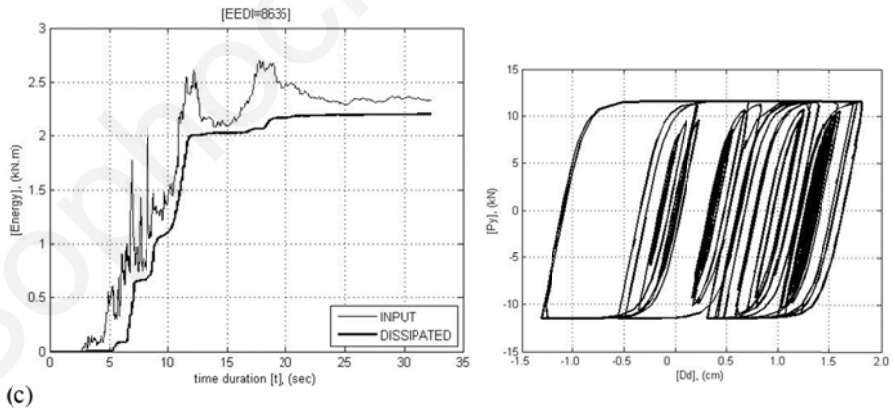

(c)

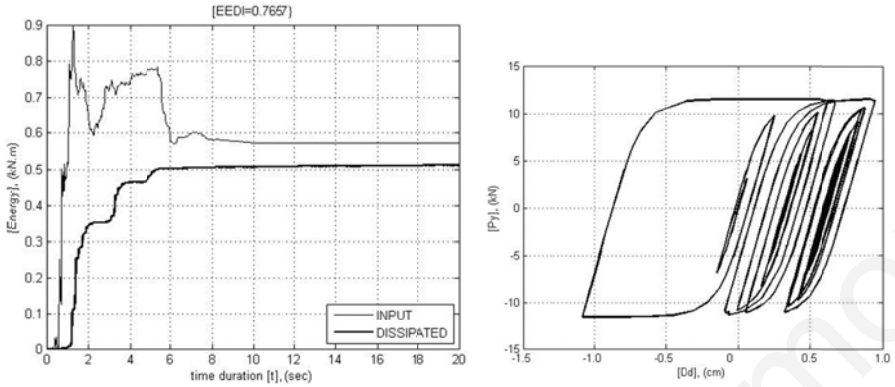

(d)

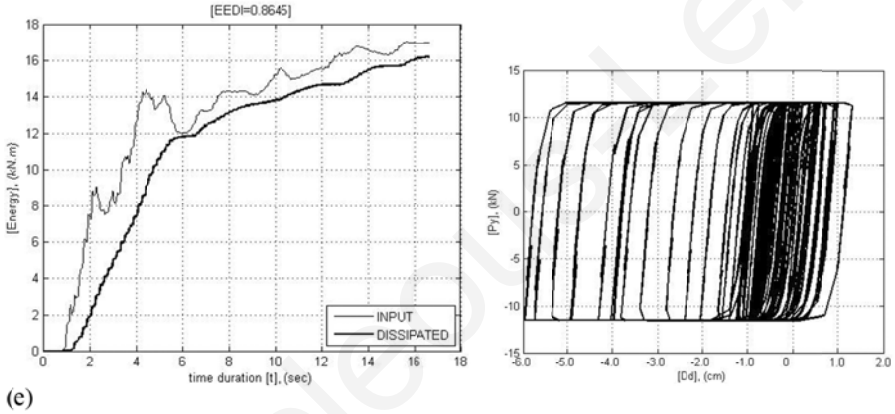

(e)

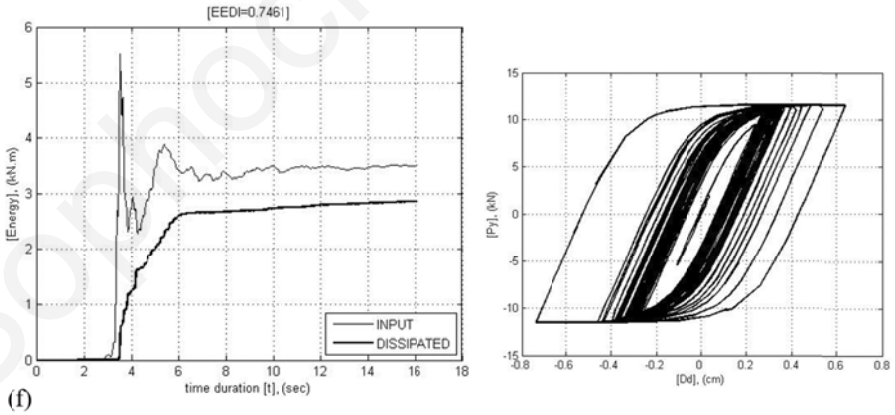

(f)

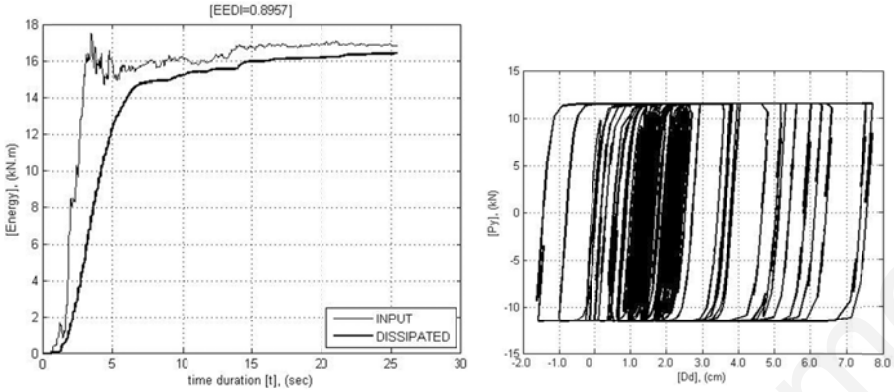

(g)

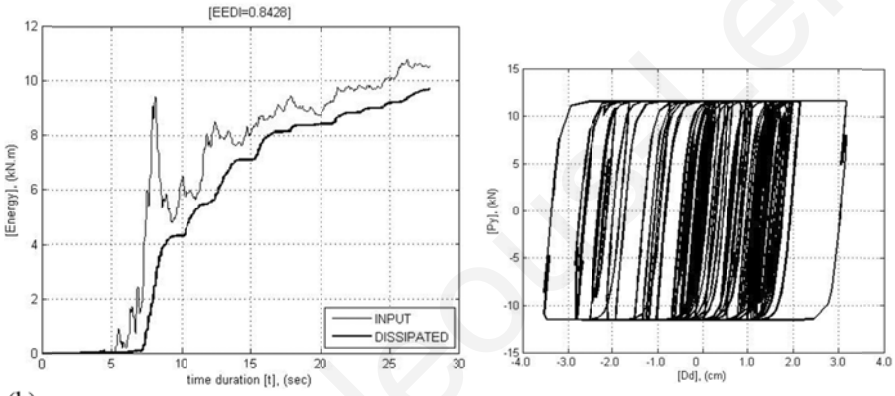

(h)

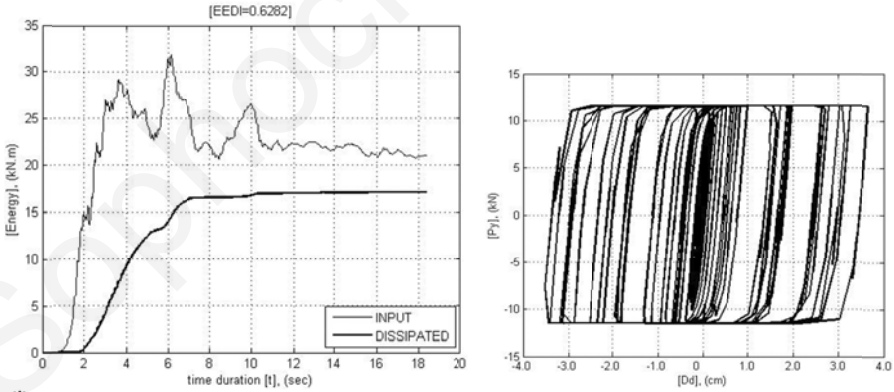

(i)

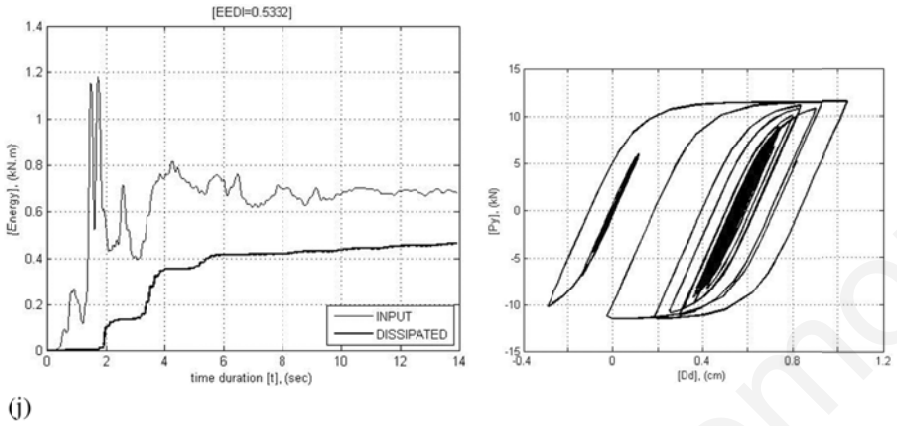

Figure 7.4 ADCS3 hysteretic damper's energy dissipation and force-deformation behavior (damper: 612155): (a) seismic case 1; (b) seismic case 2; (c) seismic case 3; (d) seismic case 4; (e) seismic case 5; (f) seismic case 6; (g) seismic case 7; (h) seismic case 8; (i) seismic case 9; (j) seismic case 10.

7.4.2 Base shear verification for ADCS3

The results obtained from the comparison of the maximum base shear responses of ADCS3 and the primary frame are presented in (Table 7.6). In 70 % of the seismic cases the maximum base shear decreases and in 20 % it increases, while in 10 % it remains at the same levels. Decrease in base shear varies as follows: 19.90 % in seismic case 1, 12.00 % in case 2, 76.00 % in case 4, 53.00 % in case 5, 8.30 % in case 6, 48.50 % in case 8 and 26.00 % in case 9. In case 10 the results are at the same levels, while an increase is observed in cases 3 and 7, by 9.50 and 41.00 % respectively. On average ADCS3 causes 19.32 % decrease of the controlled system's base shear.

Table 7.6 Primary frame's and ADCS3 (damper: 612155) maximum base shear BS.

Seismic case	Max. base shear [kN]	
	Primary frame	ADCS3
1	1577.00	1263.62
2	2048.00	1801.96
3	500.30	547.84
4	1278.00	301.38
5	1738.00	817.43
6	1361.00	1248.33
7	882.90	1245.33
8	2516.00	1295.47
9	2445.00	1809.32
10	519.10	519.39

7.4.3 Relative displacements verification for ADCS3

The maximum magnitudes for the relative displacements in absolute values for ADCS3 and the primary frame are included in (Table 7.7). In general the relative displacements are mitigated in respect to their peak values. Except for seismic cases 3 and 7, where an increase of 16.90 and 55.60 % is respectively valid, in all remaining cases the controlled system performed well. No respective variation was observed in case 6. Respective responses reductions account to 11.36 % in case 1, 2.96 % in case 2, 74.00 % in case 4, 49.00 % in case 5, 43.90 % in case 8, 19.00 % in case 9 and 0.97 % in case 10. On average ADCS3 causes 12.87 % decrease of the system's maximum relative displacements.

Table 7.7 Primary frame's and ADCS3 (damper: 612155) maximum relative displacements U_x.

Seismic case	Max. relative displacement [cm]	
	Primary frame	ADCS3
1	1.918	1.70
2	2.494	2.42
3	0.633	0.74
4	1.542	0.40
5	2.119	1.08
6	1.661	1.66
7	1.067	1.66
8	3.066	1.72
9	2.977	2.41
10	0.629	0.69

CHAPTER 8 **CONCLUSIONS**

8.1 Research Contributions

This research work focuses on the investigation of bracing-damper mechanisms, defined as Adaptable Dual Control Systems, ADCS, for earthquakes of moderately long, extremely irregular motions. ADCS provide alternative choices for the designer for passive structural control, as regards frame structures with control members for an effective energy dissipation behavior. A key difference from the research on the performance of conventional energy dissipation systems is that rods or cables are used as bracings that activate a respective kinetic mechanism by utilizing mechanical discs as connection devices of the tension-only members. The investigation in respect to the configuration and construction design of the control members has led to the present proposal for three new configuration designs and a modification of an already proposed one.

As regards previous limited studies on bracing mechanisms with hysteretic dampers, this research work provides additional information in respect to the effectiveness of the configuration designs of ADCS, when the selected input records differ in their frequency content, peak ground acceleration and time duration. The results indicate that significant portions of input energy may be dissipated, when optimum geometrical and mechanical parameters are assigned to the secondary control members, enabling the primary frame to resist elastically. At the same time the base shear and relative displacement responses of the controlled systems are kept under controllable limits.

The design configurations of the bracing-damper mechanisms investigated in the present study lead to a continuous most uniform counteraction of all structural members to resist the earthquake loading, while they practically avoid an interaction on the stiffness of the primary frame. Therefore the application of the control mechanism in ADCS1, ADCS2 and ADCS3 becomes an attractive alternative, not only for the design of earthquake resistant structures, but also for the seismic retrofit of existing ones. The proposals are

attractive within the broader architectural, aesthetic, constructability and economic context offering four alternative forms to serve differing preferences in applications.

8.2 Research Results

The code dominated capacity design for earthquake resistant systems, relies upon the inherent ductility of buildings to prevent catastrophic failure, while accepting a certain level of structural and nonstructural damage. Within this philosophy approach, the structure is designed to resist the earthquake equivalent static loads and yields reasonably successful results. However, by considering the actual dynamic nature of the earthquake phenomenon, new and innovative concepts of structural protection have been advanced.

The method of integrating hysteretic dampers within the structure, with the primary purpose to provide a source of energy dissipation and therefore reduce seismic damage, comprises an increasingly promising method for passive structural control. For the SDOF frames subjected to seismic loading, the hysteretic energy dissipation demand for the primary systems reduces with the increase of damping due to the added hysteretic devices, although the input energy also changes since it depends on the deformation. In cases with an input energy increase, associated consequences in terms of accumulated dependent damages, need to be avoided.

As far as the application of bracings is concerned, stiff members are used that interact with the stiffness of the primary frame resulting to possibly increased strength demands for the controlled system. This disadvantage could be overcome, if flexible members are used instead. Flexible bracings though are vulnerable to compression buckling and tension yielding, when the design displacements enter the inelastic region of the members' response. Therefore the application of cable-bracings for earthquake is not self evident.

In order to effectively resist seismic forces using tension-only members the design and development of a suitable kinetic mechanism is required. Energy dissipation and an effective performance of the bracing-damper mechanism may be achieved with a closed circuit in its configuration and through a dual action in its response. The displacement

dependent damper, responsible for the energy dissipation, exhibits hysteresis of the wen-plasticity model, while the response when optimum values for the design parameters are assigned, may be independent of frequency of excitation.

In the frame of the current Ph.D. thesis the development of Adaptable Dual Control Systems, ADCS, based on three new configuration alternatives and a minor modification of an already proposed one, concentrates on the investigation of the dynamic response behavior of the controlled systems under three selected international seismic input records. The systems' behavior is further verified under ten selected Mediterranean earthquakes. ADCS design proposals for frame systems, consist of added slender bracings that form a closed circuit and a hysteretic damper of steel plates. ADCS potential for effective energy deformation is investigated, while base shear and relative displacement responses are compared with the respective values of the primary frame.

ADCS innovative mechanisms differ in their configuration design: ADCS0 consists of a cross and a horizontal bracing and hysteretic damper plates placed at the midpoint of the primary beam; ADCS1 forms a portal frame assembly of tension rods and hysteretic damper plates at the midpoint, ADCS2 is formed with a chevron bracing added to the portal framing and the damper plates added at midpoint of the primary beam and ADCS3 follows a triangular shape in its bracing, while the damper is placed at the main joint region to utilize the energy dissipation component from the horizontal- and diagonal tensile members. ADCS share common features in terms of the enhancement of the elastic response of the primary structure and the dissipation of the earthquake induced energy through plastic hysteresis of the dampers. Research studies of ADCS follow simulation and modeling methods with the software SAP2000 and are based on a simplified SDOF model. The optimization procedure in the parametric studies conducted, yielded the dominant values of the damper's mechanical and geometrical properties governing each system for a related desirable performance in seismic control. In this respect the quantifiable criterion of the Effective Energy Deformation Index, EEDI and the Damper Ratio, DR, seem to govern the control efficiency of ADCS.

From the numerical analyses of the controlled systems conducted the following conclusions can be drawn:

- The integration of the bracing damper mechanism in frames enables the elastic response of the primary system.
- The control mechanism in all configuration alternatives ensures that all members contribute to the energy dissipation during a complete cycle of seismic excitation.
- Under static loading, the control mechanism does not practically influence the response of the primary system, since the overall stiffness increases practically insignificantly with the addition of the bracings and the damper within. Therefore the control mechanism may also be suitable for retrofitting purposes of existing structures.
- The use of cables in ADCS for the activation of the control mechanism, offers additional benefits of aesthetic qualities as regards architectural form, economy and ease of construction and repetition for industrial production in a broader architectural and technological content.

In respect to the dynamic behavior of the four controlled systems under investigation, the following specific conclusions are possible to be drawn:

The results of ADCS0, which was modified in terms of the damper section used, are reevaluated for the same seismic record as in the original proposal and estimated for two more records of earthquakes of the international region, yielding the following information:

- On average, for the international seismic records, the Effective Energy Deformation Index, EEDI, reaches 80.63 %, when the optimum value of Damper Ratio, DR = 265.45 1/m, (damper: 1012205, k_d = 3910 kN/m, P_y = 14.73 kN) is assigned to the integrated hysteretic damper.

The portal configuration of the bracing-damper mechanism in ADCS1 is realized with tension rods instead of cables for the bracing, since the associated required pretension is triggered high. Also a diaphragm constraint for the controlled frame at roof level and the out of plane direction should be assured. In summary ADCS1 seismic behavior is satisfactory. In particular:

- The Effective Energy Deformation Index, EEDI, reaches on average 83.48 % for the international- and 54.48 % for the Mediterranean seismic records, when the optimum Damper Ratio, DR = 392 1/m, (damper: 2282510, k_d = 9835 kN/m, P_y = 25.09 kN) is assigned to the integrated hysteretic damper.

- The average decrease of the maximum base shear accounts to 20 % for the international- and 15.91 % for the Mediterranean seismic records.

- The relative displacements of the controlled system reduce on average by 8 % for the international- and 14.84 % for the Mediterranean seismic records.

In the case when a chevron bracing is added to the portal bracing in order to form ADCS2 configuration, the earthquake response of the controlled system may be further improved. As it is verified through the investigation, the additional chevron- to the portal bracing succeeds in increasing the damper's own plastic deformations during strong seismic excitations. In particular:

- The Effective Energy Deformation Index, EEDI, reaches on average 84.38 % for the international- and 85.46 % for the Mediterranean seismic records, when the optimum value of Damper Ratio, DR = 114.3 1/m, (damper: 616355, k_d = 1003.10 kN/m, P_y = 8.78 kN) is assigned to the integrated damper.

- The average decrease of the maximum base shear accounts to 6.3 % for the international- and 1.70 % for the Mediterranean seismic records.

- The relative displacements of the controlled system reduce on average by 8 % for the international- and 19.32 % for the Mediterranean seismic records.

The third alternative configuration design studied, ADCS3, provides similarly to the former an opening at the façade, but with less bracing members. In particular:

- The Effective Energy Deformation Index, EEDI, reaches on average 79.09 % for the international- and 76.08 % for the Mediterranean seismic records, when the optimum value of Damper Ratio, DR = 466.67 1/m, (damper: 612155, k_d = 5376 kN/m, P_y = 11.52 kN) is assigned to the integrated damper.

- The average decrease of the maximum base shear accounts to 14.33 % for the international- and 19.32 % for the Mediterranean seismic records.

- The relative displacements of the controlled system reduce on average by 5 % for the international- and 12.87 % for the Mediterranean seismic records.

Respective publications of ADCS numerical analyses conducted and the controlled systems' dynamic behavior evaluation, included in international refereed scientific conference proceedings and international refereed scientific journals, are presented in the references of the present chapter ([8.1], [8.2], [8.3], [8.4], [8.5], [8.6], [8.7], [8.8], [8.9], [8.10], [8.11], [8.12])

8.3 Future Work

The results of dynamic analyses conducted in the present study are based on the model of elastic equivalent damper stiffness. A more realistic description of the controlled frame behavior can be supplied from time history analyses, whereas the real damper stiffness as based on its developed hysteretic loop is considered.

Further investigations on the applicability of ADCS concept can also address multi-storey structures as regards both the stiffness- and damping distribution over the height.

REFERENCES

[1.1] Aiken, I.D., Nims, D.K., Whittaker, A.S., Kelly, J.M., (1993), "Testing of passive energy dissipation systems", *Journal of Earthquake Spectra*, Vol. 9, No. 3, pp. 335 - 369.

[1.2] Di Sarno, L., Elnashai, A.S., (2005), "Innovative strategies for seismic retrofitting of steel and composite structures", *Journal of Progress in Structural Engineering and Materials*, Vol. 7, pp. 115 - 135.

[1.3] Filiautrault, A., Cherry, S., (1988), "Comparative performance of friction damped systems and base isolation systems for earthquake retrofit and aseismic design", *Journal of Earthquake Engineering and Structural Dynamics*, Vol. 16, pp. 389 - 416.

[1.4] Housner, G.W., Bergman, L.A., Caughey, T.K., Chassiakos, A.G., Claus, R.O., Masri, S.F., (1997), "Structural control: past, present and future", *Journal of Engineering Mechanics*, Vol. 123, No. 9, pp. 897 - 971.

[1.5] Inoue, K., Kuwahara, S., (1998), "Optimum strength ratio of hysteretic damper", *Journal of Earthquake Engineering and Structural Dynamics*, Vol. 27, pp. 577 - 588.

[1.6] Kurata, M., DesRoches, R., Leon, R.T., (2008), "Cable damper bracing for partial seismic rehabilitation", *Proceedings of 14th World Conference on Earthquake Engineering,* Beijing, China.

[1.7] Martelli, A., (2007), "Seismic isolation and energy dissipation: worldwide application and perspectives", Brebbia, C.A. (ed.), *Earthquake Resistant Engineering Structures VI*, WIT Press, Southampton, pp. 105 - 116.

[1.8] Mualla, I.H., Nielsen, L.O., Belev, B., Liao, W.I., Loh, C.H., Agrawal, A., (2002), "Performance of friction-damped frame structure: Shaking table testing and numerical simulations", *Proceedings of 7th US National Conference on Earthquake Engineering,* Boston, USA.

[1.9] Phocas, M.C., Pocanschi, A., (2003), "Steel frames with bracing mechanism and hysteretic dampers", *Journal of Earthquake Engineering and Structural Dynamics*, Vol. 32, No. 5, pp. 811 - 825.

[1.10] Phocas, M.C., Sophocleous, T., (2011), "Adaptable dual control systems for earthquake resistance", Brebbia, C.A., Maugeri, M. (eds), *Earthquake Resistant Engineering Structures VIII, ERES 2011,* WIT Press, Southampton, pp. 55 - 66.

[1.11] Renzi, E., Perno, S., Pantanella, S., Ciampi, V., (2007), "Design, test and analysis of a light-weight dissipative bracing system for seismic protection of structures", *Journal of Earthquake Engineering and Structural Dynamics*, Vol. 36, No. 4, pp. 519 - 539.

[1.12] Sophocleous, T., Phocas, M.C., (2009), "Dual earthquake resistant frames", Phocas, M., Brebbia, C.A., Komodromos, P. (eds), *Earthquake Resistant Engineering Structures VII, ERES 2009,* WIT Press, Southampton, pp. 165 - 174.

[1.13] Tremblay, R., Filiatrault, A., (1996), "Seismic impact loading in inelastic tension-only concentrically braced frames: myth or reality?", *Journal of Earthquake Engineering and Structural Dynamics*, Vol. 25, No. 12, pp. 1373 - 1389.

[1.14] Tsai, K.C., Chen, H.W., Hong, C.P., Su, Y.F., (1993), "Design of steel triangular plate energy absorbers for seismic-resistance construction", *Journal of Earthquake Spectra*, Vol. 9, pp. 505 - 528.

[1.15] Wu, B., Zhang, J., Williams, M.S., Ou, J., (2005), "Hysteretic behavior of improved Pall-typed frictional dampers", *Journal of Engineering Structures*, Vol. 27, pp. 1258 - 1267.

[1.16] Xia, C., Hanson, R.D., (1992), "Influence of ADAS element parameters on building seismic response", *Journal of Structural Engineering*, Vol. 118, No. 7, pp. 1903 – 1918.

[2.1] Engel, H., (2009), "*Structure Systems*", Hatje Cantz, Stuttgart.

[2.2] Kyprianou, C.N., (2009), "*Hybrid Structural Systems*", Department of Civil and Environmental Engineering, University of Cyprus, Nicosia, in Greek.

[2.3] Phocas, M.C., Steel Buildings, (2007), "*Construction design*". Architects and Civil Engineers, Cyprus Civil Engineers and Architects Association, Response Publications, Nicosia, No. 75, pp. 49 - 52, in Greek.

[2.4] Phocas, M.C., Sophocleous, T., (2009), "Design of structures in architecture. Architectural vision towards structural innovation", Spiridonidis, C., Voyatzaki, M. (eds), *Architectural Design and Construction Education, Experimentation towards Integration, ENHSA - EAAE Architectural Design Teachers` and Construction Teachers` Networks*, University of Genoa, Genoa, Italy, EAAE Transactions on Architectural Education, No. 45, pp. 443 - 453.

[2.5] Schlaich, J., Bergermann, R., Boegle, R., Cachola, A., Flagge, S. P., (2005), "*Light Structures*", Prestel, New York.

[3.1] Ani, N., Sigaher, B., Constantinou, C.M., (2004), "Scissor-jack-damper energy dissipation system", *Technical Report MCEER-04-0010*, Multidisciplinary Centre for Earthquake Engineering Research, Buffalo, New York.

[3.2] Black, C., Makris, N., Aiken, I., (2001), "*Component testing, stability analysis and characterization of buckling restrained braces*", Final Report to Nippon Steel Corporation, University of California, Berkeley, California.

[3.3] Chang, K.C., Shen, K.L., Soong, T.T., Lai, M.L., (1994), "Seismic retrofit of a concrete frame with added viscoelastic dampers", *Proceedings of 5th National Conference on Earthquake Engineering*, Chicago, Illinois.

[3.4] Clark, P.W., Aiken, I.D., Tajirian, F., Kasai, K., Ko, E., Kimura, I., (1999), "Design procedures for buildings incorporating hysteretic damping devices", *Proceedings of*

Conference Seminar on Seismic Isolation, Passive Energy Dissipation and Active Control of Vibrations of Structures, Cheju, South Korea.

[3.5] Constantinou, M.C., Soong, T.T., Dargush, G.F., (1998), "Passive energy dissipation systems for structural design and retrofit", *Technical Report MCEE, Monograph No.1*, Multidisciplinary Centre for Earthquake Engineering Research, Buffalo, New York.

[3.6] Constantinou, M.C., Symans, M.D., (1993), "Experimental study of seismic response of buildings with supplemental fluid dampers", *Journal of Structural Design of Tall Buildings,* Vol. 2, No. 2, pp. 93 – 132.

[3.7] Constantinou, M.C., Tsopelas, P., Hammel, W., Sigaher, A.N., (2001), "Toggle-brace-damper seismic energy dissipation systems", *Journal of Structural Engineering,* Vol. 127, pp. 105 - 112.

[3.8] Di Sarno, L., Elnashai, A.S., (2005), "Innovative strategies for seismic retrofitting of steel and composite structures", *Journal of Progress in Structural Engineering and Materials*, Vol. 7, pp. 115 - 135.

[3.9] Filiautrault, A., Cherry, S., (1988), "Comparative performance of friction damped systems and base isolation systems for earthquake retrofit and aseismic design", *Journal of Earthquake Engineering and Structural Dynamics*, Vol. 16, pp. 389 - 416.

[3.10] Filiautrault, A., Cherry, S., (1987), "Performance evaluation of friction damped braced frames under simulated earthquake loads", *Journal of Earthquake Spectra*, Vol. 3, No. 1, pp. 57 - 78.

[3.11] Grigorian, C.E., Yang, T.S., Popov, E.P., (1993), "Slotted bolted connection energy dissipators", *Journal of Earthquake Spectra*, Vol. 9, No. 3, pp. 491 - 504.

[3.12] Hanson, R.D., Soong, T.T., (2001), "Seismic design with supplemental energy dissipation devices", *Technical Report EERI, Monograph No. 8,* Earthquake Engineering Research Institute, Oakland, Canada.

[3.13] Housner, G.W., Bergman, L.A., Caughey, T.K., Chassiakos, A.G., Claus, R.O., Masri, S.F., (1997), "Structural control: past, present and future", *Journal of Engineering Mechanics*, Vol. 123, No. 9, pp. 897 - 971.

[3.14] Inoue, K., Kuwahara, S., (1998), "Optimum strength ratio of hysteretic damper", *Journal of Earthquake Engineering and Structural Dynamics*, Vol. 27, pp. 577 - 588.

[3.15] Kim, J., Choi, H., (2004), "Behavior and design of structures with buckling restrained braces", *Journal of Engineering Structures,* Vol. 26, pp. 693 - 706.

[3.16] Kim, J., Choi, H., Min, K.W., (2009), "Use of rotational friction dampers to enhance seismic and progressive collapse resisting capacity of structures", *Journal of The Structural Design of Tall and Special Buildings,* Vol. 20, pp. 515 - 537.

[3.17] Kurata, M., DesRoches, R., Leon, R.T., (2008), "Cable damper bracing for partial seismic rehabilitation", *Proceedings of 14th World Conference on Earthquake Engineering,* Beijing, China.

[3.18] Lai, M.L., Chang, K.C., Soong, T.T., Hao, D.S., Yeh, Y.C., (1995), "Full-scale viscoelastically damped steel frame", *Journal of Structural Engineering*, Vol. 121, No. 1, pp. 1443 - 1447.

[3.19] Martelli, A., (2010), "Aseismic dissipating devices and unconventional shapes in seismic areas", Cruz (ed.), *Structures and Architecture,* Taylor & Francis Group, London.

[3.20] Martelli, A., (2007), "Seismic isolation and energy dissipation: worldwide application and perspectives", Brebbia, C.A. (ed.), *Earthquake Resistant Engineering Structures VI*, WIT Press, Southampton, pp. 105 - 116.

[3.21] Mayes, R., Goings, C., Naguib, W., Harris, S., Lovejoi, J., Fanucci, J., Bystricky, P., Hayes J., (2004), "Comparative performance of buckling restrained braces and moment frames", *Proceedings of 13th World Conference on Earthquake Engineering,*

Vancouver, Canada, Paper No. 2287.

[3.22] Mualla, I.H., Belev, B., (2002), "Performance of steel frames with a new friction damper device under earthquake excitation", *Journal of Engineering Structures*, Vol. 24, pp. 365 - 371.

[3.23] Mualla, I.H., Nielsen, L.O., Belev, B., Liao, W.I., Loh, C.H., Agrawal, A., (2002), "Performance of friction-damped frame structure: Shaking table testing and numerical simulations", *Proceedings of 7th US National Conference on Earthquake Engineering,* Boston, USA.

[3.24] Nateghi, F.E., Motamedi, M., Izadi, E.Z., (2008), "Experimental behaviour of the seismic filled accordion metallic dampers, FAMD", *Proceedings of 14th World Conference on Earthquake Engineering,* Beijing, China.

[3.25] Pall, A.S, Marsh, C., (1982), "Seismic response of friction damped braced frames", *Journal of Structural Division,* Vol. 108, No. 9, pp. 1313 - 1323.

[3.26] Phocas, M.C., Pocanschi, A., (2003), "Steel frames with bracing mechanism and hysteretic dampers", *Journal of Earthquake Engineering and Structural Dynamics*, Vol. 32, No. 5, pp. 811 - 825.

[3.27] Popov, E.P., Engelhardt, M.D., (1988), "Seismic eccentrically braced frames", Journal of Constructional Steel Research, London, Vol.10.

[3.28] Renzi, E., Perno, S., Pantanella, S., Ciampi, V., (2007), "Design, test and analysis of a light-weight dissipative bracing system for seismic protection of structures", *Journal of Earthquake Engineering and Structural Dynamics*, Vol. 36, No. 4, pp. 519 - 539.

[3.29] Shen, K.L., Soong, T.T., Chang, K.C., Lai, M.L., (1995), "Seismic behaviour of reinforced concrete frame with added viscoelastic dampers", *Journal of Engineering Structures,* Vol. 17, No. 5, pp. 372 - 380.

[3.30] Sigaher, A.N., Constantinou, M.C., (2003), "Scissor-jack-damper energy dissipation

system", *Journal of Earthquake Spectra*, Vol. 19, pp. 133 - 158.

[3.31] Soong, T.T., Dargush, G.F., (1997), "*Passive energy dissipation systems in structural engineering*", Wiley, London.

[3.32] Soong, T.T., Spencer, Jr. B.F., Yao, T.P., (1997), "Structural control: Past, present and future", *Journal of Engineering Mechanics*, Vol. 123, No. 9, pp. 897 - 971.

[3.33] Symans, M.D., Charney, F.A., Whittaker, A.S., Constantinou, M.C., Kircher, C.A., Johnson, M.W., McNamara, R.J., (2008), "Energy dissipation systems for seismic applications: Current practice and recent developments", *Journal of Structural Engineering*, Vol. 1, No. 3, pp. 3-21.

[3.34] Towashiraporn, P., Park, J., Goodno, B.J., Craig, J.I., (2002), "Passive control methods for seismic response modification", *Journal of Progress in Structural Engineering and Materials*, Vol. 4, pp. 74 - 86.

[3.35] Tsai, K.C., Chen, H.W., Hong, C.P., Su, Y.F., (1993), "Design of steel triangular plate energy absorbers for seismic-resistance construction", *Journal of Earthquake Spectra*, Vol. 9, pp. 505-528.

[3.36] Tsai, C.S., Tsai, K.C., (1995), "TPEA device as seismic damper for high-rise buildings", *Journal of Engineering Mechanics*, Vol. 121, No. 10, pp. 1075 – 1081.

[3.37] Tsai, K.C., Yang, Y.F., Lint, J.L., (1993), "Seismic eccentrically braced frames", *Journal of The Structural Design of Tall Buildings*, Vol. 2, pp. 53 – 74.

[3.38] Wada, A., Huang, Y.H., Iwata, M., (1999), "Passive damping technology for buildings in Japan", *Journal of Progress in Structural Engineering and Materials*, Vol. 2, No. 3, pp. 1 - 15.

[3.39] Whittaker, A.S., Bertero, V.V., Thompson, C.L., Alonso, J.L., (1991), "Seismic testing of steel plate energy dissipation devices", *Journal of Earthquake Spectra*, Vol. 7, No. 4, pp. 563 - 604.

[3.40] Wu, B., Zhang, J., Williams, M.S., Ou, J., (2005), "Hysteretic behaviour of improved Pall-typed frictional dampers", *Journal of Engineering Structures*, Vol. 27, pp. 1258 - 1267.

[3.41] Xia, C., Hanson, R.D., (1992), "Influence of ADAS element parameters on building seismic response", *Journal of Structural Engineering*, Vol. 118, No. 7, pp. 1903 - 1918.

[4.1] Aiken, I.D., Nims, D.K., Whittaker, A.S., Kelly, J.M., (1993), "Testing of passive energy dissipation systems", *Journal of Earthquake Spectra*, Vol. 9, No. 3, pp. 335 - 369.

[4.2] Bergman, D.M., Goel, S.C., (1987), "Evaluation of cyclic testing of steel-plate devices for added damping and stiffness", *Technical Report UMCE 87-10*, The University of Michigan, Ann Arbor, Michigan.

[4.3] Chan, R.W., Albermani, F., (2008), "Experimental study of steel slit damper for passive energy dissipation", *Journal of Engineering Structures*, Vol. 30, No. 4, pp. 1058 - 1066.

[4.4] CSI, SAP2000NL, (2010), "*Theoretical and Users Manual, Release No. 14.00*", Structural Analysis Programs Computers & Structures Inc., Berkeley, California.

[4.5] Ghabraie, K., Chan, R., Huang, X., Xie, Y.M., (2010), "Shape optimization of metallic yielding devices for passive mitigation of seismic energy", *Journal of Engineering Structures*, Vol. 32, pp. 2258 - 2267.

[4.6] Kurata, M., DesRoches, R., Leon, R.T., (2008), "Cable damper bracing for partial seismic rehabilitation", *Proceedings of 14th World Conference on Earthquake Engineering*, Beijing, China.

[4.7] Li, H.N., Li, G., (2007), "Experimental study of structure with "dual function" metallic dampers", *Journal of Engineering Structures*, Vol. 29, pp 1917 - 1928.

[4.8] Martelli, A., (2010), "Aseismic dissipating devices and unconventional shapes in seismic areas", Cruz (ed.), *Structures and Architecture*, Taylor & Francis Group, London.

[4.9] Martelli, A., (2007), "Seismic isolation and energy dissipation: worldwide application and perspectives", Brebbia, C.A. (ed.), *Earthquake Resistant Engineering Structures VI*, WIT Press, Southampton, pp. 105 - 116.

[4.10] Mualla, I.H., Belev, B., (2002), "Performance of steel frames with a new friction damper device under earthquake excitation", *Journal of Engineering Structures*, Vol. 24, pp. 365 - 371.

[4.11] Mualla, I.H., Nielsen, L.O., Belev, B., Liao, W.I., Loh, C.H., Agrawal, A., (2002), "Performance of friction-damped frame structure: Shaking table testing and numerical simulations", *Proceedings of 7th US National Conference on Earthquake Engineering*, Boston, USA.

[4.12] Phocas, M.C., Pocanschi, A., (2003), "Steel frames with bracing mechanism and hysteretic dampers", *Journal of Earthquake Engineering and Structural Dynamics*, Vol. 32, No. 5, pp. 811 - 825.

[4.13] Phocas, M.C., Sophocleous, T., (2011), "Adaptable dual control systems for earthquake resistance", Brebbia, C.A., Maugeri, M. (eds), *Earthquake Resistant Engineering Structures VIII, ERES 2011,* WIT Press, Southampton, pp. 55 - 66.

[4.14] Phocas, M.C., Sophocleous, T., (2008), "Kinetic structures in architecture", *Proceedings of 14th World Conference on Earthquake Engineering,* Beijing, China.

[4.15] Renzi, E., Perno, S., Pantanella, S., Ciampi, V., (2007), "Design, test and analysis of a light-weight dissipative bracing system for seismic protection of structures", *Journal of Earthquake Engineering and Structural Dynamics,* Vol. 36, No. 4, pp. 519 - 539.

[4.16] Sophocleous, T., Phocas, M.C., (2011), "Bracing configuration in dual earthquake

resistance structure", *Proceedings of 3rd International Conference on Computational Methods in Structural Dynamics and Earthquake Engineering, COMPDYN 2011,* Corfu, Greece.

[4.17] Sophocleous, T., Phocas, M.C., (2009), "Dual earthquake resistant frames", Phocas, M., Brebbia, C.A., Komodromos, P. (eds), *Earthquake Resistant Engineering Structures VII, ERES 2009,* WIT Press, Southampton, pp. 165 - 174.

[4.18] Sophocleous, T., Phocas, M.C., (2011), "Dual structure configuration for earthquake resistance", *Proceedings of 8th International Conference on Structural Dynamics, EURODYN 2011,* Leuven, Belgium.

[4.19] Sophocleous, T., Phocas, M.C., (2010), "Dual structures towards kinetic adaptability for earthquake resistance", Cruz (ed.), *Structures and Architecture, ICSA 2010,* Taylor & Francis Group, London.

[4.20] Sophocleous, T., Phocas, M.C. (2009), "Model of analysis for earthquake resistant dual systems", *Proceedings of 2nd International Conference on Computational Methods in Structural Dynamics and Earthquake Engineering, COMPDYN 2009,* Rhodes, Greece.

[4.21] Tsai, K.C., Chen, H.W., Hong, C.P., Su, Y.F., (1993), "Design of steel triangular plate energy absorbers for seismic-resistance construction", *Journal of Earthquake Spectra*, Vol. 9, pp. 505 - 528.

[4.22] Tsai, C.S., Tsai, K.C., (1995), "TPEA device as seismic damper for high-rise buildings", *Journal of Engineering Mechanics,* Vol. 121, No. 10, pp. 1075-1081.

[4.23] Whittaker, A.S., Bertero, V.V., Thompson, C.L., Alonso, J.L., (1991), "Seismic testing of steel plate energy dissipation devices", *Journal of Earthquake Spectra*, Vol. 7, No. 4, pp. 563 - 604.

[4.24] Xia, C., Hanson, R.D., (1992), "Influence of ADAS element parameters on building seismic response", *Journal of Structural Engineering*, Vol. 118, No. 7, pp. 1903 - 1918.

[5.1] Chopra, A. K., (1995), "*Dynamics of Structures: Theory and Applications to Earthquake Engineering*", Prentice Hall, Englewood Cliffs, New Jersey.

[5.2] Clark, P., Aiken, I., Kasai, K., Ko, E., Kimura, I., (1999), "Design procedures for buildings incorporating hysteretic damping device", *Proceedings of 68th Annual Convention, Santa Barbara*, Structural Engineers Association of California, California.

[5.3] Clough, R.W., Penzien, J., (2010), "*Dynamics of Structures*", McGraw-Hill, New York.

[5.4] Constantinou, M.C., Symans, M.D., (1993), "Seismic response of structures with supplemental damping", *Journal of The Structural Design of Tall Buildings,* Vol. 2, pp. 77 - 92.

[5.5] CSI, SAP2000NL, (2010), "*Theoretical and Users Manual, Release No. 14.00*", Structural Analysis Programs Computers & Structures Inc., Berkeley, California.

[5.6] Dargush, G.F., Soong, T.T., (1995), "Behaviour of metallic plate dampers in seismic passive energy dissipation systems", *Journal of Earthquake Spectra*, Vol. 11, No. 4, pp. 545 - 568.

[5.7] Inoue, K., Kuwahara, S., (1998), "Optimum strength ratio of hysteretic damper", *Journal of Earthquake Engineering and Structural Dynamics*, Vol. 27, pp. 577-588.

[5.8] Nakashima, M., Saburi, K., Tsuji, B., (1996), "Energy input and dissipation behaviour of structures with hysteretic dampers", *Journal of Earthquake Engineering and Structural Dynamics*, Vol. 25, No. 12, pp. 483 - 496.

[5.9] Phocas, M.C., Pocanschi, A., (2003), "Steel frames with bracing mechanism and hysteretic dampers", *Journal of Earthquake Engineering and Structural Dynamics*, Vol. 32, No. 5, pp. 811 - 825.

[5.10] Phocas, M.C., Sophocleous, T., (2011), "Adaptable dual control systems for earthquake

resistance", Brebbia, C.A., Maugeri, M. (eds), *Earthquake Resistant Engineering Structures VIII, ERES 2011,* WIT Press, Southampton, pp. 55 - 66.

[5.11] Phocas, M.C., Sophocleous, T., (2008), "Kinetic structures in architecture", *Proceedings of 14th World Conference on Earthquake Engineering,* Beijing, China.

[5.12] Sophocleous, T., Phocas, M.C., (2011), "Bracing configuration in dual earthquake resistance structure", *Proceedings of 3rd International Conference on Computational Methods in Structural Dynamics and Earthquake Engineering, COMPDYN 2011,* Corfu, Greece.

[5.13] Sophocleous, T., Phocas, M.C., (2009), "Dual earthquake resistant frames", Phocas, M., Brebbia, C.A., Komodromos, P. (eds), *Earthquake Resistant Engineering Structures VII, ERES 2009,* WIT Press, Southampton, pp. 165 - 174.

[5.14] Sophocleous, T., Phocas, M.C., (2011), "Dual structure configuration for earthquake resistance", *Proceedings of 8th International Conference on Structural Dynamics, EURODYN 2011,* Leuven, Belgium.

[5.15] Sophocleous, T., Phocas, M.C., (2010), "Dual structures towards kinetic adaptability for earthquake resistance", Cruz (ed.), *Structures and Architecture, ICSA 2010,* Taylor & Francis Group, London.

[5.16] Sophocleous, T., Phocas, M.C. (2009), "Model of analysis for earthquake resistant dual systems", *Proceedings of 2nd International Conference on Computational Methods in Structural Dynamics and Earthquake Engineering, COMPDYN 2009,* Rhodes, Greece.

[5.17] Tsai, C.S., Tsai, K.C., (1995), "TPEA Device as seismic damper for high-rise buildings", *Journal of Engineering Mechanics*, Vol. 121, No. 10, pp. 1075 – 1081.

[5.18] Tsai, K.C., Chen, H.W., Hong, C.P., Su, Y.F., (1993), "Design of steel triangular plate energy absorbers for seismic-resistance construction", *Journal of Earthquake Spectra*, Vol. 9, pp. 505 - 528.

[5.19] Uang, C.M., Bertero, V.V., (1988), "Use of energy as a design criterion in earthquake-resistant design", *Technical Report UCB/EERC-88/18*, University of California, Berkeley, California.

[5.20] Whittaker, A., Constantinou, M., Tsopelas,P., (1998), "Displacement estimates for performance–based seismic design", *Journal of Structural Engineering,* Vol. 124, No. 8, pp. 905 - 912.

[6.1] Chopra, A.K., (1995), "*Dynamics of Structures*", Prentice Hall, Englewood Cliffs, New Jersey.

[6.2] Clough, R.W., Penzien, J., (2010), "*Dynamics of Structures*", McGraw-Hill, New York.

[6.3] CSI, SAP2000NL, (2010), "*Theoretical and Users Manual, Release No. 14.00*", Structural Analysis Programs Computers & Structures Inc., Berkeley, California.

[6.4] Phocas, M.C., Pocanschi, A., (2003), "Steel frames with bracing mechanism and hysteretic dampers", *Journal of Earthquake Engineering and Structural Dynamics*, Vol. 32, No. 5, pp. 811 - 825.

[6.5] Phocas, M.C., Sophocleous, T., (2011), "Adaptable dual control systems for earthquake resistance", Brebbia, C.A., Maugeri, M. (eds), *Earthquake Resistant Engineering Structures VIII, ERES 2011*, WIT Press, Southampton, pp. 55 - 66.

[6.6] Phocas, M.C., Sophocleous, T., (2008), "Kinetic structures in architecture", *Proceedings of 14th World Conference on Earthquake Engineering,* Beijing, China.

[6.7] Sophocleous, T., Phocas, M.C., (2011), "Bracing configuration in dual earthquake resistance structure", *Proceedings of 3rd International Conference on Computational Methods in Structural Dynamics and Earthquake Engineering, COMPDYN 2011,* Corfu, Greece.

[6.8] Sophocleous, T., Phocas, M.C., (2009), "Dual earthquake resistant frames", Phocas, M., Brebbia, C.A., Komodromos, P. (eds), *Earthquake Resistant Engineering Structures VII, ERES 2009,* WIT Press, Southampton, pp. 165 - 174.

[6.9] Sophocleous, T., Phocas, M.C., (2011), "Dual structure configuration for earthquake resistance", *Proceedings of 8th International Conference on Structural Dynamics, EURODYN 2011,* Leuven, Belgium.

[6.10] Sophocleous, T., Phocas, M.C., (2010), "Dual structures towards kinetic adaptability for earthquake resistance", Cruz (ed.), *Structures and Architecture, ICSA 2010,* Taylor & Francis Group, London.

[6.11] Sophocleous, T., Phocas, M.C. (2009), "Model of analysis for earthquake resistant dual systems", *Proceedings of 2nd International Conference on Computational Methods in Structural Dynamics and Earthquake Engineering, COMPDYN 2009,* Rhodes, Greece.

[7.1] Phocas, M.C., Sophocleous, T., (2011), "Adaptable dual control systems for earthquake resistance", Brebbia, C.A., Maugeri, M. (eds), *Earthquake Resistant Engineering Structures VIII, ERES 2011,* WIT Press, Southampton, pp. 55 - 66.

[7.2] Phocas, M.C., Sophocleous, T., (2008), "Kinetic structures in architecture", *Proceedings of 14th World Conference on Earthquake Engineering,* Beijing, China.

[7.3] Sophocleous, T., Phocas, M.C., (2011), "Bracing configuration in dual earthquake resistance structure", *Proceedings of 3rd International Conference on Computational Methods in Structural Dynamics and Earthquake Engineering, COMPDYN 2011,* Corfu, Greece.

[7.4] Sophocleous, T., Phocas, M.C., (2009), "Dual earthquake resistant frames", Phocas, M., Brebbia, C.A., Komodromos, P. (eds), *Earthquake Resistant Engineering Structures VII, ERES 2009,* WIT Press, Southampton, pp. 165 – 174.

[7.5] Sophocleous, T., Phocas, M.C., (2011), "Dual structure configuration for earthquake resistance", *Proceedings of 8th International Conference on Structural Dynamics, EURODYN 2011,* Leuven, Belgium.

[7.6] Sophocleous, T., Phocas, M.C., (2010), "Dual structures towards kinetic adaptability for earthquake resistance", Cruz (ed.), *Structures and Architecture, ICSA 2010,* Taylor & Francis Group, London.

[7.7] Sophocleous, T., Phocas, M.C. (2009), "Model of analysis for earthquake resistant dual systems", *Proceedings of 2nd International Conference on Computational Methods in Structural Dynamics and Earthquake Engineering, COMPDYN 2009,* Rhodes, Greece.

[8.1] Phocas, M.C., Sophocleous, T., "Adaptable dual control systems: A comparative parametric analysis", *Journal of Safety and Security Engineering,* submitted 2012.

[8.2] Phocas, M.C., Sophocleous, T., (2011), "Adaptable dual control systems for earthquake resistance", Brebbia, C.A., Maugeri, M. (eds), *Earthquake Resistant Engineering Structures VIII, ERES 2011,* WIT Press, Southampton, pp. 55 – 66.

[8.3] Phocas, M.C., Sophocleous, T., "Cable bracing design in adaptable dual control systems", Brebbia, C.A. (ed.), *Earthquake Resistant Engineering Structures IX, ERES 2013,* WIT Press, Southampton, in print.

[8.4] Phocas, M.C., Sophocleous, T., "Dual system configuration for earthquake safety", *Journal of Advances in Structural Engineering*, submitted 2012.

[8.5] Phocas, M.C., Sophocleous, T., (2008), "Kinetic structures in architecture", *Proceedings of 14th World Conference on Earthquake Engineering,* Beijing, China.

[8.6] Phocas, M.C., Sophocleous, T., "Numerical verification of a dual's system's seismic response", *Journal of Earthquakes and Structures*, in print.

[8.7] Sophocleous, T., Phocas, M.C., (2011), "Bracing configuration in dual earthquake resistance structure", *Proceedings of 3rd International Conference on Computational Methods in Structural Dynamics and Earthquake Engineering, COMPDYN 2011,* Corfu, Greece.

[8.8] Sophocleous, T., Phocas, M.C., (2012), "Bracing design in dual systems for earthquake resistance", *Proceedings of 15th World Conference on Earthquake Engineering* Lisbon, Portugal.

[8.9] Sophocleous, T., Phocas, M.C., (2009), "Dual earthquake resistant frames", Phocas, M., Brebbia, C.A., Komodromos, P. (eds), *Earthquake Resistant Engineering Structures VII, ERES 2009,* WIT Press, Southampton, pp. 165 - 174.

[8.10] Sophocleous, T., Phocas, M.C., (2011), "Dual structure configuration for earthquake resistance", *Proceedings of 8th International Conference on Structural Dynamics, EURODYN 2011,* Leuven, Belgium.

[8.11] Sophocleous, T., Phocas, M.C., (2010), "Dual structures towards kinetic adaptability for earthquake resistance", Cruz (ed.), *Structures and Architecture, ICSA 2010,* Taylor & Francis Group, London.

[8.12] Sophocleous, T., Phocas, M.C. (2009), "Model of analysis for earthquake resistant dual systems", *Proceedings of 2nd International Conference on Computational Methods in Structural Dynamics and Earthquake Engineering, COMPDYN 2009,* Rhodes, Greece.